Ministero dell'Università e della Ricerca

Università degli studi di Palermo

Dipartimento di Ingegneria Nucleare Università di Palermo

Dipartimento di Ingegneria Nucleare

Preparation of fluorinated polymer matrixes modified for biomedical applications

PhD thesis of **Ferro Loredana**

Supervisor
Prof. Alessandro Galia

Head of the PhD board
Prof. Francesco Castiglia

Ciclo XXII: 2008-2010

INDEX

INTRODUCTION

During the last years many studies were performed to develop a new generation of polymer materials to use in biomedical applications such as drug controlled release, the selective permeation of drugs from biological fluids, protein immunoblot and antibacterial packaging. The fluoropolymers are an important class of biocompatible polymers having excellent properties of chemical and mechanical resistance useful for these applications. Among these, the PVDF-based polymers have been widely investigated. Vinylidene fluoride-hexafluoropropylene (VDF-HFP) random copolymers represent an important class of fluoropolymers and they can be used as membrane materials for fuel cells and biomedical applications. Their properties can be tuned from those of a semi-crystalline thermoplastic to those of a fully amorphous elastomer by increasing the HFP content. Actually they are industrially produced using aqueous emulsion or suspension processes, generating large amount of waste water and requiring high energy for drying. Therefore, their production has heavy environmental issues that could be overcome by replacing the conventional solvent (water) with the alternative dispersing medium supercritical carbon dioxide, defined as a "green solvent". Recently, several studies showed that the $scCO_2$ is a promising alternative to traditional polymerization solvents, in fact DuPont has just built the first industrial plant for the production of tetrafluoroethylene fluoropolymer in $scCO_2$.

The first section of this thesis summarizes the existent literature on the use of supercritical CO_2 as polymerization medium, focused mainly on the fluoropolymer synthesis. Successively, the thesis reports the experimental study of the free radical heterogeneous copolymerization process of

vinylidene fluoride and hexafluoropropylene in supercritical carbon dioxide, aimed particularly to solve the problem of the main reaction locus. Indeed, since the process is carried out in heterogeneous conditions, the system is characterized by the presence of two phases: the continuous (sc-CO_2) and the polymer phase, which could be two potential reaction loci. This is a key aspect that needed a valid investigation in view of an industrial scale production of the copolymer because depending on the contribute of each phase as reaction locus the resulting copolymer can exhibit different properties and performances.

The second section of the thesis concerns the description of the grafting methods used more frequently to modify hydrophobic polymers, such as PVDF, and to confer them hydrophilic properties and pH sensitivity. Moreover it reports the existent literature on the grafting polymerization processes performed in supercritical carbon dioxide on PVDF since they represents a valid alternative to that performed in condensed systems. In fact, in CO_2/polymer systems the monomers and initiator not only can diffuse into the pores of membranes, wetting their internal volume, but moreover their distribution between the polymeric substrates and scCO_2 could be controlled by the fluid phase density. Accordingly, it was interesting to study the preparation of hydrophilic and pH-sensitive PVDF membranes by addition of acrylic acid units, using supercritical carbon dioxide as solvent, which has good swelling capability towards amorphous fluoropolymers. Among several experimental routes attempted, the graft copolymerization of AA on the PVDF membrane was successfully performed by mean a radical initiator, which initiates the reaction by thermal decomposition. In particular in the last section are described the results obtained from the study of the influence of the main operative parameters on the final properties exhibited of the

membranes, such as microstructure, crystallinity, microscopic morphology, thermal stability, water permeation and pH sensitivity.

CHAPTER 1

SUPERCRITICAL CARBON DIOXIDE AS POLYMERIZATION MEDIUM

1.1 Supercritical fluids (SCFs) as alternative solvent media

Actually the industrial activities make use of excessive amounts of organic solvents, in particular the polymer industry which uses these compounds either as reaction media in the polymerization process or as media for polymer processing such as shaping, extraction, impregnation, or viscosity reduction. Indeed, due to this industrial activity, about 20 million tonnes of volatile organic compounds (VOCs) are emitted into the atmosphere each year. In order to reduce these emissions most of the efforts of the processes are connected with the solvent recovery. A typical scheme of a conventional catalytic polymerization process based on organic solvents, including a step of solvent recovery is shown in Figure 1.1. Some processes use water as solvent in place of the conventional organic solvents but then the problems are reflected on the large amounts of hazardous aqueous waste that require treatment. As a result of these environmental concerns, actually, the most of research studies of the chemical industry are directed to the development of more sustainable processes, where the use of organic solvents is highly reduced. These studies suggest two possibilities: the development of solvent-free processes or the replacement of conventional solvents with environmentally benign products. Generally, the polymerizations carried out in absence of solvent are characterized by several problems related to the polymer processing due to the increased viscosities and the mass transfer limitations.[1]

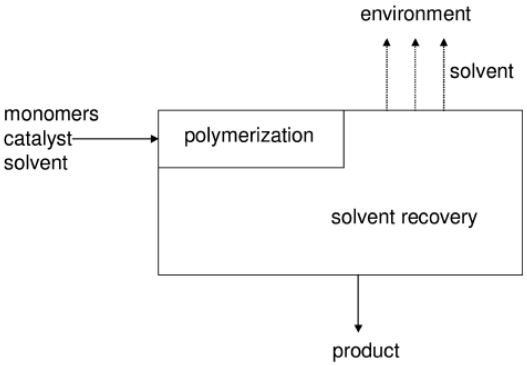

Fig. 1.1-Schematic representation of a conventional catalytic polymerization process based on organic solvents, which needs of a solvent recovery step to reduce the emission of VOCs.[2]

The solvent replacement would be the most promising alternative, if it is associated with a solvent removal step requiring a low energy consumption. A solution could be use a reactant in excess in the feed so that it acts also as solvent, anyway the problem is shifted toward the solvent removal step because this excess of reactant have to be removed. Therefore, the simplest solution consists in the use of a volatile solvent which makes the solvent removal step easier.

Actually, the potential environmentally benign products alternative to organic solvents can be ionic liquids and supercritical fluids.[3] Ionic liquids are room-temperature molten organic salts which have a negligible vapour pressure. Although their use in existing equipments significantly reduces the VOCs emission, it becomes more difficult their separation from the process streams. Moreover, the cost of a room-temperature molten salt is substantial. Concerning the supercritical fluids, a valid alternative could be the

supercritical water which is a very effective reaction medium for oxidation reactions.[4,5] Nevertheless, the processes based on supercritical water require very extreme operative conditions, because to the high critical point of the water. These severe conditions induce to problems connected with corrosion of materials that cause the increase the investment costs. Moreover these processes need of proper oxidation processes for waste water treatment.[6]

The critical properties of common substances used as supercritical fluids are shown in Table 1.1. Among these substances, carbon dioxide and water are the fluids most frequently used in a wide range of applications. An example of industrial application of carbon dioxide is the process of the Dow Chemical Company in which CO_2 is used as blowing agent to replace chlorofluorocarbon in the manufacture of polystyrene foam sheet.[7,8]

Solvent	T_c (K)	P_c (MPa)	Solvent	T_c (K)	P_c (MPa)
Acetone	508.1	4.70	Hexafluoroethane	293.0	3.06
Ammonia	405.6	11.3	Methane	190.4	4.60
Carbon dioxide	304.1	7.38	Methanol	512.6	8.09
Cyclohexane	553.5	4.07	*n*-hexane	507.5	3.01
Diethyl ether	466.7	3.64	Propane	369.8	4.25
Difluoromethane	351.6	5.83	Propylene	364.9	4.60
Difluoroethane	386.7	4.50	Sulfur hexafluoride	318.7	3.76
Dimethyl ether	400.0	5.24	Tetrafluoromethane	227.6	3.74
Ethane	305.3	4.87	Toluene	591.8	41.1
Ethylene	282.4	5.04	Trifluoromethane	299.3	4.86
Ethyne	308.3	6.14	Water	647.3	22.1

Table 1.1-Critical conditions of several substances.[9]

Until now, supercritical CO_2 represents the more promising alternative to the conventional solvents in chemical processes due to several aspects, some which are in following reported. It is naturally abundant, indeed it exists in

natural reservoirs located throughout the world. In addition, it is generated in large quantities as a byproduct in ammonia, hydrogen, and ethanol production plants and in electrical power generation stations that burn fossil fuels. It can also be a sustainable source of carbon[10] in place of the fossil fuels so contributing to reduce the emission of greenhouse gas CO_2. Moreover, it is inexpensive, non-flammable and non-toxic.

1.2 Advantages of the use of CO_2 in the supercritical state

A substance is in the supercritical state if it is at temperature and pressure conditions upper than its corresponding critical values.[11-13] Once the supercritical state is reached, the pressure and temperature can be increased simultaneously or individually without involving a phase change. In Figure 1.2-a, representing the pressure-temperature phase diagram of carbon dioxide, it observes the boiling line which separates the vapour and liquid regions and ends at the critical point. Indeed, above the critical point, the vapour-liquid coexistence line no longer exists.

The supercritical state was discovered in 1822 by Baron Cagniard de la Tour[14], who defined it as a state of matter where the liquid and vapour phases are indistinguishable. Another definition of supercritical state it has given, on a characteristic microscale of approximately 10–100 Å, by Baldyga[15] who defined the supercritical state as a state of matter composed by statistical clusters of higher density with a structure close to that of liquids, surrounded by less dense and more chaotic regions of compressed gas. According to this theory, the number and dimensions of these clusters vary significantly with pressure and temperature, resulting in high compressibility of the substance near the critical point. The physical properties, that are responsible of the importance gain by SCFs in the

industrial processes, are density, viscosity and diffusion. A comparison of these properties for typical gases, liquids and SCFs is given in Table 1.2. According to this values, it is possible to revise the supercritical state as an "hybrid state" in fact supercritical fluids can have gas-like diffusivities and liquid-like densities.

Properties	Gas	Supercritical fluid	Liquid
ρ (kg m^{-3})	1	100–800	1000
η (Pa s)	0.001	0.005–0.01	0.05–0.1
$\mathcal{D}$ (m^2 s^{-1})	$1 \cdot 10^{-5}$	$1 \cdot 10^{-7}$	$1 \cdot 10^{-9}$

Table 1.2 -Typical values of physical properties of gases, supercritical fluids and liquids.[16] ρ = density, η = viscosity, D =diffusivity.

By studying the phase behaviour of SCFs it was observed that they can exhibit changes in solvent density with small changes in temperature or pressure within the critical region. This behaviour can be observed in the density-pressure phase diagram (Fig. 1.2 b). The diagram presents a region where exists the coexistence of the two phases liquid-vapour in equilibrium, moreover, at the critical point, the densities of the equilibrium liquid phase and the saturated vapour phase become equal, resulting in the formation of a single supercritical phase.

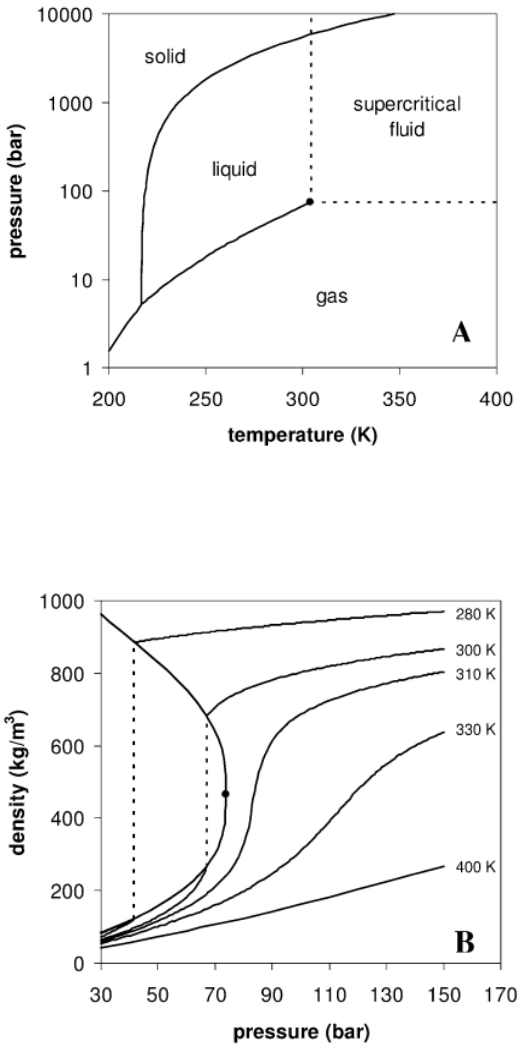

Fig. 1.2- (A) Phase diagram pressure - temperature of CO_2 in which it is evidenced the supercritical fluid region at the end of the vapor-liquid equilibrium line. (B) Phase diagram density-pressure of CO_2 at different temperatures.[2]

Supercritical carbon dioxide is the most extensively studied supercritical fluid medium for polymerization reactions and organic transformations. Its critical temperature and pressure were discovered in 1875 by Andrews[17] (30.95°C and 72.8 atm) and the first technological application of $scCO_2$ dates at 1970 when it was used for the extraction of caffeine from coffee beans.[18] This application was followed by several other applications, such as the supercritical chromatography used to separate polar compounds.[19,20] Nowadays, the interest in supercritical fluid-based processes is remarkable increased indeed actually the industrial applications of supercritical fluids concern a wide range of industrial fields such as food, agriculture, petrochemical and pharmaceutical industry. CO_2 finds particularly advantageous applications in the polymer industry for the synthesis and processing of polymers. Indeed, it can be regarded as a viable alternative solvent because, apart from the environmental benefits, it has also desirable physical and chemical properties. These include its chemical inertness, readily accessible critical point, excellent wetting characteristics, low viscosity, and highly tuneable solvent behaviour. Moreover, because it is an ambient gas, the final products can be isolated from the reaction media by simple depressurization, resulting in a dry polymer product. This feature eliminates energy-intensive drying procedures required in polymer manufacturing to remove solvent and represents potential cost and energy savings. Moreover, it is possible to carry out the process providing the recycle of the solvent and other components, like catalyst and monomers, back to the reactor feed. Figure 1.3 illustrates the scheme of a CO_2-based polymerization system as a closed-loop process.

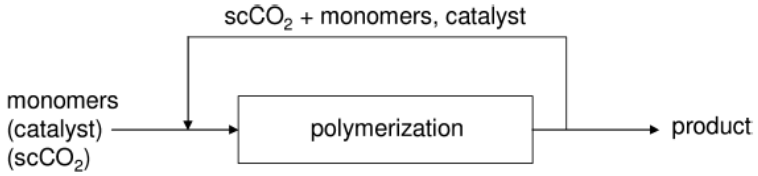

Fig. 1.3 - Schematic representation of a closed-loop process of a catalytic polymerization system based on CO_2 as solvent.[2]

1.3 Solubility of Polymers and Monomers in carbon dioxide

The parameters that govern solubility of polymers and monomers in CO_2 are not fully understood, indeed several studies have been performed focusing the attention on the nature of solute-solvent interactions between polymers and CO_2. The main intermolecular interaction forces are dispersion, dipole-dipole, dipole-quadrupole, and quadrupole-quadrupole. These interactions are highly temperature sensitive. The solvent strength of carbon dioxide for solutes is dominated by low polarizability and a strong quadrupole moment (Table 1.3). CO_2 is a nonpolar substance but it is able to dissolve most nonpolar and some polar molecules of low molar weight, while it is a poor solvent for most high molar mass polymers under mild conditions (<100 °C, <350 bar). Anyway a good miscibility with many compounds, including vinyl monomers, can be obtained at high density for which it is required high pressure. Moreover, as molecular weight increases at a given temperature, the pressure where this substance is still completely miscible in CO_2 rises sharply. As consequence, most of polymers exhibit very limited solubility in carbon dioxide so excluding its use for the manufacture of such polymers by solution polymerization. That also means that dispersion, emulsion or precipitation are viable techniques for synthesizing high molecular weight polymers in $scCO_2$. The only polymers that show good solubility in CO_2

under mild conditions are polyalkene oxides, perfluorinated polypropylene oxide, polymethyl acrylate, polyvinyl acetate, polyalkyl siloxanes and polyether carbonate.

Solvent	$\alpha \cdot 10^{25}$ (cm^3)	μ (D)	$Q \times 10^{26}$ ($erg^{1/2}cm^{5/2}$)
Methane	26	0.0	
Ethane	45.0	0.0	–0.7
Ethyne	33.3	0.0	+3.0
Hexafluoroethane	47.6	0.0	–0.7
Carbon dioxide	27.6	0.0	–4.3
n-hexane	118.3	0.0	
Methanol	32.3	1.7	
Acetone	63.3	2.9	

Table 1.3 - Physical properties of various solvents,[16,21,22] where $\boldsymbol{\alpha}$ is the polarizability, $\boldsymbol{\mu}$ is the dipole moment and $\boldsymbol{Q}$ is the quadrupole moment.

Another important feature of supercritical CO_2 is its high solubility in a lot of polymers that influences remarkably the mechanical and physical properties of the polymers, such as for example diffusivity, viscosity, glass transition, melting point, compressibility, and expansion. In particular, it causes the polymer plasticization, which results in the lowering of the polymer's glass transition temperature (Tg). This aspect will be widely explained in the followed of this thesis, however, now it is important to remark that the plasticization effect of CO_2 is due to the polymer-solvent interactions[23] and moreover it is a very important property of CO_2 because can decisively facilitate many polymer processing operations such as polymer impregnation, extraction, chemical modification and foaming.

1.4 Future developments

From what has been discussed until now, it is evident that a $scCO_2$-based technology represents an interesting alternative to several existing industrial processes, mainly that of polymer synthesis and processing. Anyway, this technology is not still widely adopted in the industry. The reasons could be the limited solubility of the reactants for specific reactions, but also economic issues. Indeed, a $scCO_2$-based process requires high pressures that means higher operative costs and, moreover, when high pressures are involved, the costs and some aspects related to safety must also be carefully considered, especially while planning for scale-ups.

However, actually it forecasts that the main future applications of supercritical CO_2 will concern the food and pharmaceutical industry, but the results collected until now by the scientific community concerning feasibility studies suggest the application possibility of supercritical fluid technology also in polymer processes. An industrial example is represented by DuPont[24] which is commercializing the production of fluoropolymers in $scCO_2$.

References

[1] J.M. DeSimone, Science, 2002, 297, 799.

[2] M.F. Kemmere, T. Meyer, Supercritical Carbon Dioxide in Polymer Reaction Engineering, Wiley-VCH, Weinheim, 2005.

[3] P.T. Anastas, Green chemistry as applied to solvents, in Clean solvents alternative media for chemical reactions and processing, eds.: M.A. Abraham, L. Moens, ACS Symposium Series 819, Washington, 2002.

[4] M. Modell, US Patent 4338199, 1982.

[5] T. B. Thomason, M. Modell, Hazard Waste, 1984, 1(4), 453.

[6] J.W. Griffith, D.H. Raymond, Waste Management, 2002, 22, 453.

[7] G. C. Welsh, US Patent 5266605, 1993.

[8] G. C. Welsh, US Patent 5250577, 1993.

[9] W. Leitner, P.G. Jessop, Chemical synthesis using supercritical fluids, Wiley-VCH, Weinheim, 1999.

[10] D.J. Darensbourg, M.W. Holtecamp, Coordination Chemistry Reviews, 1996, 153, 155.

[11] S. Angus, B. Armstrong, K.M. de Reuck, International Thermodynamic Tables of the Fluid State. Carbon Dioxide, Pergamon Press, Oxford, 1976.

[12] R. Span, W. Wagner, J. Phys. Chem. Ref. Data, 1996, 25, 1509.

[13] J. A. Darr, M. Poliakoff, Chem. Rev., 1999, 99, 495.

[14] C. Cagniard de la Tour, Ann. Chim. Phys., 1822, 22, 127.

[15] J. Baldyga, M. Henczka, B.Y. Shekunov, Fluid dynamics, mass transfer and particle formation in supercritical fluids, in Supercritical fluid technology for drug product development, eds.: P. York, U.B. Kompella, B. Shekunov, M. Dekker, New York, 2004.

[16] R. C. Reid, J.M. Prausnitz, B.E. Poling, The Properties of Gases and Liquids, 4th edn., McGraw-Hill, New York, 1987.

[17] T. Andrews, Proc. R. Soc., 1875, 24, 455.

[18] M.A. McHugh, V. J. Krukonis, Supercritical fluid extractions: principles and practice, 2nd edn., Butterworth-Heinemann, Stoneham, MA, 1994.

[19] T. A. Berger, J. Chromatogr. A, 1997, 785, 3.

[20] G. O. Cantrell, J. A. Blackwell, J. Chromatogr. A, 1997, 782, 237.

[21] J.M. Prausnitz, R.N. Lichtenthaler, E.G. de Azevedo, Molecular Thermodynamics of Fluid Phase Equilibria, 2nd edn., Prentice-Hall, Englewood Cliffs, 1986.

[22] C. F. Kirby, M.A. McHugh, Chem. Rev., 1999, 99, 565.

[23] S.G. Kazarian, Polym. Sci., Ser. C, 2000, 42(1), 78.

[24] G. Parkinson, Chem. Eng., 1999, 106,May, 17.

CHAPTER 2

SYNTHESIS OF FLUOROPOLYMERS BY RADICAL POLYMERIZATION IN SUPERCRITICAL CARBON DIOXIDE

2.1 General remarks on homogeneous radical polymerization

The ideal homogeneous kinetic model[1] usually used for the radical polymerizations consists of a sequence of three steps: initiation, propagation, and termination. The initiation step is considered to involve two reactions. The first is the production of free radicals, which can be produced by a thermal, photochemical, or redox method. The thermal method, inducing the homolytic dissociation of an initiator I to yield a pair of radicals R• (primary radicals), is the most widely used in the academic studies as well as in commercial processes. The second part of the initiation involves the addition of a primary radical to the first monomer molecule to produce the first radical.

$$I \xrightarrow{k_d} 2R^{\bullet} \qquad 2.1$$

$$R^{\bullet} + M \xrightarrow{k_i} P_1^{\bullet} \qquad 2.2$$

Where k_d is the rate constant for the initiator dissociation, M represents a monomer molecule and k_i is the rate constant for the initiation step.

In most polymerizations, the second step is much faster than the first one. Thus the homolysis of the initiator represents the rate-determining step in the initiation sequence, and the rate of initiation can be expressed by:

$$R_i = 2fk_d[I] \qquad 2.3$$

where [I] is the concentration of the initiator and *f* is the initiator efficiency that is defined as the fraction of the radicals produced in the homolysis reaction. Its value is usually less than unity due to side reactions with the solvent or with polymer macroradicals which form inactive species.

The number of different types of compounds that can be used as thermal initiators is rather limited. A limit is due to bond dissociation energy values which have to be in the range 100–170 kJ/mol. In fact, compounds with higher or lower dissociation energies will dissociate too slowly or too rapidly, respectively. Only few classes of compounds possess the desired range of dissociation energies. Generally, the peroxides and azo-compounds find extensive use as radical sources, while the other classes of compounds are usually either not readily available or not stable enough.

Several different types of peroxy compounds are widely used. As example, here it is reported the benzoyl peroxide:

$$\phi - CO - O - O - CO - \phi \xrightarrow{\Delta T} 2CO - O\cdot$$

Among the azo compounds major used an example is 2,2-Azobisisobutyronitrile (AIBN):

$$CH_3 - C(CH_3CN) - N = N - C(CH_3CN) - CH_3 \xrightarrow{\Delta T} 2CH_3 - C(CH_3CN)\cdot + N_2$$

The various initiators are used at different temperatures depending on their rates of decomposition which can be conveniently expressed in terms of "initiator half-life" ($t^{1/2}$) defined as the time needed in order that the initial concentration of initiator decreases to one half. The kinetic of thermal

decomposition of an initiator is the first order under ideal conditions, that is in presence of an inert solvent to the decomposition reaction. In particular:

$$-\frac{dc}{dt} = kC \qquad 2.4$$

$$t = \ln(\frac{c_o}{c_t}) / \frac{1}{k} \qquad 2.5$$

$$t^{1/2} = \ln\frac{2}{k} \qquad 2.6$$

It is evident from the equation 2.6 that the $t^{1/2}$ depends exclusively on the intrinsic rate constant *k*. Therefore, all the factor influencing *k*, involve a change of the $t^{1/2}$. Indeed, the halflife of an initiator depends on temperature as well as pressure. For example a decrease in temperature of about 5-10°C duplicates the value of $t^{1/2}$, instead an increase in pressure penalizes the decomposition rate so causing a decrease in halflife. Anyway the pressure effect is more weak than that of temperature, in fact the halflife is twice when the pressure is 3000 bar rather than that at atmospheric pressure. Another parameter that influences this characteristic time is the type of solvent and in particular its polarity. Indeed, the solvent can attack directly the initiator and induce its decomposition. A demonstration is the fact that usually the decomposition rate valuated in suitable solvents is different from that in polymerization media.

Concerning the propagation step, it consists of the growth of P_1• by the successive additions of hundreds and sometimes thousands of monomer molecules. Each addition creates a new radical that has the same identity as the one previously, except that it is larger by one monomer unit. The successive additions may be represented by the follow equation:

$$P_n^{\bullet} + M \xrightarrow{k_P} P_{n+1}^{\bullet} \qquad 2.7$$

The rate of propagation is therefore the sum of a lot of individual propagation steps. Since the rate constants for all the propagation steps are assumed the same, the propagation rate can be expressed by:

$$v_p = k_p[M]\sum[P^{\bullet}] \cong k_p[M][P^{\bullet}] \qquad 2.8$$

$$P\cdot = \sum P_i \cdot \qquad 2.9$$

where k_p is the rate constant for propagation and [P•] is the total concentration of all radical growing chains, independently of their length. The simplification adopted with the equation 2.6 it has been experimentally validated. In particular, since the effect of the radical sizes on their reactivity is almost non influential after the formation of oligomeric radicals, it is valid to suppose that all the radical have the same reactivity.

The bimolecular terminations between two radicals can occur by combination (coupling), two radicals react each with other, or more rarely by disproportionation, in which a hydrogen radical that is in beta to one radical site is transferred to another radical site. The two mechanism are shown in following.

$$P_n^{\bullet} + P_m^{\bullet} \xrightarrow{K_{tc}} P_{n+m} \qquad \text{Combination} \qquad 2.10\text{-a}$$

$$P_n^{\bullet} + P_m^{\bullet} \xrightarrow{K_{td}} P_n + P_m \qquad \text{Disproportionation} \qquad 2.10\text{-b}$$

where k_{tc} and k_{td} are the rate constants for termination by coupling and disproportionation, respectively.

In particular, the polymer obtained by the former mechanism will have a molecular weight equal to the sum of the ones of radicals coupled. While, by disproportionation two polymer molecule will be obtained, one saturated and one unsaturated, with the same molecular weight. In general it is possible to use a termination constant k_t obtained as sum of the two ones in order to define a mathematical expression of the termination rate (v_t).

$$v_t = k_t \left[P^\bullet\right]^2 \qquad 2.11$$

In several polymerization systems it has been evidenced that a growing radical can undergoes to premature termination because it could react with other molecular species existing in the polymerization system, by transferring the radical site so obtaining a dead polymer molecule and another radical which then reinitiates polymerization. In this way the total radical concentration is unchanged but the molecular weight of the final polymer results diminished. These radical displacement reactions are termed chain-transfer reactions and may be depicted as:

$$P_n^\bullet + A - B \xrightarrow{k_{tr}} P_n - A + B^\bullet \qquad 2.12$$

$$v_{tr} = k_{tr} \left[P^\bullet\right]\left[AB\right] \qquad 2.13$$

where the A-B specie can be the monomer, initiator, polymer or solvent, and v_{tr} is chain-transfer reaction rate.

2.2 Polymerization rate

The polymerization rate is expressed as rate of monomer disappearance. In particular, since monomer disappears in the initiation reaction as well as in the propagation reaction, the polymerization rate is given by

$$\frac{-d[M]}{dt} = R_i + R_P \qquad 2.14$$

where R_i and R_p are the rates of initiation and propagation, respectively. However, in a process producing polymer with high molecular weight, the number of monomer molecules reacting in the initiation step is far less than the number in the propagation step. Thus, the former can be neglected and the polymerization rate can be assumed as the propagation rate.

$$\frac{-d[M]}{dt} = R_P = k_P[M][P^{\bullet}] \qquad 2.15$$

In order to calculate a value for R_p this equation is not directly applicable because it requires the knowledge of radical concentration that is difficult to measure quantitatively, since it is very low (~10-8 M). To solve this problem the steady-state assumption can be made. Indeed, although the radical concentration increases initially, it almost instantaneously reaches a constant value (steady-state value). According to this, it is possible to assume zero the rate of change of the concentration of radicals during the polymerization.

$$\frac{dP\bullet}{dt} = 2fk_d[I] - k_t[P\bullet]^2 \cong 0 \qquad 2.16$$

This is equivalent to stating that the rates of initiation R_i and termination R_t of radicals are equal, obtaining the following expression for the radical concentration.

$$\left[P^{\bullet}\right]=\left(\frac{2fk_d[I]}{k_t}\right)^{1/2} \qquad 2.17$$

In this way, replacing [P•] in the eq. 2.15 it will have:

$$R_P = k_P[M]\left[P^{\bullet}\right] = k_P[M]\left(\frac{2fk_d[I]}{k_t}\right)^{1/2} \qquad 2.18$$

Therefore, according the ideal kinetic scheme described until now, the polymerization rate is proportional to monomer concentration and to the square root of the initiator concentration. This behaviour was confirmed in several polymerization systems and for different pairs initiator-monomer in a wide range of concentrations.

Moreover, this ideal kinetic scheme is used also to obtain a primary qualitative description of the behaviour of more complex systems.

2.3 Autoacceleration of the polymerization rate

In batch polymerization systems one would normally expect a diminution of the reaction rate with time since the monomer and initiator concentrations decrease. Instead, the exact opposite behaviour is observed in almost all polymerizations: the reaction rate increases with conversion (autoacceleration). Such behaviour is referred to as “gel effect” or

"Trommsdorff-Norrish effect" (in recognition of the early workers in the field) and it is observed under isothermal reaction conditions.

The typical trends of the conversion versus time are shown in Figure 2.1 for a generic radical polymerization system, at different feed monomer concentration in the solvent. Similar behaviour has been observed for a variety of monomers, including styrene, vinyl acetate, and methyl methacrylate.[2-6]

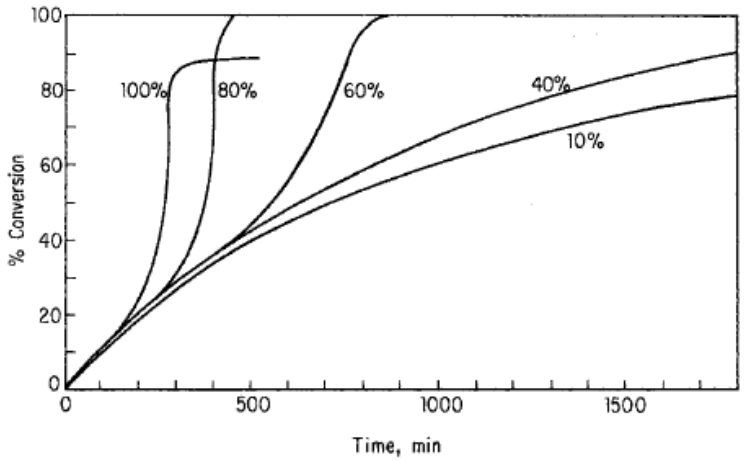

Figure 2.1 - Autoacceleration in a radical polymerization. The different curves represent different concentrations of monomer feed in solvent.

As it is possible to see in the figure, the real systems with higher monomer concentration exhibit autoacceleration.

Plotting $R_P/[M][I]^{1/2} = k_P(2fk_d/k_t)^{1/2}$ against time (or conversion) it is possible to identify three stages in some polymerizations, rather than a constant trend (see Figure 2.2). Stage I involves either a constant rate (IA) or

declining rate (IB) with time, stage II constitutes the autoaccelerated region (gel effect) and stage III involves either a constant (IIIA) or declining (IIIB) rate.

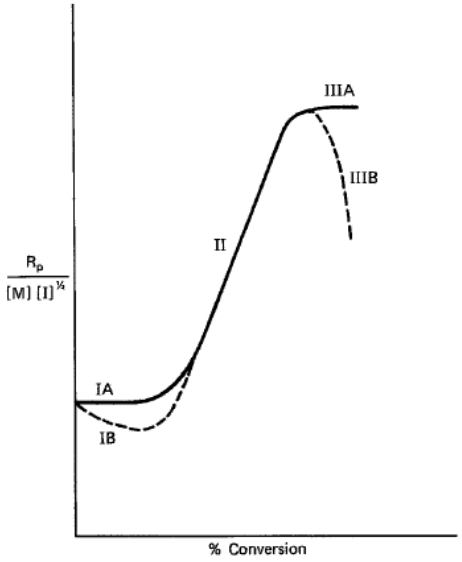

Figure 2.2 – Effect of conversion on polymerization rate in which it is evident the gel effect.

Here we'll explain the mechanisms related to the second stage, which cause the gel effect. In order to do this, it is necessary to look at the termination as a diffusion controlled reaction, described as three-step process.[7,8]

The first one consists in the translational diffusion of two growing radicals (i.e., movement of the whole radicals) until they are in close proximity to each other; the second stage is the rearrangement of two radical molecules by segmental diffusion of the chains, that is, by the movement of segments of a polymer chain relative to other segments. This rearrangement is

fundamental in order that the two radical ends are sufficiently close to react together. Finally, the last stage is the chemical reaction between the two radical ends.

In general, segmental diffusion and translational diffusion are differently influenced by the conversion, that is by the increase of polymer concentration in the medium during the polymerization. Indeed, since the size of the growing radical (coil) during the propagation in solution becomes smaller and there is an effective higher concentration gradient across this one, the segmental diffusion of the radical end out of the coil increases. Instead, at sufficiently high polymer concentrations, the polymer radicals become more entangled with each other leading to the decreasing of translational diffusion. Generally, up to a certain value of conversion the two effects are exactly counterbalanced therefore k_t remains constant (stage IA). Exist anyway some case in which the initial increase in segmental diffusion is greater than the decrease in translational diffusion, so k_t increases and the polymerization rate decreases (stage IB). After this initial trend, the chain entanglements sensibly increase, due to the more viscous medium and longer polymer chain, inducing a decrease of translational diffusion faster than the increase in segmental diffusion. Therefore k_t decreases and the ratio $(k_P/k_t)^{1/2}$ increases causing a rapid acceleration of the polymerization rate with the conversion (stage II).

2.4 Radical Copolymerization

Copolymerization is a process in which two monomers are simultaneously polymerized giving a final product named “copolymer” containing variable amounts of units of both monomers. A generic copolymerization process can be represented as follow:

$$M_1 + M_2 \longrightarrow \approx M_1M_2M_2M_1M_1M_1M_1M_2M_1M_2M_2M_2M_1 \approx$$

The two monomers enter into the copolymer in overall amounts depending on their relative concentrations feed in the system and their reactivity.
Primarily, copolymerizations were used to study the reactivity of several monomers and the effect of the chemical structure on their reactivity. Indeed, much of the knowledge of the reactivity of monomers, free radicals, carbocations, and carbanions in radical polymerization comes from copolymerization studies. Moreover, since the final properties exhibited by the copolymer are mainly influenced by its composition and the arrangement of the two monomers in the chain, studies on kinetics of copolymerization are very useful to understand how to produce a polymer product with specifically desired properties.

2.4.1 Terminal kinetic model

The final copolymer composition is usually different from the composition of the comonomer feed because different monomers can have different reactivity. Moreover, it was observed that some monomers are more reactive in copolymerization with another monomer than in their homopolymerization, while other monomers are less reactive. As consequence, the composition of a copolymer cannot be determined simply from a knowledge of the homopolymerization rates of the two monomers.[9]
To estimate the copolymer composition it can refers to the "Terminal kinetic model" which is based on three main assumptions. In particular the model assumes: irreversible propagation reactions; the chemical reactivity of the growing chain in a copolymerization is dependent only on the identity of the monomer unit at the growing end and independent of the chain composition

preceding the last monomer unit;[10-13] side reactions are neglected. According to this model, four propagation reactions are then possible in which monomers M_1 and M_2 can each add either to a propagating chain ending in M_1 or to one ending in M_2.

$$\sim M_1^{\bullet} + M_1 \xrightarrow{k_{P11}} \sim M_1^{\bullet} \qquad 2.19\text{-a}$$

$$\sim M_1^{\bullet} + M_2 \xrightarrow{k_{P12}} \sim M_2^{\bullet} \qquad 2.19\text{-b}$$

$$\sim M_2^{\bullet} + M_1 \xrightarrow{k_{P21}} \sim M_1^{\bullet} \qquad 2.19\text{-c}$$

$$\sim M_2^{\bullet} + M_2 \xrightarrow{k_{P22}} \sim M_2^{\bullet} \qquad 2.19\text{-d}$$

where k_{ii} is the rate constant of M_i homopropagation (self-propagation), k_{ij} that of the reaction between a chain ending in M_i and a monomer M_j (crosspropagation or crossover reaction). To estimate the instantaneous composition of a copolymer, obtained from a mixture of two monomers with known composition, it is necessary to consider the rates of disappearance of the two monomers (that are synonymous with their rates of entry into the copolymer) and their reactivity ratios (r_1 and r_2). In particular:

$$\frac{d[M_1]}{d[M_2]} = \frac{[M_1](r_1[M_1] + [M_2])}{[M_2]([M_1] + r_2[M_2])} \qquad 2.20$$

$$r_1 = k_{p11} / k_{P12} \qquad 2.21$$

$$r_2 = k_{P22} / k_{P21} \qquad 2.22$$

r is the ratio of the rate constant for a reactive propagating specie adding its own type of monomer to the rate constant for its addition with the other

monomer. It also indicates the tendency of two monomers to copolymerize for *r* values between zero and unity. While, a r_1 value greater than unity means that M_1• preferentially adds M_1 instead of M_2, while an r_1 value less than unity means that M_1• preferentially adds M_2. A r_1 value equal to zero would mean that M_1 is incapable of undergoing homopolymerization.

The copolymerization equation 2.20 can also be expressed in terms of mole fractions instead of concentrations. Indeed, if f_1 and f_2 are the mole fractions of monomers M_1 and M_2 in the feed, and F_1 and F_2 are the mole fractions of M_1 and M_2 in the copolymer, the copolymer equation, termed of Mayo-Lewis, will be:

$$F_1 = \frac{r_1 f_1^2 + f_1 f_2}{r_1 f_1^2 + 2 f_1 f_2 + r_2 f_2^2} \qquad 2.23$$

Different types of copolymers are obtained depending on the values of reactivity ratios of the monomers selected for the process. In fact copolymerizations can be of three types depending on whether the product of the two monomer reactivity ratios ($r_1 \cdot r_2$) is unity, less than unity, or greater than unity.

If their product is equal to one the copolymerization is termed ideal. In this case, if $r_1 = r_2 = 1$, the two monomers show equal reactivity toward both propagating species so the copolymer composition is the same as the mixture feed with a randomic placement of the two monomers along the copolymer chain. When the two monomer reactivity ratios are different, one of the monomers results more reactive than the other toward both propagating species so the copolymer will contain a larger proportion of the more reactive monomer in randomic placement. Therefore, resuming in a ideal copolymerization the final copolymer has a structure random with a

composition depending on the monomer reactivity ratios values: The copolymer is richer in M_1 when $r_1 > 1$ and is poorer in M1 when $r_1 < 1$, it has the feed composition if $r_1 = 1$

As the $r_1 \cdot r_2$ product decreases from one toward zero, there is an increasing tendency toward alternation of the two units. Perfect alternation occurs when r_1 and r_2 are both zero so the two monomers enter into the copolymer in equimolar amounts.

If both r_1 and r_2 are greater than unity (and therefore, also $r_1 \cdot r_2 > 1$) there is a tendency to form a block copolymer in which there are blocks of both monomers in the chain.

After this brief description on the type of copolymerization it is evident that the final composition and the physical-chemical properties exhibited by the copolymer are closely related to both reactivity ratios of the two monomer species under study.

2.5 Advantages of use $scCO_2$ as solvent in a radical polymerization

In this section the advantages arising from the use of supercritical CO_2 as polymerization medium will be discussed. They are mainly due to the polymerization kinetic at high pressure and to the physico-chemical properties exhibited by the species present in the system in supercritical conditions. In conventional liquid solvents the polymerization rates are often limited by the local increase of the viscosity during the process which penalizes the mass transfer rate of the monomer to the reaction site. While in supercritical CO_2, the lower viscosity of the medium and higher diffusion coefficients of the reacting species contribute to overcome this limitation so favouring the monomer conversion and also attenuating the issues of Tromsdorf effect and autoacceleration.

Another advantage consists in the possibility to modulate, by tuning temperature and pressure, the values of several properties such as density, dielectric constant, heat capacity and viscosity which can affect the performances of the polymerization process. In the follow the effect of pressure on the kinetic of radical polymerization is described. The increase of pressure generally influences the polymerization through changes in concentrations, rate constants and equilibrium constants.[14-16]

High pressure can have appreciable effects on polymerization rates and polymer molecular weights manifesting by changes in the three rate constants of initiation, propagation, and termination. At constant temperature, the quantitative effect of pressure on a rate constant is given by the following expression:

$$\frac{d \ln k}{dP} = \frac{-\Delta V^{\ddagger}}{RT} \qquad 2.24$$

where k is the reaction constant and $\Delta V^{\ddagger}$ is the volume of activation, that is, the change in volume (cm^3/mol) in going from the reactants to the transition state.[17] A negative value of $\Delta V^{\ddagger}$ leads to an increase in the reaction rate constant as consequence of an increased pressure. While positive values correspond to a decrease in the reaction rate constant with increase pressure as the volume of the transition state is larger than that of the reactants.

The variation of the polymerization rate with pressure will depend on the variation of the term $k_p(k_d/k_t)^{1/2}$ with pressure in accordance with equation 2.18. In particular:

$$\frac{d \ln(k_P (k_d / k_t)^{1/2}}{dP} = \frac{-\Delta V_R^{\ddagger}}{RT} \qquad 2.25$$

Therefore the effect of pressure on the polymerization rate will depend from $\Delta V_R^{\ddagger}$ that is the overall volume of activation for the polymerization process and it is given by:

$$\Delta V_R^{\ddagger} = \frac{\Delta V_d^{\ddagger}}{2} + \Delta V_P^{\ddagger} - \frac{\Delta V_t^{\ddagger}}{2} \qquad 2.26$$

The $\Delta V_d^{\ddagger}$ is the volume of activation for the initiation reaction. If the initiation occurs by thermal decomposition of an initiator, it is positive, since the reaction is a unimolecular decomposition involving a volume expansion for the initiator going to the transition state. Thus the initiation rate decreases as pressure increases. The volume of activation for propagation $\Delta V_P^{\ddagger}$ is negative, since the reaction involves two species coming together in going to the transition state. The volume of activation for bimolecular termination $\Delta V_t^{\ddagger}$ is positive even if it involves a decrease in volume when two radicals come together in the transition state. In fact, since the termination step is diffusion controlled, an increase of pressure increases the viscosity of the reaction medium inducing decrease of k_t.[18-20]

Anyway. the three terms are such that the value of $\Delta V_R^{\ddagger}$ results negative for most monomers thus the rate of polymerization increases with high pressures. This theoretical prevision is coherent with the experimental results of several studies. As example is reported in Figure 2.3 the effect of the pressure on polymerization rate and polymer molecular weight for the radiation-initiated polymerization of styrene.[21]

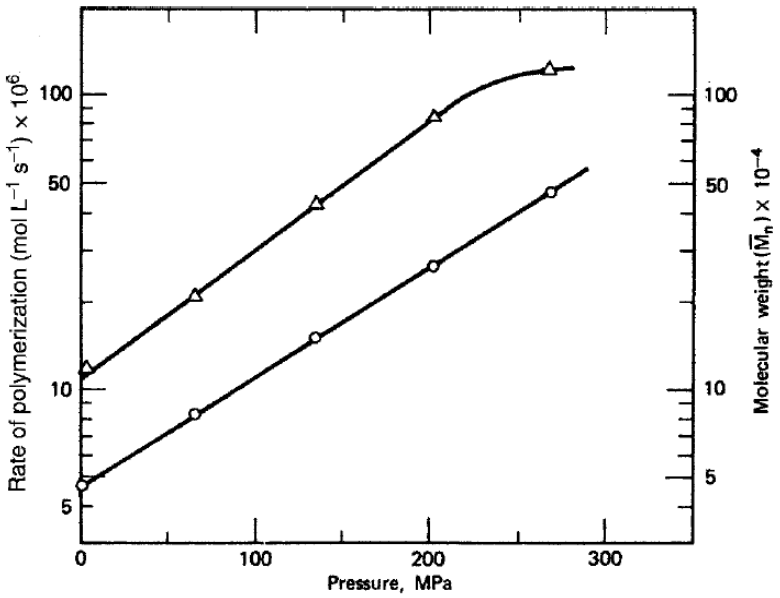

Figure 2.3 - Effect of pressure on the polymerization rate (o) and polymer molecular weight (Δ) of radiation-initiated polymerization of styrene at 25°C.

It is worth noting that the relative effect of pressure on polymerization rate is less than that of temperature from the practical viewpoint. For example, for a polymerization with $\Delta V_R^{\ddagger}$ = -25 cm^3/mol an increase in pressure from 0.1 to 400 MPa at 50°C yields about the same increase in R_p as does an increase in temperature from 50 to 105°C.

Concerning the effect of pressure on the equilibrium constant of a reaction, the variation of the equilibrium constant with pressure, at constant temperature, has the same form of the equation 2.24 for the rate constant:

$$\frac{d\ln K}{dP} = \frac{-\Delta V}{RT} \qquad 2.27$$

where ΔV is the reaction volume that is the difference in volume between products and reactants. Since ΔV is negative in a polymerization, the equilibrium constant increases with increase pressure (ΔV values are generally in the range -15 to -25 cm^3/mol). As consequence, polymerization results thermodynamically more favoured at high pressure.

Another advantage of $scCO_2$ consists in its chemical inertness to free radicals, eliminating chain transfer to solvent as a side reaction.[22]

2.6 General remarks on fluorinated polymers

A fluoropolymer or fluoroplastic is defined as a polymer consisting of carbon (C) and fluorine (F) atoms. Sometimes these are referred to as perfluoropolymers to distinguish them from partially fluorinated polymers. The latter molecules include hydrogen (H) atoms in addition to fluorine and carbon atoms. Partially fluorinated fluoropolymers are significantly different from the perfluoropolymers with respect to properties and processing characteristics. For example, perfluoropolymers are more thermally stable but physically less hard than partially fluorinated polymers.[23]

The consumption of fluoropolymers has increased over the years as technological advancement has required the properties of these plastics. These useful properties include: chemical resistance, thermal stability, cryogenic properties, low coefficient of friction, low surface energy, low dielectric constant and flame resistance. These basic properties arise from the atomic structure of fluorine, carbon, and their covalent bonding in specific chemical structures. The properties are weakened as the chemical structure becomes less "perfluorinated," as in polyvinylidene fluoride. Because tetrafluoroethylene polymer (PTFE) has a linear structure ([(–CF_2–CF_2–)$_n$]), it is a good subject for discussion of extreme properties. The

backbone is formed of carbon-carbon and carbon-fluorine bonds. Both are extremely strong bonds (C–C = 607 KJ/mole and C–F = 552 KJ/mole.).[24,25] The basic properties of PTFE originate from these two very strong chemical bonds. The size of the fluorine atom allows the formation of a uniform and continuous sheath around the carbon-carbon bonds and protects them from attack, thus imparting chemical resistance and stability to the molecule. The fluorine sheath is also responsible for the low surface energy (18 dynes/cm)[26] and low coefficient of friction (0.05–0.08, static)[27] of PTFE. Another attribute of the uniform fluorine sheath is the electrical inertness (or non-polarity) of the PTFE molecule.

In the last 40 years many fluoropolymers have been developed and made commercially available. The structures of some of these polymers are shown in Table 2.1.

Name	Abbreviation	Structure
Poly(tetrafluoroethylene)	PTFE	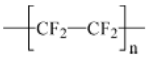
Poly(tetrafluoroethylene-*co*-hexafluoropropylene)	FEP	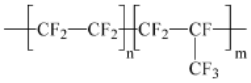
Poly(ethylene-*alt*-tetrafluoroethylene)	ETFE	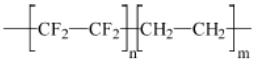
Poly(chlorotrifluoroethylene)	PCTFE	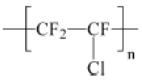
Poly(vinylidene fluoride)	PVDF	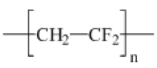
Poly(tetrafluoroethylene-*co*-perfluoropropyl vinyl ether)	PFA	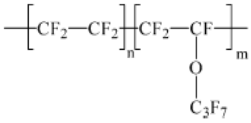
Poly(vinylidene fluoride-*co*-hexafluoropropylene)	PVDF-*co*-HFP	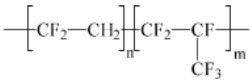
Poly(vinyl fluoride)	PVF	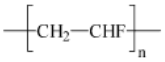

Table 2.1 - Main commercially available fluoropolymers

The applications of fluoropolymers are very wide, typically from household uses to the aerospace and electronic industries. However, the final applications for fluoropolymers always exploit one or more of the properties that select them from other plastics. The table 2.2 summarized the major applications and some uses of fluoropolymers.

For example, in the chemical processing industry these polymers are selected for their resistance to chemical attack and also for their thermal stability for

use at high temperatures. Moreover, because they do not react with process streams, they help prevent contamination of products.

In food processing, the Food and Drug Administration (FDA) has approved fluoropolymer grades as fabrication material for equipment due to their resistance to oil and cleaning materials, and their low friction properties.

Also in medical field the long-term stability of fluoropolymers as well as their low surface energy and chemical resistance are fundamental properties for surgical patches and cardiovascular grafts.

Industry/Application Area	Key Properties	Typical Uses
Chemical Processing	Chemical resistance Good mechanical properties Thermal stability Cryogenic properties	Gaskets, vessel liners, valve and pipe liners, tubing, coatings
Electrical & Communications	Low dielectric constant High volume/surface resistivity High dielectric breakdown voltage Flame resistance, thermal stability	Wire and cable insulation, connectors
Automotive & Office Equipment	Low coefficient of friction Good mechanical properties Cryogenic properties Chemical resistance	Seals and rings in automotive power steering, transmission, and air-conditioning. Copier roller and food processing equipment covering.
Houseware	Thermal stability Low surface energy Chemical Resistance	Cookware coatings
Medical	Low surface energy Stability Excellent mechanical properties Chemical resistance	Cardiovascular grafts, heart patches, and ligament replacement
Architectural Fabric	Excellent weatherability Flame resistance Low surface energy	Coated fiberglass fabric for stadium and airport roofs
Semiconductor Fabrication	Chemical resistance Purity Non-shedding Thermal stability	Process surfaces Wafer carrier basket Tubing, valves, pumps, and fittings

Table 2.2 - Typical applications and uses of fluoropolymers[23]

Fluoropolymers are typically synthesized in aqueous polymerization systems (both emulsion and suspension), non-aqueous systems (Freon-113), or in hybrid Freon- 113/aqueous hybrid systems.[28] Anyway, such processes require the use of large quantities of water, CFCs (for non-aqueous polymerizations), and fluorinated surfactants for emulsion polymerization. It is evident that the chemical process industry has to comply with regulatory issues and more stringent quality demands, which necessitates focusing on green chemistry. The term "green chemistry", is defined as the utilization of a set of principles that reduces or eliminates the use or generation of hazardous substances in the design and manufacture of chemical products.[29]

2.7 State of the art on fluoropolymers synthesis in $scCO_2$

As aforementioned the use of $scCO_2$ as reaction medium in polymer industry has already been implemented on industrial scale for some processes, while for others the scientific and technological feasibility is currently under study. Until now, major of studies related to the polymer synthesis in sc-CO_2 concerns the polymerization of fluorinated monomers because in particular way these processes exhibit better performances using a sc-CO_2–based technology exploiting all the advantageous properties of CO_2 as polymerization medium. The common fluorinated monomers used to produce fluoropolymers in $scCO_2$ are shown in Figure. 2.4

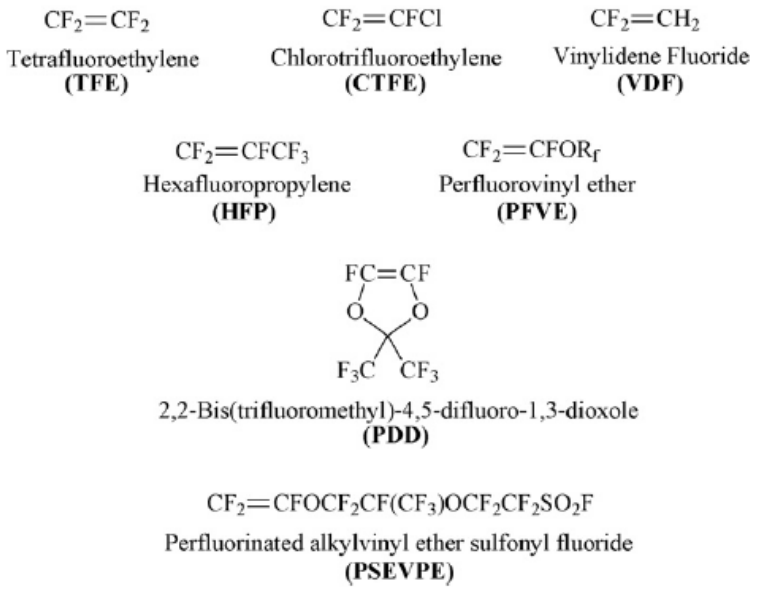

Figure 2.4 - Main fluoroolefins polymerized in supercritical carbon dioxide

Their handling is generally very difficult because many of these monomers are flammable and some are also explosive. For example, TFE is flammable when mixed with air and has a high propensity for explosion during expansion from its liquid phase under pressure to a gas. Further, at elevated temperatures TFE is a gas highly explosive. In the presence of oxygen it will undergo autopolymerization, a process sufficiently exothermic to ignite an explosion. Previously, TFE was handled as a liquid azeotropic mixture with hydrochloric acid (HCl) (33mol% TFE and 67mol% HCl) before polymerization. However, the disposal of the large amount of HCl and the toxicity potential of the acid were considerable disadvantages.

Successively, it has been demonstrated that CO_2/TFE mixtures were less susceptible to ignition as TFE forms a ‘‘pseudo’’azeotrope with CO_2.[30] This makes handling and delivering monomer much safer. According to this

result, a set of fluoropolymers based on TFE were produced in CO_2. Among these there are TFE/vinyl acetate polymers, Nafion® and Teflon® AF-type materials.

Aqueous suspension and dispersion polymerizations of copolymers of TFE with a variety of comonomers including hexafluoropropylene (HFP) and various perfluoroalkyl vinyl ethers (PAVE's) typically provide a final product exhibiting high levels of carboxylic acid end groups, while IR analysis confirmed that if they are synthesized in sc-CO_2 exhibit acid end group levels an order of magnitude below.[31,32] This result could be attribute to the plasticizing effect of CO_2 that induce a more efficient diffusion of monomer into the polymer phase, so increasing the probability of existence of a monomer molecule near to the active chain ends. In this way the bimolecular propagation step could result favoured over the β-scission process (see mechanism in Figure 2.5). Another explanation may be found in the lower operative temperatures used in CO_2 systems that may favour cross propagation over β-scission.

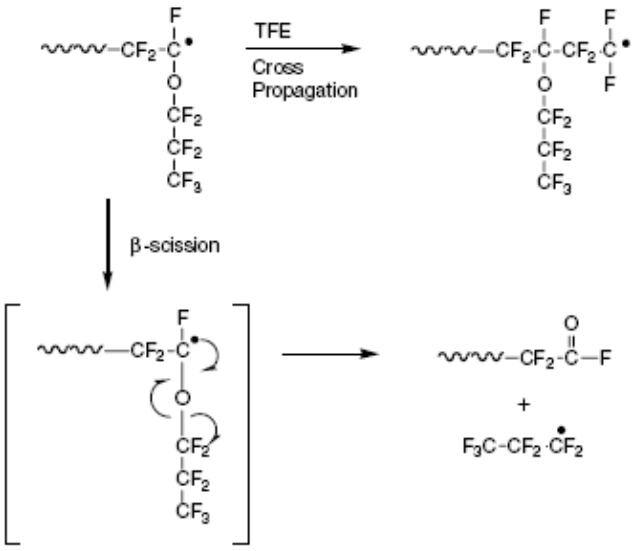

Figure 2.5 - Mechanism of β-scission competitive with cross propagation of TFE.[33]

Teflon® products were commercialized by DuPont in North Carolina and they were the first commercial example of fluoropolymer resins made using supercritical carbon dioxide as solvent, instead of 1,1,2-trichloro-1,2,2-trifluoroethane or water and surfactant,[34] which provides a product with superior properties.

A very interesting material having combined properties between those of amorphous and fluorinated materials is Teflon® AF, that is a copolymer of TFE and 2,2-bis (trifluoromethyl)-4,5-difluoro-1,3-dioxole (PDD). Among its properties there are good optical transparency and good solubility in organic solvents with high thermal stability, excellent chemical stability, and low surface energy. Additionally, these materials possess the lowest refractive index and the lowest dielectric constant of any known solid organic polymer.[35] A range of copolymers with various compositions and different molecular weights were synthesized in supercritical carbon dioxide

obtaining yields as high as 74% and their properties were compared to commercially available Teflon® AF. [36] The results obtained suggested that the low reaction temperature and the use of a perfluorinated initiator make the properties of copolymers comparable to those of the analogous commercial product (Teflon® AF 1601). Moreover, with a $scCO_2$ technology it is possible to isolate the final product directly from the reactor without contamination from solvents or surfactants.

One of the more difficult issues associated with the use of CO_2 as a polymerization medium has been the limited solubility of most high molecular weight polymers in CO_2. In fact, much of the works reported for polymerizations in CO_2 are typically heterogeneous precipitation, dispersion or emulsion processes as the ones above discussed.

It has been demonstrated that 1,1-dihydroperfluorooctyl acrylate (FOA), an amorphous fluoropolymer with high molecular weight (>250,000), can be synthesized homogeneously in CO_2 utilizing free radical initiators.[37,38] Indeed this highly fluorinated polyacrylate exhibit exceptional solubility in supercritical CO_2, allowing to use reaction conditions milder in terms of temperature and pressure rather than of conventional solvent based processes.[37]

Another class of fluoropolymers known to be readily soluble in CO_2 are perfluoropolyethers (PFPEs).[39] PFPE polymers and copolymers are high performance materials, exhibiting low surface energies and excellent thermal and chemical stabilities. PFPEs are primarily found in high performance lubricant applications such as heat exchanger fluids.

One of the main industrial processes for the production of PFPEs is photooxidation of fluoroolefins.[40] Currently, only TFE and HFP are used commercially in this process. Typically, HFP is photooxidized in bulk owing to its very low reactivity while TFE requires an inert diluent in order to

prevent homopolymerization of the olefin. DeSimone[41] and coworkers reported recently the photooxidation of various concentrations of HFP in CO_2. According to the collected data in this study, it was demonstrated that there is a strong dependence of molecular weight and composition on HFP concentration.

2.8 VDF based fluoropolymers synthesized in $scCO_2$

Poly(vinylidene fluoride) has the second largest production volume among all fluorinated thermoplastics. Much of its unique properties arise from the alternating arrangement of CH_2 and CF_2 groups in the polymer backbone. Actually, it is used in the production of several commercial thermoplastic[42-45] and elastomeric[46] fluoropolymers such as coating materials for cable insulation. More recently, porous polyvinylidene fluoride membrane has received much attention from researchers in various fields since it was found that PVDF membrane could be applied in chemical engineering, electronics, textile industry, food processing and biochemistry, due to its excellence in chemical stability, thermal stability, and toughness. For example PVDF membranes are used for protein immunoblot[47,48] due to their low affinity for amino acids.

Most of the VDF-based fluoropolymers are commercially synthesized by free radical emulsion polymerization, using perfluorooctanoic acid (PFOA) or other fluorinated surfactants, or by suspension polymerization in water.[42]

Until now several studies were performed on the synthesis of VDF-based polymers using $scCO_2$ as solvent in homogeneous[49,50] (e.g. T = 140°C and P = 150 MPa for PVDF[49]) as well as in heterogeneous conditions.[50-54] Anyway, concerning the VDF radical polymerization[51,55-59] most of the recent studies

in supercritical medium involve heterogeneous systems, because to the milder operative conditions (e.g., T<80°C and P<40MPa).

VDF has been synthesized in CO_2 in a continuous precipitation process using a continuous stirred tank reactor (CSTR)[60] to circumvent the potential economic disadvantages associated with batch reactors. Figure 2.6 shown a simplified scheme of the experimental set-up which could be widely applicable for the precipitation polymerization of various monomers in $scCO_2$ with or without surfactants. The CSTR system consisted of an intensely mixed tank and was followed by two high-pressure filters in parallel, where the polymer was collected. Carbon dioxide and monomer were pumped continuously by high pressure syringe pumps in constant flow mode and mixed by an eight-element static mixer before to enter the CSTR. The initiator solution was also pumped continuously into the reactor by a high-pressure syringe pump in constant flow mode, entering as a separate stream. All of the feed lines were equipped with check valves to prevent back flow and with rupture disks for safety in case of over pressurization. The PVDF polymers were collected as dry, free-flowing powders with molecular weights up to 150 kg/mol.

The system was also used in the precipitation homopolymerization of acrylic acid in absence of surfactant,[61] anyway it could be modified by adding parallel lines for copolymerization processes.[62]

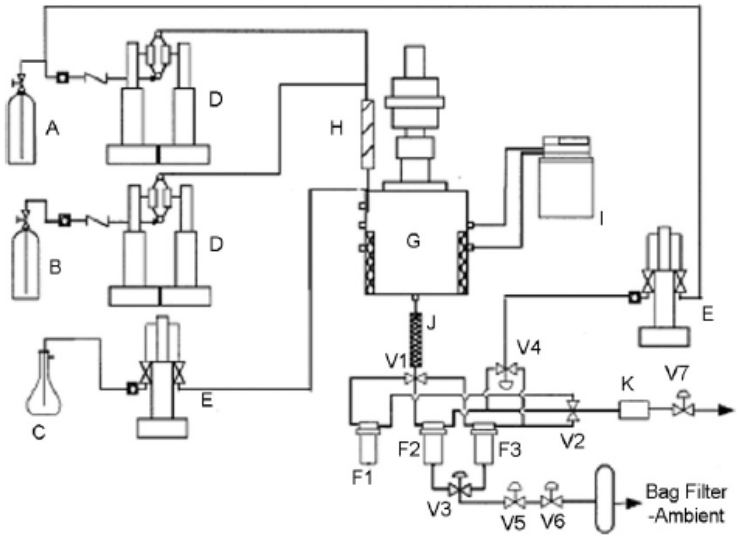

Fig. 2.6 - Continuous polymerization apparatus: (A) CO_2 cylinder; (B) monomer; (C) initiator solution; (D) continuous syringe pumps; (E) syringe pumps; (F1) steady-state filter; (F2, F3) non-steady-state filter; (G) thermostated autoclave; (H) static mixer; (I) chiller/heater unit; (J) effluent cooler; (K) gas chromatograph; (V1, V2) four-way valves; (V3, V4) three-way valves; (V5, V6) two-way valves; (V7) heated control valve (copyright).

The advantage of a continuous process over a batch process is that the monomer and the CO_2 can be removed and recycled, leading to a high rate of polymerization. Indeed, significantly higher polymerization rates of VDF in the CSTR were observed than the average rates achievable in batch polymerizations under similar conditions.

Another important class of fluoropolymers is the one of vinylidene fluoride-hexafluoropropylene (VDF-HFP) random copolymers having properties that change according to the HFP content in the copolymer. Indeed, in absence of HFP, the PVDF homopolymer is semi-cristalline (thermoplastic) while by

increasing the HFP content the copolymer becomes fully amorphous with elastomeric properties. Actually, this copolymer is used as construction material of tubing, valves and fittings[63,64,65] and it is industrially produced by several companies (e.g. DuPont, Solvay Solexis and 3M/Dynon) with a maximum HFP content of 22-23 mol%.

Copolymers with a low content of HFP (up to 5 mol%) were studied for the preparation of membranes for fuel cell applications[66,67] because PVDF can be an interesting alternative to Nafion for the fabrication of proton-conducting membranes for fuel cells. In fact, they seem to offer promising performances, combining high room temperature proton conductivity, chemical stability and good mechanical properties. But, since this fluorinated copolymer has an hydrophobic nature; in order to confer hydrophilic properties and, consequently, proton conductivity, it has to be subjected to a chemical modification. For example by grafting with styrene comonomers, which allows to link sulfonic groups.

PVDF-HFP membrane with an excellent antibacterial activity was developed by Chen Yao et al.[68] The membranes were first subjected to plasma pre-treatment followed by UV-induced surface graft copolymerization of 4-vinylpyridine (4VP) and quaternization of the grafted pyridine groups with hexylbromide. This is a possible method to prevent the microbial colonization of polymer surfaces, which are generally used for antibacterial or antifungicidal packaging, in order to extend the shelf-life of food, and as surgical sutures or wound dressings, to prevent an inflammatory response or stimulate wound healing.

Also VDF-HFP copolymers are industrially produced using aqueous emulsion or suspension processes,[64] generating large amount of waste water and requiring high energy for drying. As mentioned above, their production

has heavy environmental issues that could be overcome by replacing the conventional solvent with $scCO_2$.

Concerning the properties exhibited from the PVDF polymers synthesized in $scCO_2$, several studies of independent groups[51,56] observed that bimodal molecular weight distributions (MWDs) are obtained when monomer concentration exceeding a threshold value of about 2 mol/L. In fact after this value the curves exhibit a second mode, that is more shifted towards the high molecular weight as monomer concentration increases (Figure 2.7).

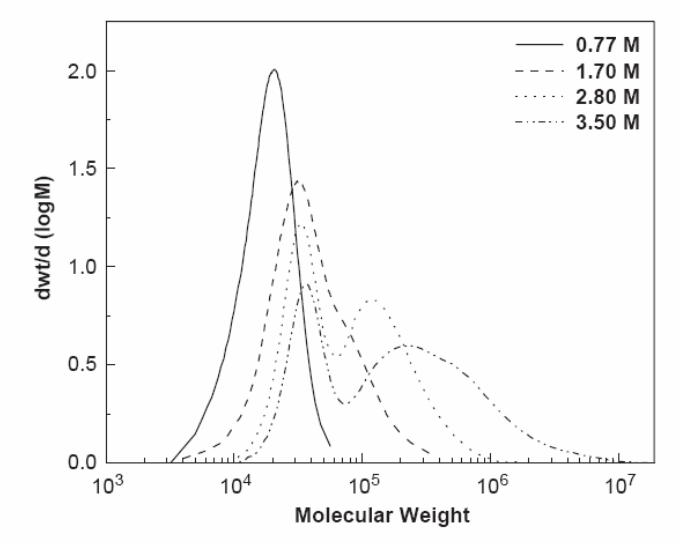

Figure 2.7 - Precipitation polymerization of VDF in scCO2 (CSTR, P=275 bar, T=75°C, I_2=3mM)[55]

Bimodality of MWD was observed also in the case of VDF-HFP copolymers.[69] Anyway, although several studies were performed on the polymerizations in $scCO_2$ by precipitation[51,53,56] as well as by dispersion,[52,57-

[59] it is still under debate a crucial aspect of the heterogeneous copolymerization kinetics of VDF-HFP in supercritical CO_2 that is: which is the contribution of each phase as reaction locus?

This question is originated from the presence of two phases in a reaction system of heterogeneous polymerization in $scCO_2$: the continuous fluid phase ($scCO_2$) and the polymer phase. Indeed, in a reaction of polymerization carrying out in heterogeneous conditions, the nucleation corresponding to particle formation step is completed within the first few minutes of reaction,[53,70] when monomer conversion is quite low. Then, the precipitated polymer particles may undergo a coagulation process leading to the formation of large, irregular-shape aggregates in the case of precipitations, or to well defined, micron sized spherical particles, if a suitable surfactant is used. The latter is the case of dispersions. The models proposed until now were mainly based on homogeneous (1-locus model) or heterogeneous (2-loci model) kinetics polymerization.

In the following will be presented the several proposed models for the PVDF case together with the more important obtained results.

Saraf et al.[51] proposed a model presuming the polymerization reaction taking place exclusively in the supercritical continuous phase. In this model it was assumed that the increase in MWD polydispersity index (PDI) was due to chain transfer to polymer which induces polymer branching. Anyway, such model was able to reproduce only PDI experimental data but not the bimodal distribution. To well describe also the latter aspect, the same group proposed a different model taking into account the decrease in mobility of the macroradicals at increasing chain length, thus making the termination rate constant chain-length-dependent.[55] Indeed, in this way the MWD resulted well reproduced. Finally, a further modification of the same one-phase model has been proposed very recently taking into account both chain

transfer to polymer and diffusion controlled termination at the same time.[71] The latter was assumed to take place when macroradical sizes exceed a critical value (n_{cr}) which can be estimated by direct fitting to the experimental data.

To resume, in all the aforementioned models (1-locus models) it was assumed that the whole polymerization process, including radical generation, growth and termination step, occurs in the continuous supercritical phase.

Differently, Mueller et al.[56] proposed a model that explains the two modes in the MWD as representative of polymer chains produced in the CO_2-rich continuous phase and in the polymer-rich dispersed phase (2-loci model). The model presumes that monomer and initiator are partitioned between the two phases at equilibrium, while radicals, generated in the continuous phase having low viscosity, can diffuse into the polymer phase before their termination, thus continuing their propagation in the latter phase. The rate of this mass transfer process depends both on the relative amount of the two phases, as well as on the polymer morphology. In fact, if the system is characterized by the presence of smaller polymer particles, that is consistent to have a major total interphase area, A_p, the contribution of the reaction in the polymer dispersed phase will be larger due to the enhanced transport rate of active chains from the continuous phase towards the polymer particles. Mueller et al.[56,57] showed that such 2-loci model is able to predict the VDF polymerization kinetics under precipitation and dispersion conditions, i.e. with different total interphase area values, as well as the occurrence of MWD bimodality by minimal parameter adjustment.

Until now, despite the very different mechanistic picture proposed, both the 1-locus and the 2-loci model are able to describe bimodal MWDs. Anyway, it is necessary understand the role of each reaction locus because the problem has a practical relevance related to achievement of an efficient

control of the quality product, which is needed to realize the scale-up in view of industrial scale production.

References

[1] G. Odian, Principles of Polymerization, Chap. 3, fourth edition, eds.,Wiley-Interscience, New York, 2004

[2] Balke, S. T, A. E. Hamielec, J. Appl. Polym. Sci., 17, 905 (1973).

[3] Cardenas, J. N, K. F. O'Driscoll, J. Polym. Sci. Polym. Chem. Ed., 14, 883 (1976); 15, 1883, 2097 (1977).

[4] Small, P. A., Adv. Polym. Sci., 18, 1 (1975).

[5] Turner, D. T., Macromolecules, 10, 221 (1977).

[6] Yamamoto, K. and M. Sugimoto, J. Macromol. Sci. Chem., A13, 1067 (1979).

[7] Mahabadi, H. K. and K. F. O'Driscoll, J. Polym. Sci. Polym. Chem. Ed., 15, 283 (1977a); Macromolecules, 10, 55 (1977b).

[8] North, A. M., Reactivity, Mechanism and Structure in Polymer Chemistry, Chap. 5, A. D. Jenkins, A. Ledwith, eds.,Wiley-Interscience, New York, 1974.

[9] G. Odian, Principles of Polymerization, Chap. 6, fourth edition, eds.,Wiley-Interscience, New York, 2004

[10] Alfrey, T., Jr., G. Goldfinger, J. Chem. Phys., 12, 115, 205, 332 (1944).

[11] Mayo, F. R., F. M. Lewis, J. Am. Chem. Soc., 66, 1594 (1944).

[12] Wall, F. T., J. Am. Chem. Soc., 66, 2050 (1944).

[13] Walling, C., Free Radicals in Solution, Chap. 4, Wiley, New York, 1957.

[14] Ogo, Y., J. Macromol. Sci. Rev. Macromol. Chem. Phys., C24, 1 (1984).

[15] Weale, K.E., Chap. 6 in Reactivity, Mechanism and Structure in Polymer Chemistry,A.D. Jenkins and A. Ledwith, eds.,Wiley-Interscience, New York, 1974.

[16] Zutty, N.L., R. D. Burkhart, Chap. 3 in Polymerization and Polycondensation Processes, N.A.J. Platzker, ed., American Chemical Society, Van Nostrand Reinhold, New York, 1962.

[17] Asano, T., W. J. Le Noble, Chem. Rev., 78, 407,1978.

[18] Nicolson, A. E., R. G. W. Norrish, Disc. Faraday Soc., 22, 104, 1956.

[19] O'Driscoll, K. F., Makromol. Chem., 178, 899, 1977.

[20] O'Driscoll, K. F., Makromol. Chem., 180, 2053, 1979.

[21] Moore, P.W., F.W. Ayscough, J.G. Clouston, J. Polym. Sci. Polym. Chem. Ed., 15, 1291, 1977.

[22] Davidson TA, DeSimone JM. In: Jessop PG, Leitner W, editors. Chemical synthesis using supercritical fluids. New York, Chichester, Brisbane, Singapore, Toronto: Wiley-VCH Weinheim; 1999. p. 297.

[23] Ebnesajjad S, Khaladkar P.R, Fluoropolymer Applications in Chemical Processing Industries, William Andrew, Inc., New York, 2005

[24] Cottrell, T. L., The Strength of Chemical Bonds, 2nd ed., Butterworths, Washington, DC, 1958

[25] Sheppard, W. A., Sharts, C. M., Organic Fluorine Chemistry, W. A. Benjamin, Inc., New York ,1969

[26] Zisman, W. A., Surface Properties of Plastics, Record of Chemical Progress, 26, (1965)

[27] Gangal, S. V., Polytetrafluoroethylene, Kirk-Othmer Encyclopedia of Chemical Technology, 4th ed., 11, 621–644, John Wiley & Sons, New York, 1994

[28] Resnick RP, Buck WH, Modern fluoropolymers, John Wiley & Sons, 1997

[29] M.F. Kemmere, T. Meyer, Supercritical Carbon Dioxide in Polymer Reaction Engineering, Wiley-VCH, Weinheim, 2005.

[30] Van Bramer DJ, Schiflett MB, Yokozeki A. United States Patent 5,345,013, 1994.

[31] Hogue CC & EN. August 30, 2004, p. 17.

[32] Romack TJ, DeSimone JM. Macromolecules 1995;28:8429.

[33] DeYoung JP, Romack TJ, DeSimone JM. In: Hougham G, Cassidy PE, Johns K, Davidson T, editors. Fluoropolymers 1: synthesis. New York: Kluwer Academic/Plenum Publishers; 1999. p. 191–205.

[34] Parkinson G., Chem Eng 1999;106:17.

[35] Resnick RP, Buck WH. In: Scheirs J, editor. Modern fluoropolymers. Chichester: John Wiley & Sons; 1997. p. 397.

[36] U. Michel, P. Resnick, B.E. Kipp, J.M. DeSimone, Macromolecules 36 (2003) 7107.

[37] DeSimone JM, Guan Z, Elsbernd C. Science 1992;257:945.

[38] DeSimone JM. US Pat. 5,739,223, 1998.

[39] McHugh MA, Krukonis V. Supercritical fluid extraction. 2nd ed. Butterworth Heinemann; 1994.

[40] Sianesi D, Marchionni G, DePasquale RJ. In: Banks RE, Smart BE, Tatlow JC, editors. New York: Plenum Press; 1994. p. 431.

[41] Bunyard WC, Romack TJ, DeSimone JM. Macromolecules 1999;32:8224.

[42] A.E. Feiring, Fluoroplastics, in: R.E. Banks, B.E. Smart, J.C. Tatlow (Eds.), Organofluorine Chemistry: Principles and Commercial Applications, Plenum Press, New York, London, 1994, p. 339.

[43] D.E. Hull, B.V. Johnson, I.P. Rodricks, J.B. Staley, THV fluoroplastic, in: J. Scheirs (Ed.),ModernFluoropolymers: High Performance Polymers forDiverse Applications, John Wiley & Sons, Chichester, NewYork, Weinheim, Brisbane, Singapore, Toronto, 1997, p. 257.

[44] D.A. Seiler, PVDF in chemical process industry, in: J. Scheirs (Ed.), Modern Fluoropolymers: High Performance Polymers for Diverse Applications, John Wiley & Sons, Chichester, NewYork,Weinheim, Brisbane, Singapore, Toronto, 1997, p. 487.

[45] C. Tournut, Thermoplastic copolymers of vinylidene fluoride, in: J. Scheirs (Ed.), Modern Fluoropolymers: High Performance Polymers for Diverse Applications, John Wiley & Sons, Chichester, New York, Weinheim, Brisbane, Singapore, Toronto, 1997, p. 577.

[46] A.L. Logothetis, in: R.E. Banks, B.E. Smart, J.C. Tatlow (Eds.), Organofluorine Chemistry: Principles and Commercial Applications, Plenum Press, New York, London, 1994, p. 373.

[47] Pluskal, M. G.; Przekop, M. B.; Kavonian, M. R.; Vecoli, C.; Hicks, D. A. Biotech. 1986, 4, 272-283.

[48] Bronstein, I.; Voyta, J. C.; Murphy, O. J.; Bresnick, L.; Kricka, L. J. Biotech. 1992, 12, 748-753.

[49] Beuermann, S.; Imran-Ul-Haq, M. J. Pol. Sci.: Part A: Pol. Chem. 2007, 45, 5626-5635.

[50] Ahmed, T. S.; DeSimone, J. M.; Roberts, G. W. Macromolecules 2006, 39, 15-18.

[51] Saraf, M. K.; Gerard, S.; Wojcinski, L. M.; Charpentier, P. A.; DeSimone, J. M.; Roberts, G. W. Macromolecules 2002, 35, 7976-7985.

[52] Tai, H. ; Wang, W. ; Howdle, S. M. Macromolecules 2005, 38, 9135-9142.

[53] Beginn, U.; Najjar, R.; Ellmann, J.; Vinokur, R.; Martin, R.; Moller, M. J. Pol. Sci.: Part A: Pol. Chem. 2006, 44, 1299-1316.

[54] Galia, A.; Caputo, G.; Spadaro, G.; Filardo, G. Ind. Eng. Chem. Res. 2002, 41, 5934-5940.

[55] Ahmed, T. S.; DeSimone, J. M.; Roberts, G. W. Chem. Eng. Sci. 2004, 59, 5139-5144.

[56] Mueller, P. A.; Storti, G.; Morbidelli, M.; Apostolo, M.; Martin, R. Macromolecules 2005, 38, 7150-7163.

[57] Mueller, P. A.; Storti, G.; Morbidelli, M.; Costa, I.; Galia, A.; Scialdone, O.; Filardo, G. Macromolecules 2006, 39, 6483-6488.

[58] Galia, A.; Giaconia, A.; Scialdone, O.; Apostolo, M.; Filardo, G. J. Pol. Sci.: Part A: Pol. Chem. 2006, 44, 2406-2418.

[59] Tai, H.; Wang W.; Howdle, S. M.; Macromolecules 2005, 38, 1542-1545.

[60] Charpentier PA, Kennedy KA, DeSimone JM, Roberts GW. Macromolecules 1999;32:5973–5.

[61] P.A. Charpentier, K.A. Kennedy, J.M. DeSimone, G.W. Roberts, Macromolecules 32 (1999) 5973.

[62] T.S. Ahmed, J.M. DeSimone, G.W. Roberts, Macromolecules 40 (2007) 9322.

[63] Ebnesajjad, S.; Khaladkar, P. R. Fluoropolymers Applications in Chemical Processing Industries - The Definitive User's Guide and Databook; William Andrew Publishing: Norwich, NY, 2005.

[64] Albert L. M. Fluoroelastomers Handbook – The Definitive User's Guide and Databook; William Andrew Publishing: Norwich, NY, 2006.

[65] Ameduri, B. Chem. Rev. 2009, 109, 6632–6686.

[66] Soresi, B.; Quartarone, E.; Mustarelli, P.; Magistris, A.; Chiodelli, G. Solid State Ionics 2004, 166, 383-389.

[67] Kim, J. R.; Choi, S. W.; Jo, S. M.; Lee, W. S.; Kim, B. C. J. Electrochem. Soc. 2005, 152, A295-A300.

[68] Chen Yao, Xinsong Li, K.G. Neoh, Zhilong Shi, E.T. Kang, Applied Surface Science 255 (2009) 3854–3858

[69] Beginn, U.; Najjar, R.; Ellmann, J.; Vinokur, R.; Martin, R.; Moller, M. J. Pol. Sci.: Part A: Pol. Chem. 2006, 44, 1299-1316.

[70] Fehrenbacher, U.; Ballauff, M. Macromolecules 2002, 35, 3653-3661.

[71] Ahmed, T. S.; DeSimone, J. M.; Roberts, G. W. Chem. Eng. Sci. 2010, 65, 651-659.

CHAPTER 3

FREE RADICAL COPOLYMERIZATION OF VDF AND HFP IN SUPERCRITICAL CARBON DIOXIDE

3.1 Introduction

In this work were carried out selected free radical heterogeneous copolymerizations of vinylidene fluoride (VDF) and hexafluoropropylene (HFP) in supercritical carbon dioxide to understand whether the process occurs in one or in two phases, and, in the latter case, to identify the contribute of each phase as reaction locus. This is an important aspect which have to be clarified in view of an industrial scale production, because the reaction locus can influence notably the final properties exhibited by the copolymer (e.g. molecular weight distribution). To achieve this goal it was used a proper experimental strategy based only on experimental evidences; initially it was studied the effect of polymer content and interphase area on the copolymer composition. Carrying out batch reactions, the former was changed increasing the polymerization time, while the latter was manipulated comparing precipitation and dispersion reactions. Moreover it was investigated also the effect of polymer content and interphase area on the copolymer molecular weight distribution. In this way it could be possible to emphasize the effect of the interfacial area (A_p) on the properties exhibited by copolymer (e.g. on the composition and the MWD), to discriminate between the two mechanistic views. Indeed, by manipulating A_p no effect is expected on the final properties according to the 1-locus models because

according to the homogeneous mechanism the particle phase is not involved in the polymerization process. Instead, from the view point of the 2-loci model, increasing the A_p, the interphase radical transport from the continuous to the polymer phase is enhanced so inducing to an increment of the relative amount of polymer produced in the dispersed phase.[1,2]

3.2 Materials

Vinylidene fluoride and hexafluoropropylene monomers were supplied by Solvay Solexis and CO_2 by Air Liquide (99.998% pure) were used as received. The diethylperoxidicarbonate (DEPDC) initiator was synthesized according to a procedure described in the literature,[1] using water as solvent and extracting the initiator into Freon 113 (HPLC grade). The concentration of active peroxide in the solution was determined by iodine titration technique, ASTM method E 298-91. All chemicals used in the synthesis of the DEPDC solution were used as received by Aldrich. All manipulations of the initiator solution were performed at 0 °C and the final product was stored under dark at -22 °C. The ammonium carboxylate perfluoropolyether salts FLK 7850A (ca. 500 g/mol), FLK 7004A (ca. 1000 g/mol) and Fomblin DA (ca. 3000 g/mol), all supplied by Solvay Solexis, were used as steric stabilizers because it is known they are very effective in stabilizing PVDF dispersions.[3,4] Their structures and the conventional code are reported in Table 3.1. The stabilizers had an initial water content ranging from 1 to 2% (w/w) and were used after drying in vacuum at 50°C overnight.

Stabilizer	Code	M_w [g mol^{-1}]
$[Cl–(CF_2CF(CF_3)O)_nCF_2COO^–]NH4^+$	FLK 7850A	500
	FLK 7004A	1000
$[CF_3(CF_2CF(CF_3)O)_m$-$(CF(CF_3)O)_n(CF_2O)pCOO^-]NH_4^+$	Fomblin DA	3000

Table 3.1 - Ammonium Carboxylate Perfluoropolyether Stabilizers used in this work

3.3 Polymerization Apparatus and Reaction Procedure

Polymerization experiments were carried out in an AISI 316 batch reactor, schematized in Figure 3.1, having a volume of about 27 mL. The reactor was equipped with high pressure valve (PARKER), pressure transducer (Barksdale UPA3, estimated accuracy by calibration with a high-precision manometer of ± 0.05 MPa) and Pt 100 temperature sensor (estimated accuracy of ± 0.3 K).

In the surfactant assisted copolymerizations, the first component introduced in the reactor was the dried surfactant. Then the vessel was purged by a controlled flow rate of low pressure gaseous CO_2 maintained for at least 15 min to remove air. The reactor was sealed and the desired amount of monomers was added at room temperature (Figure 3.2). HFP was introduced first by heating its vessel using an electrical heating tape, while the liquid VDF was added by a 250D ISCO syringe pump. Both monomers were charged by weighting the vessel using an electronic balance (Sartorius, max 8 kg, precision 0.01g) to reach the nominal concentration of the copolymerization mixture.

The reactor was connected to monomer vessels by means of high pressure tubes (1/8 in OD) that were purged by flowing the corresponding monomer to remove air.

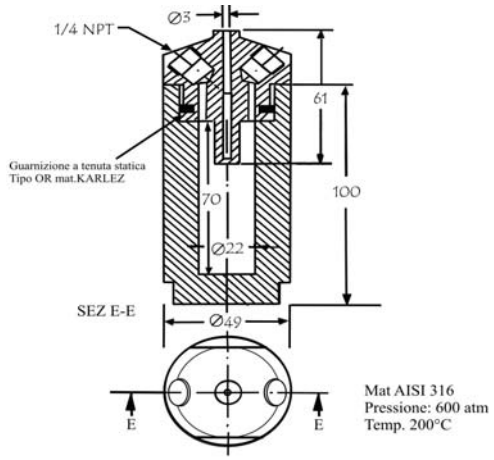

Figure 3.1 - Schematic representation of the batch reactor

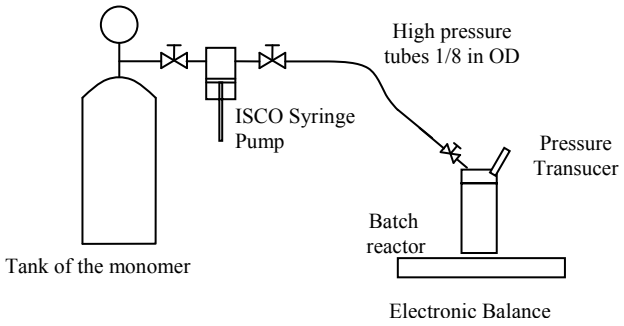

Figure 3.2 - Experimental set-up to charge of both monomers. The ISCO Syringe pump was used only for VDF monomer

After loading the monomers, the reaction vessel was put in a bath of water, connected to an automated temperature-control system, and heated at the reaction temperature (T = 50°C) under a continuous stirring by a magnetic bar (Figure 3.3).

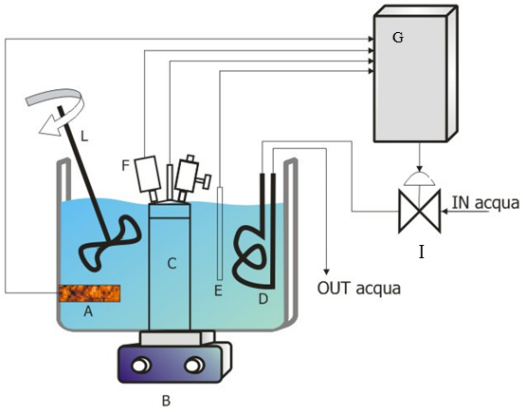

Figure 3.3 - Schematic diagram of the grafting apparatus: Heating electric resistance (A), magnetic stirrer (B), reactor (C), cooling coil (D), Pt100 temperature sensor (E), pressure transducer (F), control system (G), electro-valve (I), mechanical stirrer of the thermostatic bath (L).

When the reactor reached the set-point temperature, the initiator solution was loaded in a sample loop of suitable volume and delivered inside the reactor by a stream of liquid CO_2 pumped by an air driven Maximator pump up to the desired value of total pressure. The apparatus used to pump CO_2 and DEPDC into the reactor is represented in Figure 3.4. The loading time of initiator and CO_2 was about 2-4 minutes, after which the reaction time was set to zero. At the end of the desired reaction time, the reactor was quenched

by immersion in ice and water bath and slowly depressurized until to a total venting of the solvent (CO_2) and unreacted monomers.

Finally, the amount of copolymer formed was obtained by subtracting from the weight of the reactor measured after venting, the weight of the empty reactor and of the (non volatile) surfactant loaded. Before characterization, the copolymer obtained in the presence of surfactants was subjected to an extraction procedure with a controlled flow of $scCO_2$ at 40°C and 20 MPa for 2 hours (ISCO SFX 2-10 extractor) to remove the surfactant. This procedure proved to be effective for a quantitative recovery of the adopted stabilizers[5] and, moreover, it was showed that this process ($scCO_2$ extraction) does not affect the polymer MWD[6] by comparing GPC elution curves of extracted and untreated samples.

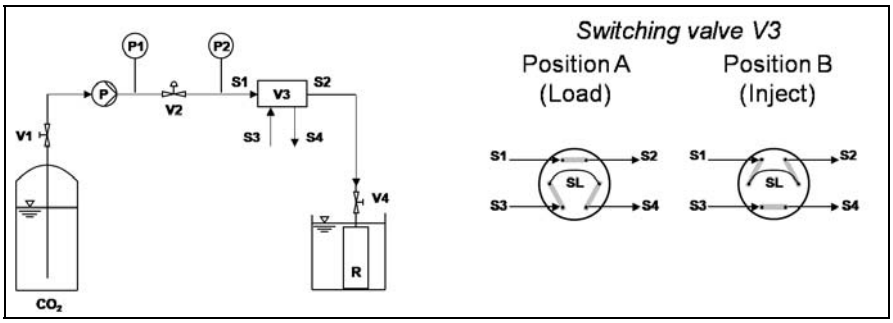

Figure 3.4. - Left: Sketch of the experimental apparatus used to feed CO_2 and DEPDC into the batch reactor. V1, V4: valves; V2: reducing pressure regulator; V3: switching valve; P: air driven pump; P1, P2 manometers; R: reactor; S1, S2: CO_2 stream line; S3, S4: stream line of DEPDC solution; SL: sampling loop. Right: Schematic representation of the switching valve (V3): with V4 closed and V3 in position A, the CO_2 feed line is pressurized and the DEPDC solution is fed into the SL. Then V3 is switched to B, V4 is opened and the CO_2 pumped into R through SL. When the desired pressure is reached, V4 is closed.

3.4 Polymer Characterization

Monomer conversion, X_w, was determined gravimetrically as the ratio between the mass of copolymer formed at the end of the polymerization experiments and the total mass of monomers feed into the reactor. The polymer volume fraction at the end of the reaction, ϕ_P, was estimated as:

$$\phi_P = \frac{X_w M_0}{\rho_p V_R} \qquad 3.1$$

where M_0 is the total mass of monomers feed into the reactor, V_R the reactor volume and ρ_P is the density of the polymer. In Eq. 3.1 we used a constant value for copolymer density of ρ_P = 1.75 g/mL.[7] By this choice, swelling of the polymer phase and influence of temperature and pressure are neglected. For these reasons the values of ϕ_P have to be considered as reasonable estimations.

The particle morphology was analyzed by a Philips scanning electron microscope (SEM). The samples were putted on the sample stubs by means of double-sided adhesive tapes and then were sputter-coated with gold to a thickness of about 200 Å.

The complete MWD was measured at 45°C with a GPC instrument equipped with 2 x PL-Gel Mix-B LS columns, RI and viscosity detectors. These measurements were performed by preparing solutions of polymer samples at about 1.5 g/L in DMF (HPLC grade) modified with 1 g/L LiBr. Columns were calibrated using PMMA standards (Mp = 2,680 to 3,900,000 g/mol; Polymer Labs. Ltd, UK). On-line measurements of both RI and relative viscosity allowed the evaluation of the molecular weight distributions (MWDs) by the universal calibration approach.

^{19}F-NMR spectra were measured in deuterated DMSO (ARMAR Chemicals) at 80°C at 188 MHz with a Bruker instrument. Chemical shifts were related to the $CFCl_3$ signal at 0 ppm. A typical ^{19}F NMR spectrum for poly(VDF-co-HFP) is depicted in Figure 3.5. The detailed chemical shifts, available in the literature,[8,9] are: group of signals assigned to VDF repeat units are located at -91.4 to -96.2 ppm for head-to-tail normal additions (-$CH_2C\mathbf{F}_2$-CH_2CF_2-), at -108.6 to -112.3 ppm for CF_2 groups adjacent to a HFP unit (-$CH_2C\mathbf{F}_2CF_2CF(CF_3)$-), and at -113.6 and -115.9 ppm for the head-to-head reversed addition (-$CH_2C\mathbf{F}_2$-CF_2CH_2-). Group of signals assigned to HFP units are centered at -70.3 and -75 ppm for the side CF_3 group (-$CF_2CF(C\mathbf{F}_3)$-), at -115.3 and -117 to -119.2 ppm for the perfluoromethylene group in the HFP unit (-$C\mathbf{F}_2CF(CF_3)$-), and at -181.4 and -184.1 ppm for the CF group (-$CF_2C\mathbf{F}(CF_3)$-). Moreover, according to Beginn et al.,[10] the average HFP mole fraction incorporated in the copolymer, $\underline{F}_{HFP}$ is calculated by either one of the following equations:

$$\underline{F}_{HFP} = \frac{2C}{B} \qquad 3.2$$

$$\underline{F}_{HFP} = \frac{2A}{3B} \qquad 3.3$$

where A denotes the sum of the areas of NMR signals in the range from -70 to -76 ppm (CF_3 group), B from -91.4 to -119.2 ppm (CF_2 group) and C from -181.4 to -184.1 ppm (CF group). Differences between values obtained by the two equations were within 1% and the average values were considered.
Both the GPC and 19F-NMR analysis were performed by the research group of Prof. Morbidelli in ETH, Zurich.

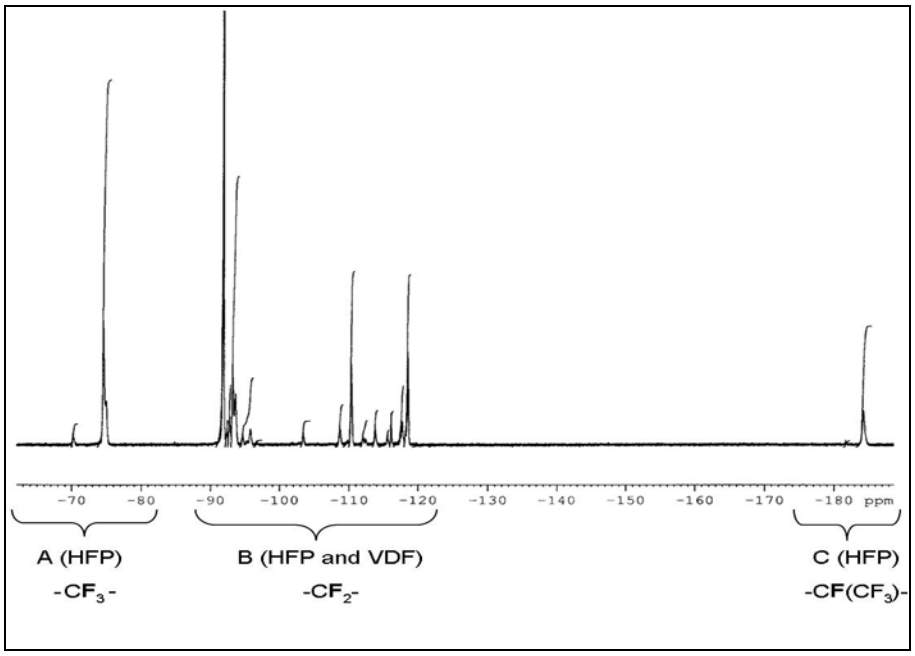

Figure 3.5 - ^{19}F-NMR spectrum of a P[VDF-co-HFP] sample polymerized at T = 50°C in $scCO_2$. Data in the regions A, B and C, indicated in the figure together with the corresponding repeating units, were used to estimate the average copolymer composition $\underline{F}_{HFP}$.

3.5 Effect of monomer feed composition on interphase area of the copolymer

As first aim of this study, it was necessary to define experimental conditions in which either dispersion or precipitation polymerization takes place in order to study the effect of A_p on the copolymer composition and MWD. In particular, for case of dispersion, the experimental conditions had to ensure the efficacy of the surfactant in stabilizing copolymers thus inducing higher values of the interphase area compared to those of the copolymer obtained by precipitation. For the VDF homopolymerization it was shown in a

previous study[4] that in order to obtain a stable dispersion when perfluoropolyether surfactants are used at T = 50°C, relatively high pressure (P > 35 MPa) and monomer concentration ($[VDF]_0 \cong 5.5$ mol/L) are necessary. This finding can be explained by the cumulative effect of increased solvency of the supercritical medium with density together with the cosolvent effect of the fluorinated monomer, which favour a more extended conformation of the stabilizer perfluoropolyether tails, thus imparting more efficient steric stabilization.

Accordingly, suitable reactions of copolymerization were carried out increasing HFP comonomer initial mole fraction, $f_{HFP,0}$, using experimental conditions similar to those aforementioned for PVDF dispersions. In particular were performed experiments with $f_{HFP,0}$ up to about 0.4 and their details are indicated in Table 3.2, which groups experimental runs as a function of the initial feed HFP content ($f_{HFP,0}$) and shows the adopted experimental conditions and some results from the characterization methods such as final conversion (X_w), mole fraction of HFP in the final product (F_{HFP}), the corresponding number average molecular weight (MW_n) and polydispersity (PDI).

Because of the low reactivity of HFP,[11] both the reaction rate and weight average molecular weights decreased when its initial feed concentration was increased. In fact it is possible to note this effect looking at runs 6, 8, 12, and 13 in Table 3.2 representing dispersion reactions at equal reaction time but with a major content of HFP feed. Moreover, relatively large values of the polydispersity index (PDI=MWw/MWn) were found in most cases, although the termination is believed to occur predominantly by radical coupling.[12] Instead, there were no significant differences in the reaction rate between the precipitation and dispersion processes.

Run	Surfactant [g/L]	f_{HFP_0} [mol %]	Reaction time [min]	Xw [wt%]	F_{HFP} [mol%]	MW_n [kg/mol]	PDI	ϕ_p, %
1	0	21.5	60	8.7	6.7	74	2.7	2.3
2	0	20.0	180	23.9	7.1	98	2.9	5.8
3	0	20.6	360	41.5	7.9	104	3.1	10.9
4	0	28.6	30	4.3	9.4	67	1.7	1.3
5	0	30.0	120	14.4	10.7	73	2.1	4.1
6	17.8	15.2	180	30.8	4.9	131	3.0	7.5
7	17.7	20.5	60	6.2	6.3	85	2.0	1.5
8	17.7	22.6	180	18.2	7.1	152	2.3	4.8
9	18.4	21.4	360	35.5	7.1	160	2.5	9.4
10	18.0	30.0	30	4.5	10.2	67	1.5	1.3
11	17.9	28.2	120	15.6	9.2	94	2.3	4.6
12	18.3	30.0	180	21.6	9.9	97	2.2	6.1
13	17.6	43.3	180	12.3	15.7	83	1.8	4.4

Table 3.2 - Main Characterization Results for the Copolymerization of VDF and HFP in $scCO_2$. Operating conditions: T = 50°C, P_0 = 38.5 MPa, [DEPDC] = 5.8 mM, monomer feed concentration [VDF]+[HDP] = 5.5 M

From SEM images, showed in figure 3.6 and 3.7, it is possible to observe the morphologies exhibited by the copolymers obtained with $f_{HFP,0} \cong 0.2$ (Table 3.2, runs 3 and 9 and Figure 3.6) and $f_{HFP,0} \cong 0.3$ (Table 3.2, runs 5 and 11 and Figure 3.7), by dispersions and as well as by precipitations. In both cases occurred the formation of microparticles but the dispersions provided more segregated and well defined particles compared to precipitations, which exhibited particles coalesced and irregularly shaped.

From image analyses we could estimate that the average size of the aggregates in the case of precipitations was about 2-3 times larger than in the corresponding dispersions. This, for the same total polymer volume, implies about 10-30 time less particles and A_p values smaller by a factor 2-3.

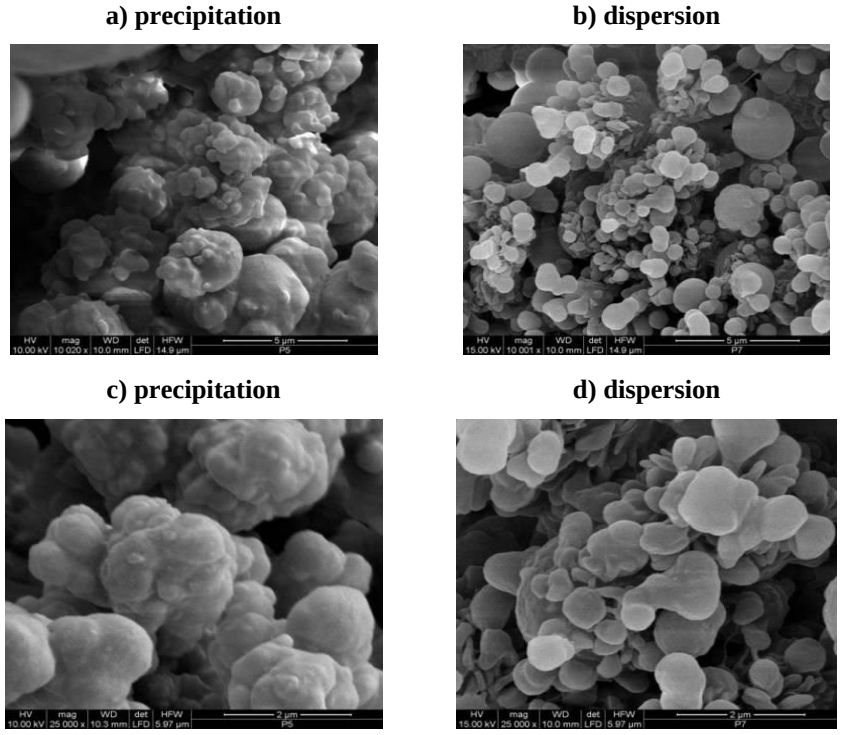

Figure 3.6. - Effect of the surfactant concentration on the copolymer morphology for reactions with initial monomer composition $f_{HFP,0} \cong 0.2$: a,c) precipitation (Table 3.2, run 3); b,d) dispersion (Table 3.2, run 9).

a) precipitation **b) dispersion**

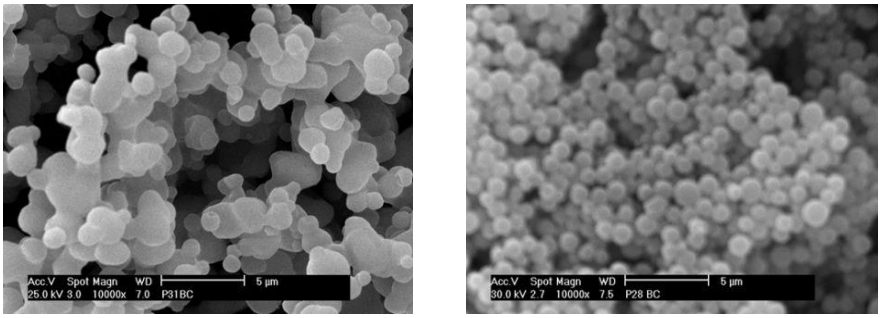

Figure 3.7 - Effect of the surfactant concentration on the copolymer morphology for reactions with initial monomer composition $f_{HFP,0} \cong 0.3$: a) precipitation (Table 3.2, run 5); b) dispersion (Table 3.2, run 11).

It is important to evidence here that, at the operating conditions under examination, the system is below the copolymer cloud point. In fact, independent groups showed that the copolymer is essentially insoluble in supercritical medium (also up to $f_{HFP,0} \cong 0.30$) and precipitates just after the first few minutes of reaction.[13,10] Therefore, the experiments were carried out in heterogeneous conditions.

When $f_{HFP,0}$ reached the value of 0.43 (Table 3.2, run 13) the polymer particles were completely coalesced (Figure 3.8-a) also in presence of surfactant. This strong change in the morphology can be probably due to the enhanced solubility of CO_2, since there are more amorphous domains[6] increasing the HFP content. That means that a major plasticization effect of CO_2 softens the polymer phase which becomes more similar to an expanded, liquid-like polymer rather than to a solid matrix. An experimental evidence of this behaviour it was observed by contacting with $scCO_2$ a commercial copolymer ($\underline{F}_{HFP}$ = 0.22, X_{cr} = 0); the figure 3.8-b shows that the sample exhibited a liquid-like behaviour already at mild temperature and pressure

conditions, in contrast to the case of the VDF homopolymer, which remains solid and rigid.[14]

Resuming, the copolymer was composed by microparticles for feed composition up to $f_{HFP,0} \cong 0.3$, in both precipitation and dispersion techniques, but the dispersions were characterized by a higher interphase area, while for upper composition ($f_{HFP,0} = 0.43$) it consists of coalesce polymer particles also in presence of the surfactant.

a) b)

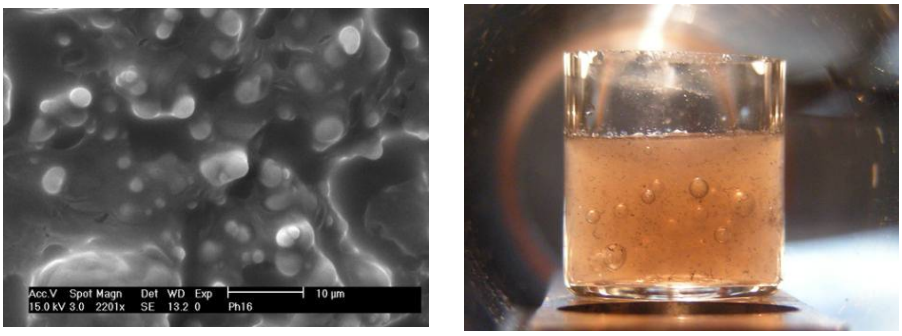

Figure 3.8 - a) SEM image of a sample produced by dispersion polymerization with initial monomer composition $f_{HFP,0} = 0.43$ (Table 3.2, run 13). b) Picture of a commercial copolymer (Tecnoflon N 935 from Solvay-Solexis, $\underline{F}_{HFP} = 0.22$, $MW_n =$ 110 kg/mol) contacted with CO_2 at $T = 50$ °C and $P < 140$ bar.

3.6 Copolymer composition

The "instantaneous" composition of the copolymer, F_{HFP}, is directly related to the monomers composition in the feed mixture through the Mayo-Lewis equation (Eq. 2.20), which is in follow represented for case of VDF and HFP copolymerization:[15]

$$F_{HFP} = \frac{r_{HFP} f_{HFP}^2 + f_{VDF} f_{HFP}}{r_{HFP} f_{HFP}^2 + 2 f_{VDF} f_{HFP} + r_{VDF} f_{VDF}^2} \qquad 3.4$$

where r_{VDF} and r_{HFP} are the reactivity ratios of the two monomers (defined by Eqs. 2.21, 2.22) under study:

$$r_{VDF} = \frac{k_{pVDF-VDF}}{k_{pVDF-HFP}}; \qquad r_{HFP} = \frac{k_{pHFP-HFP}}{k_{pHFP-VDF}} \qquad 3.5$$

Since the reaction can occur in both phases, differences in copolymer composition could in principle be observed when moving from precipitation to dispersion regimes if the two phases are characterized by different reactivity ratios or monomer compositions. Therefore, in principle copolymer composition could be used to detect the main reaction locus.[16]

For the copolymerization reaction of VDF and HFP, the reactivity ratios reported in the literature for aqueous emulsion/suspension or acetonitrile solution polymerization are in the range r_{VDF} = 2.5-6.7 and $r_{HFP} \approx$ 0-0.1,[11] which are very similar to those reported for reactions in $scCO_2$, i.e. r_{VDF} = 3.6-5.1 and $r_{HFP} \approx$ 0-0.1.[13,17,10,18] It is thus reasonable to expect reactivity ratios similar in the two phases.

Indeed, as it is possible to see in Figure 3.9, which reports the average $\underline{F}_{HFP}$ measured by ^{19}F NMR for precipitation (empty symbols) and dispersion

(filled symbols) reactions as a function of conversion with initial HFP mole fractions $f_{HFP,0}$ of about 0.2, the composition drift with conversion was limited to values lower than few percents, and no significant change in $\underline{F}_{HFP}$ was observed when the main reaction locus was changed from the homogeneous to the dispersed phase by increasing polymer hold-up and A_p. Therefore, polymer chains have similar instantaneous composition in both reaction phases under the selected operative conditions, so the monomer composition is not significantly different in the continuous and in the dispersed phase, and the copolymer composition cannot be used to clearly identify the main reaction locus.

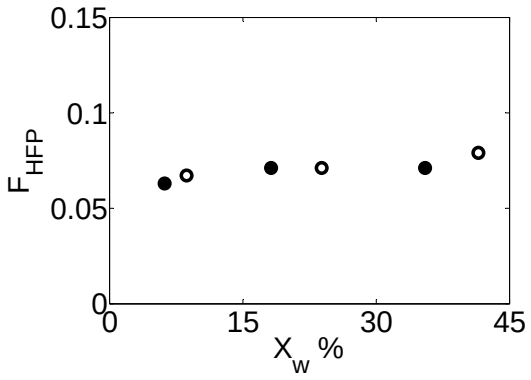

Figure 3.9. - Drift of average copolymer composition as a function of conversion for precipitation (○) and dispersion (●) copolymerization of VDF and HFP in $scCO_2$ at $f_{HFP,0} \cong 0.2$ (Table 3.2, runs 1-3 and 7-9, respectively).

3.7 Effect of interphase area on MWD of the homopolymer PVDF

In a previous research activity carried out by Filardo's group on the homopolymerization of VDF in supercritical CO_2, were compared the particle morphology and its relation with the MWD of selected homopolymers produced by precipitation and dispersion. The main results of this study are shown in Table 3.3.

Run	**Surfactant [g/L]**	**Reaction time [min]**	***Xw* [wt%]**	***MW*$_n$ [kg/mol]**	**PDI**	**ϕ_p, %**
1	0	30-180	results non reproducible; polymer not soluble			
2	3.6	180	43.8	77	35.5	8.8
3	17.6	69	41.2	102	3.2	7.7
4	18.4	180	60.8	137	3.6	12.2

Table 3.3 - Main Characterization Results for the homopolymerization of VDF in $scCO_2$. Operating conditions: T = 50°C, P_0 = 38.5 MPa, [DEPDC] = 5.8 mM, monomer feed concentration [VDF] = 5.5 M

In particular, a surfactant-free VDF homopolymerization (precipitation) at monomer concentration of 5.5 M (Table 3.3, run 1) produced a dry product extremely hard and not fully soluble in the GPC solvent, thus it was impossible to analyse its MWD. (Similar results were reported by Saraf et al.[12] for a continuous stirred tank reactor (CSTR) at about 6 M inlet monomer concentration for which the reactor entered an "inoperability region" and after the reactor was shut down it was found filled with a hard-insoluble material). Moreover, the polymer exhibited an irregular structure

(Figure 3.10-a) and a non-reproducible kinetic behaviour (Figure 3.11). Indeed, in repeated polymerization runs, conversion values ranging from 24 to 57% were measured at 1 h reaction time and from 44 to 68% at 3 h reaction time, indicating a loss of reaction control.

When the reaction was performed with a concentration of 3.6 g/L of surfactant (Table 3.3, run 2), corresponding to 1% w/w with respect to VDF, only partial stabilization of the polymer particles was achieved. Indeed, the polymer morphology was characterized by the presence of domains containing microspherical particles (Figure 3.10-b) as well as domains with a morphology similar to that of the precipitation (Figure 3.6-a). In this case the polymer was soluble in GPC solvent and it was possible to perform the GPC analysis. From the latter a marked bimodality was measured, typical of VDF polymerizations by precipitation having monomer concentration higher than ca. 2-3 M.[1,12]

The reactions performed at a major content of surfactant (Table 3.3, runs 3 and 4) led to a highly soluble polymer characterized by an much larger interphase area, in fact it contained exclusively well defined microspherical particles (Figure 3.10-c). Moreover, the conversion values obtained were higher than that of the dispersion at lower interphase area (cf. Table 3.3, runs 3 and 4), while the MWD was still broad but monomodal.

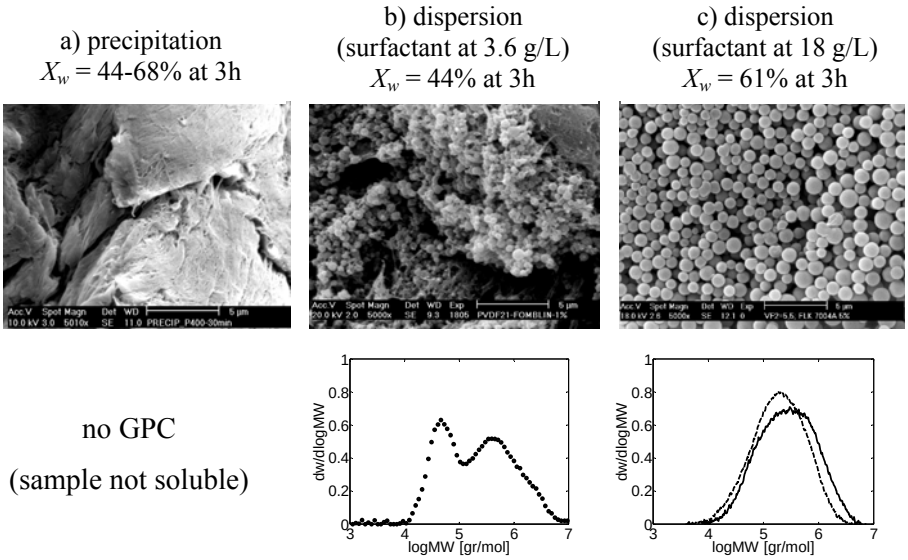

Figure 3.10 - Effect of the surfactant concentration on the morphology and MWD of PVDF produced in $scCO_2$: a) without surfactant (Table 3.3, run 1, SEM refers to 30 minute reaction); b) surfactant at 3.6 g/L, (Table 3.3, run 2); c) surfactant at 18 g/L (Table 3.3, run 3, dashed line in the MWD; Table 3.3, run 4, SEM image and continuous line).

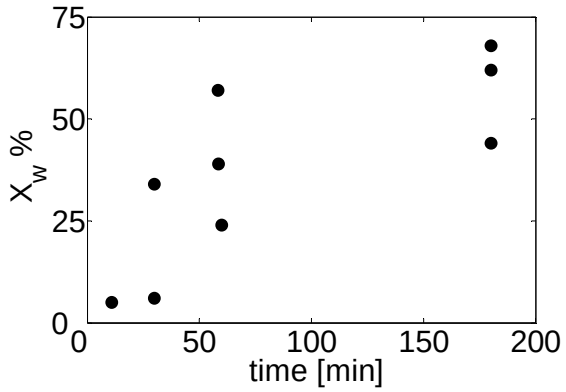

Figure 3.11 - Conversion as a function of time for repeated precipitation polymerization runs of VDF (●, Table 3.3, run 1).

The results shown until now are compatible only with a model that considers the existence of two reaction loci. Indeed, when the surfactant is totally effective (Figure 3.10-c) the very high interphase area enhances the radicals interphase transport,[1] so the most of the growing radicals, poorly soluble in the continuous phase,[19] enter the polymer dispersed phase which therefore constitutes the main reaction locus. Accordingly, the resulting MWD exhibits a single mode in the high MW region, representative of chains produced in the dispersed phase. While at smaller A_p values (Figure 3.10-b), the flow of radicals from the continuous to the dispersed phase is lower and it is more probable that a portion of the radicals generated in the continuous phase terminate in the same phase before precipitating. In this case both phases are operative as reaction loci, each giving rise to its characteristic MWD mode, and the resulting overall MWD is bimodal.

3.8 Effect of interphase area on MWD of the copolymer

Concerning the effect of the interfacial area on the MWD of the copolymers the results plotted in figure 3.12 indicate the same behaviour of the precipitation and dispersion (Table 3.2, runs 3 and 9) observed in the homopolymer case. In particular, bimodal and monomodal MWDs were measured for precipitation and dispersion polymerization, respectively. Figure 3.13 shows the MWDs measured for a precipitation and a dispersion (runs 5 and 11 of Table 3.2) reaction at $f_{HFP,0} \cong 0.3$. The MWD has a tail in the range of the high molecular weights in both cases, but with a portion of macromolecules in the high MW region increased for the dispersion case. It is important remark that in the two sets of experiments investigated until now the polymer morphology is the only relevant difference that could affect

the MWD. Such behaviour is consistent with a 2-loci model and not with an homogeneous model.

Note that inoperability was not observed in the case of copolymerization reactions, in agreement with previous literature results.[10,17]

When $f_{HFP,0}$ reached the value of 0.43 (Table 3.2, run 13) it was no possible to find a relation between the interfacial area and the copolymer molecular weight distribution, because the polymer particles were completely coalesced, as explained in section 3.4. Resuming, in that systems for which it is possible to obtain an enough interfacial area by adding a suitable surfactant, it was observed an increase of the amount of polymer chains produced at higher molecular weight and that is consistent with a two-loci model for which A_p affects the reaction progress.

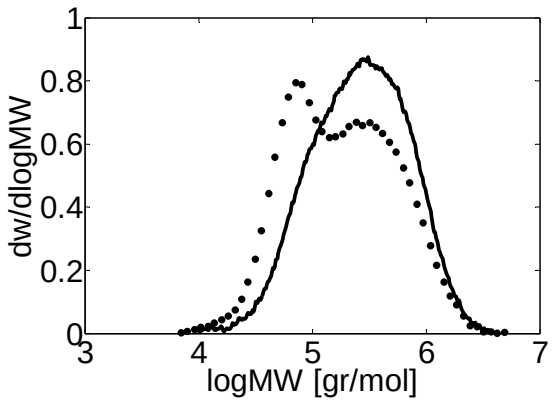

Figure 3.12. - Effect of the interphase area, A_p, on the measured molecular weight distribution for samples produced at initial monomer composition $f_{HFP,0} \cong 0.2$ under precipitation (●, Table 3.2, run 3), and dispersion conditions (continuous line, Table 3.2, run 9).

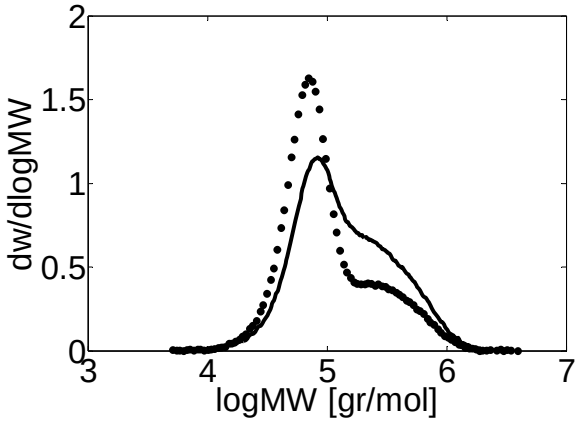

Figure 3.13 - Effect of the interphase area, A_p, on the measured molecular weight distribution for samples produced at initial monomer composition $f_{HFP,0} \cong 0.3$ under precipitation (●, Table 3.2, run 5), and dispersion conditions (continuous line, Table 3.2, run 11).

3.9 Effect of copolymer hold-up on molecular weight distribution

In order to better understand the effect of the interphase area, A_p, on the system behaviour, the MWDs normalized to the copolymer conversion (that is, with area proportional to the total mass of produced copolymer) are represented at increasing reaction time and therefore at increasing polymer hold-up, ϕ_p, for precipitation (Figure 3.14) and dispersion (Figure 3.15) polymerizations, respectively.

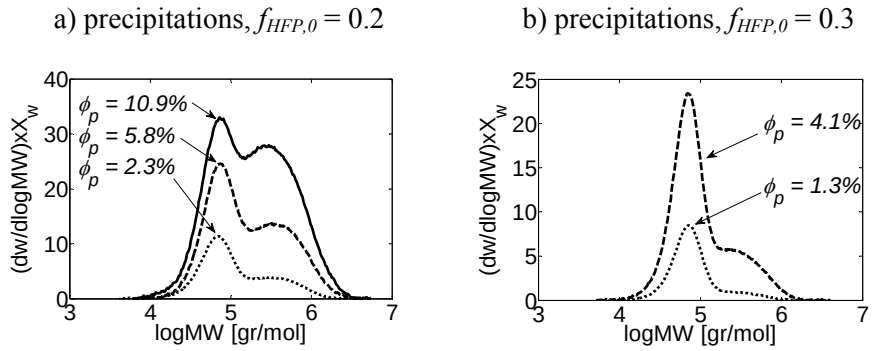

Figure 3.14 - Effect of reaction time and polymer hold-up, ϕ_p, on molecular weight distributions for samples produced under precipitation conditions. a) Initial monomer composition $f_{HFP,0} \cong 0.2$ (Table 3.2, runs 1-3); b) initial monomer composition $f_{HFP,0} \cong 0.3$ (Table 3.2, runs 4-5).

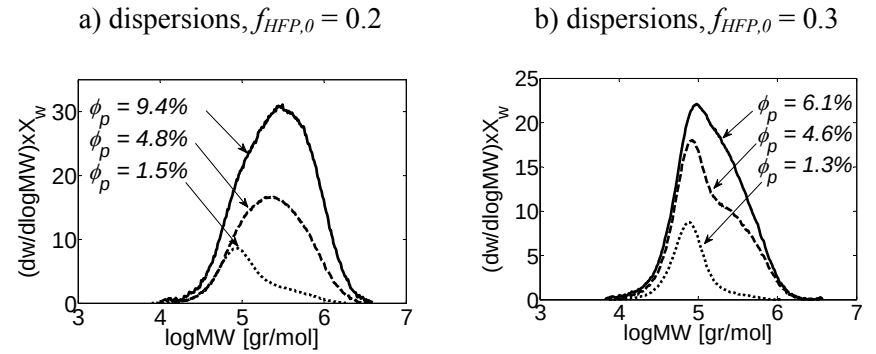

Figure 3.15 - . Effect of reaction time and polymer hold-up, ϕ_p, on molecular weight distributions for samples produced under dispersion conditions. a) Initial monomer composition $f_{HFP,0} \cong 0.2$ (Table 3.2, runs 7-9); b) initial monomer composition $f_{HFP,0} \cong 0.3$ (Table 3.2, runs 10-12).

In the case of precipitation reactions at short polymerization time and low ϕ_p, the MWDs exhibit a dominant low MW peak with some tailing in the high MW region at $f_{HFP} \cong 0.2$ (Figure 3.14-a) as well as at $f_{HFP} \cong 0.3$ (Figure 3.14-b). At increasing reaction time and ϕ_p, the second mode in the high MW region becomes more visible in both cases, even though the low MW peak remains the dominant one. The MWD profiles for dispersions are comparable to those observed for precipitations at the shortest reaction time. However, at longer reaction times, the high MW tail becomes the dominant one, eventually leading to very broad but still monomodal MWDs. Also this behaviour can be explained with a 2-loci model associating the peak at lower MW to the polymer formed in the continuous phase and the one at higher MW to that formed in the dispersed phase.

The moving of the tail toward the high MW with the polymer hold-up for dispersions could be such explained: at low conversion the small polymer amount (ϕ_p smaller than 2.5%) collects only a small fraction of the growing radicals, and the continuous phase is the main reaction locus. At increasing time and polymer hold-up, the dispersed phase increases its relevance as reaction locus and it becomes the predominant one, so the fraction of the higher MW mode increases. Under otherwise constant conditions, this evolution is regulated by the amount of available interphase area, A_p, which controls the transfer of the radicals from the continuous to the particulate phase. Since precipitation polymerization exhibits lower A_p values, this transition is much slower, and in fact even at the highest ϕ_p value in Figure 3.14-a the contributions of the two reaction loci are still comparable and the corresponding MWD is still bimodal.

The mechanism of the two reaction loci is able to interpret also the experimental results reported by Ahmed et al.[38] In particular, they carried out experiments opportunely designed in order to discriminate among

continuous, interfacial or polymer particle reaction locus. Indeed, the Authors evaluated the effect of the polymer hold-up on precipitation copolymerization kinetics in a continuous stirred tank reactor up to ϕ_p values of about 2.5%, and using a 1-locus polymerization model, they obtained good predictions in terms of reaction rate and number average molecular weight.

Instead, according the results shown in Figure 3.14, under these conditions the contribution of the continuous phase to the overall polymerization still prevails over the one of the polymer particles and the corresponding data do not allow to detect the role of the dispersed phase as site of polymerization. Finally, therefore we can state that there is not a single reaction site all along the reaction but a gradual transition from one site (continuous phase) to the other (dispersed phase).

3.10 Conclusions

In this work selected experiments of VDF and HFP copolymerization in $scCO_2$were designed and performed to collect information on the existence of two potential reaction loci. In particular, the experiments carried out in the presence of ammonium carboxylate perfluoropolyether surfactants with a HFP mole fraction in the feed ranging from 0 to 0.3, exhibited higher interphase area A_p, enhancing the kinetics of radical transport and the contribution of the polymer phase as reaction locus compared to precipitation reactions with much smaller A_p. While looking at the effect of polymer hold-up increment, the significant MWD changes clearly indicate that the polymerization started in all cases in the supercritical phase, but it quickly shifted to the polymer phase provided that enough interface area became available. Moreover, the MWD of the final product reflected the

relative contribution of both loci. Indeed, under the experimental conditions considered in this work, longer polymer chains were produced in the dispersed phase compared to those produced in the continuous phase, leading to bimodal or monomodal MWD for precipitation or dispersion reactions, respectively.

Although 1-locus models can be used at low conversion values when polymer hold-ups smaller than few percents are reached, the same models cannot cover the whole process because they do not account for the effect of the interfacial area on the final molecular weight distribution. According to the reported experimental evidences, the general 2-loci polymerization scheme previously proposed by Mueller et al.[1] for precipitation/dispersion reactions in supercritical carbon dioxide applies to both VDF homopolymerization and its copolymerization with HFP up to initial HFP feed mole fractions of 0.30. Above this value, the plasticization effect caused by the CO_2 sorption softened the copolymer causing particle coalescence and thus prevented to study the effect of the interfacial area on the MWD.

Reference:

[1] Mueller, P. A.; Storti, G.; Morbidelli, M.; Apostolo, M.; Martin, R. *Macromolecules* 2005, 38, 7150-7163.

[2] Mueller, A. P.; Storti, G.; Morbidelli, M.; Mantelis, C. A.; Meyer, T. *Macromol. Symp.* 2007, 259, 218-225.

[3] Mueller, P. A.; Storti, G.; Morbidelli, M.; Costa, I.; Galia, A.; Scialdone, O.; Filardo, G. *Macromolecules* 2006, 39, 6483-6488.

[4] Galia, A.; Giaconia, A.; Scialdone, O.; Apostolo, M.; Filardo, G. *J. Pol. Sci.: Part A: Pol. Chem.* 2006, 44, 2406-2418.

[5] Scialdone, O.; Galia, A.; Raimondi, S.; Filardo, G. *J. Supercrit. Fluids* 2007, 39 347-353.

[6] Supporting Information.

[7] Mekhilef, N. *J. Appl. Pol. Sci.* 2001, 80, 230-241.

[8] Pianca, M.; Bonardelli, P.; Tatò, M.; Cirillo, G.; Moggi, G. *Polymer* 1987, 28, 224–230.

[9] Isbester, P. K.; Brandt, J. L.; Kestner, T. A.; Munson, E. J. *Macromolecules* 1998, 31, 8192–8200.

[10] Beginn, U.; Najjar, R.; Ellmann, J.; Vinokur, R.; Martin, R.; Moller, M. J. Pol. Sci.: Part A: Pol. Chem. 2006, 44, 1299-1316.

[11] Ameduri, B.; Boutevin, B.; Kostov, G. Prog. Pol. Sci. 2001, 26, 105-187.

[12] Saraf, M. K.; Gerard, S.; Wojcinski, L. M.; Charpentier, P. A.; DeSimone, J. M.; Roberts, G. W. Macromolecules 2002, 35, 7976-7985.

[13] Ahmed, T. S.; DeSimone, J. M.; Roberts, G. W. Macromolecules 2006, 39, 15-18.

[14] Briscoe, B. J.; Lorge, O.; Dang, P. Philos. Mag. 2002, 82, 2081-2091.

[15] Odian, G. Principles of Polymerization, 4th ed.; John Wiley & Sons: New York, 2004.

[16] Nomura, M.; Satpathy, U. S.; Kouno, Y.; Fujita, K. J. Pol. Sci.: Part C: Pol. Lett. 1988, 26, 385-390.

[17] Tai, H. ; Wang, W. ; Howdle, S. M. Macromolecules 2005, 38, 9135-9142.

[18] Möller, E.; Schreiber, U.; Beuermann, S. Macromol. Symp. 2010, 289, 52-63.

[19] Bonavoglia, B.; Storti, G.; Morbidelli, M. Ind. Eng. Chem. Res. 2006, 45, 3335-3342.

CHAPTER 4

pH SENSITIVE PVDF MEMBRANES

4.1 Application fields of polymeric membranes

Actually, synthetic polymeric membranes are the object of intensive research in the field of polymer, physical and chemical sciences. Many membrane separation processes have been developed in a wide number of industries such as chemical, pharmaceutical, food, fuels, gas, cellulose processing, textile and automobile. Particularly, strong development and growth of membrane technology can be observed in the purification of wastewater and the production of drinking water. Generally, membrane separation processes: offer appreciable energy savings; they are environmentally benign; the technology is clean and easy to operate; they replace conventional processes of filtration, distillation, and ion exchange; they produce high-quality products and offer greater flexibility in system design. Actually, membrane technology has widespread applications in chemical and pharmaceutical industries and its use in various other fields is increasing rapidly.

A membrane can essentially be defined as a barrier between two phases that allows the transport of molecular/ionic species of liquids or gases in contact with its surface under the influence of a driving force. It can provide selective transport of one specie over another and regulate the transport of various species at different controlled rates. The former property is called selectivity (degree of separation), whereas the latter is known as permeability. The preferential transport of molecular/ionic species through a membrane occurs due to differences in size, shape, chemical properties or

electrical charge of the components in the mixture to be separated. Anyway the transport occurs as consequence of a driving force, i.e. a difference in chemical potential by a gradient across the membrane, e.g. concentration or pressure, or by an electrical field. The membrane thickness can vary from 100 nm to several millimetres.

Table 4.1 summarizes typical membrane separation processes along with their fields of application and corresponding driving forces.

Membrane type	Membrane process	Driving force	Phase	Field of application
Dense	Dialysis	ΔC	Liquid/liquid	Purification of polymer solutions, haemodialysis, controlled-release, alcohol reduction in beer
Dense	Reverse osmosis	ΔP	Liquid/liquid	Desalination
Porous	Microfiltration	ΔP	Solid/liquid	Clarification of beverages, cell harvesting, reduction of bacteria and particulate turbidity, production of ultra-pure water for semiconductor industry
Porous	Ultrafiltration	ΔP	Liquid/liquid	Purification and concentration of juices and polymer solution, protein recovery and waste water purification in dairy industry, starch recovery and pharmaceuticals
Porous	Hyperfiltration	ΔP	Liquid/liquid	Desalination of brackish and sea water, purification of waste water, metal recovery from galvanic industry waste water, concentration of juice and milk
Dense/porous	Electrodialysis	ΔE	Liquid/liquid	Production of salt and ion free water from seawater, reduction of acidity of citrus juices, chloro-alkali, production of sulfuric acid
Dense	Pervaporation	ΔP, C and T	Liquid/vapor/liquid	Dehydration of organic solvents, separation of isomer solvents, recovery from water
Dense	Membrane distillation	ΔP, C and T	Liquid/vapor/liquid	Production of pure water, solvent recovery
Dense/composite	Gas separation	ΔP	Gas/gas	Natural gas purification, oxygen enrichment
Dense	Piezodialysis	ΔP	Liquid/liquid	Salt enrichment, separation of electrolytes

Table 4.1- Typical membrane separation processes along with their field of application and the corresponding driving forces. (DC; concentration difference; DP; pressure difference; DE; potential difference; T, temperature).[1]

In principle, membranes can be divided into two categories: symmetric and asymmetric, according to their structural characteristics which can have significant impacts on their performance (Figure 4.1). Symmetrical membranes have an homogeneous structure and composition along of the entire membrane thickness; such membranes can be either dense films or microporous.

Dense membranes consist of a dense film through which permeants are transported by diffusion under the effect of a driving force. The separation of various components of a solution is related directly to their relative transport rate within the membrane, which is determined by their diffusivity and solubility in the membrane material. An important property of nonporous, dense membranes is that even permeants of similar size may be separated when their concentration in the membrane material (i.e. their solubility) differs significantly. Most gas separation, pervaporation, and reverse osmosis membranes use dense membranes to perform the separation. However, these membranes usually have an asymmetric structure to improve the flux.

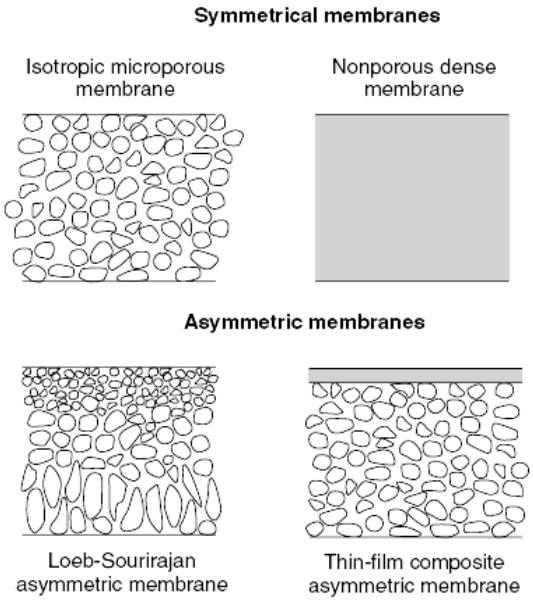

Fig. 4.1- Schematic representations of the principal types of membrane.

Porous membranes are used widely in microfiltration and they have a rigid, highly voided structure with randomly distributed, interconnected pores (0.1- to 10-μm diameter). The shape of the pores is strongly dictated by the method of preparation of the membranes. Exist membranes that show essentially straight pores (cylindrical pores) across the membrane thickness, but the majority of porous membranes, however, have interconnected pores with tortuous paths. As shown in Figure 4.2, microporous membranes can be generally characterized by the average pore diameter d, the membrane porosity ε (the fraction of the total membrane volume that is porous), and the tortuosity of the membrane, τ , (a term reflecting the length of the average pore through the membrane compared to the membrane thickness). The separation of solutes by microporous membranes is mainly a function of molecular size and pore size distribution.

Since the flow rate through a membrane is inversely proportional to the membrane thickness, it is very desirable to make the homogeneous membrane layer as thin as possible. However, very thin membranes typically do not exhibit the mechanical strength needed to withstand the usual handling procedures and processing pressure gradients. Therefore, a practical solution to this problem has been the development of an asymmetric or composite membrane composed by an extremely thin surface layer supported on a much thicker porous, dense substructure. In this "anisotropic" arrangement, separation of the species of the feed stream and the most flow resistance (or pressure drop) take place primarily in the thin membrane layer. While, the underlying support should be mechanically strong and porous enough that it does not cause the flow resistance.

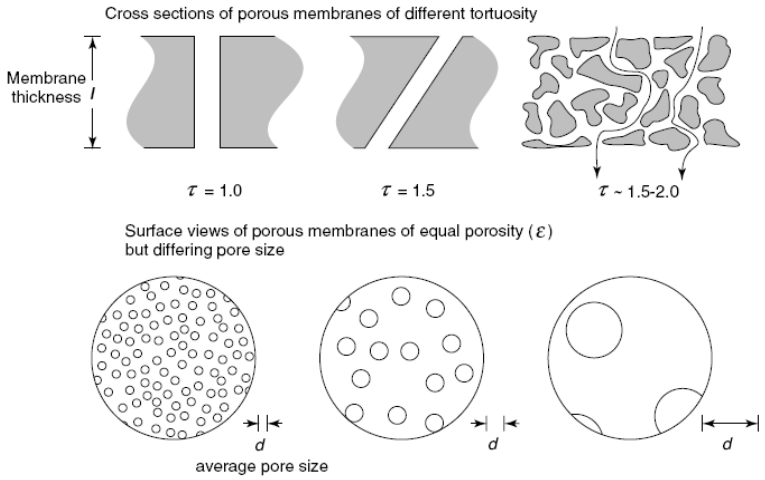

Fig. 4.2. (**a**) Cross sections of porous membranes containing cylindrical pores, with a tortuosity τ (**b**) Surface views of porous membranes of equal porosity ε but differing average pore size d.

Normally ion exchangers are solid water insoluble "high-molecular" substances that can exchange ions bound to other free-in-solution ions of the same charge; usually ion exchangers are resins composed of cross-linked polymers that possess electrically active functional groups. Electrically charged membranes can be dense or microporous, but are most commonly microporous, with the pore walls carrying fixed positively or negatively charged ions. A membrane with positively charged ions is referred to as an anion-exchange membrane because it binds anions in the surrounding fluid. Similarly, a membrane containing negatively charged ions is called a cation-exchange membrane (Figure 4.3). Two key factors determine the effectiveness of an ion exchanger: its affinity for the ion in question and the number of active sites available per unit mass of the membrane.

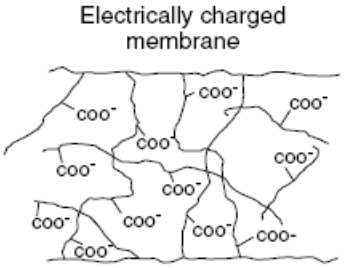

Figure 4.3- Schematic representation of a ion exchange membrane.

4.2 Techniques of grafting

In the polymeric age, it is essential to modify the properties of a polymer according to tailor-made specifications designed for target applications. There are several means to modify polymer properties, viz. blending, grafting, and curing. 'Blending' is the physical mixture of two (or more) polymers to obtain the requisite properties. 'Grafting' is a method wherein one or more monomers are covalently bonded (modified) onto the polymer chain, whereas in curing, the polymerization of an oligomer mixture forms a coating which adheres to the substrate by physical forces. Actually there is no time scale for the process of grafting, which can take minutes, hours or even days, whereas curing is usually a very rapid process, occurring in a fraction of second. The schematic presentation of the different methods for polymer modification is presented in figure 4.4.

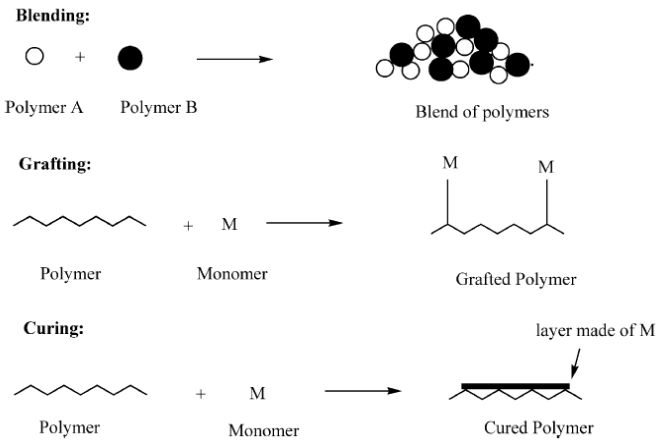

Figure 4.4- Schematic representation of the methods of polymer modification[2]

Among the methods of modification of polymers, grafting is one of the more promising. In principle, graft copolymerization is a process in which side chain grafts are covalently attached to the main chain of a polymer backbone to form branched copolymer. A graft copolymer can be represented as follows:

$$-A-A-\underset{\displaystyle B_n}{\underset{|}{A}}-A-A-\underset{\displaystyle B_m}{\underset{|}{A}}-A-A-$$

where, A denotes the main polymer chain, B_n and B_m are the side chain grafts originated from the monomer B having n and m repeat units respectively. The extent of polymerization in B_n and B_m grafts is called the degree of grafting (grafting yield) which can be gravimetrically determined as the percentage of mass increase. Both the backbone and side chain grafts can be either homopolymer or copolymer. Graft copolymerization takes

place as a result of formation of active sites on the polymer backbone. The active sites may be free radicals or ionic chemical groups, which initiate polymerization reaction. The formation of active sites on the polymer backbone can be carried out by several methods such as plasma treatment, ultraviolet (uv) light radiation, decomposition of chemical initiator and high energy radiation (ionizing radiation).

4.2.1 Grafting initiated by chemical routes

In the chemical process, the role of initiator is very important as it determines the path of the grafting process. The grafting can proceed along two major paths: free radical and ionic. In a free radical grafting process, free radicals are produced from the initiators and transferred to the substrate to react with monomer to form the graft co-polymers. For example, one can consider the generation of free radicals by redox reaction, e.g. M^{n+}/H_2O_2, persulphates[3]

$$Fe^{2+} + H_2O_2 \rightarrow Fe^{3+} + OH^- + OH^{\bullet}$$
$$Fe^{2+} + {}^{-}O_3S\text{-}OO\text{-}SO_3^- \rightarrow Fe^{3+}\, SO_4^{2-} + SO_4^{-\bullet}$$

It may be observed that the active species in the decomposition of H_2O_2 and persulphate induced by Fe^{2+} are $OH^{\bullet}$ and $SO_4^{-\bullet}$ respectively.

The most useful sources of radicals for free radical grafting are organic peroxides, which, if thermally activated, supplies free radicals by the homolitic cleavage of the labile oxygen-oxygen bond at appropriate temperatures. The decomposition rate of a peroxide depends not only on the class of peroxide but also on the nature of its chemical groups. Anyway, free radical species generated from peroxides are very reactive and have short

lifetimes. To initiate free-radical grafting the peroxides have to generate primary free radicals sufficiently reactive to abstract hydrogen atoms from polymer chain to form the corresponding macroradicals. Moreover, a good peroxide for a given grafting reaction should meet at least the following criteria: low toxicity and volatility, appropriate half life, and high grafting initiator efficiency. Furthermore the nature of decomposition products (toxicity, odour, volatility), the residual amount in the final polymer and the physical form of the peroxide are important parameters.

Unlike, azo-initiators are rarely used for free radical grafting because of their short half life and low hydrogen abstracting capacity.

It is possible to define an initiator efficiency, f_g, for free radical grafting as the fraction of primary radicals able to abstract hydrogen atoms from the polymer backbone forming the corresponding macroradicals. An important factor affecting the initiator efficiency is the so-called “cage effect”. The cage effect is related to the fact that primary radicals originating from the initiator decomposition are formed in a cage made of solvent, monomer and/or preformed polymer molecules. In general, not all primary radicals generated within this cage can diffuse out of it and react with the polymer backbone, instead they terminate before by combination with other radicals present in the cage. The hydrogen abstracting capacity depends not only on the nature of primary radicals but also on the type of carbon-hydrogen bonds (C-H) associated with the chemical structure of the polymer. In general, a lower dissociation energy makes easier the hydrogen atom abstraction and correspondingly the stability of the radical formed by removal of a hydrogen atom is higher. Thus, abstracting a hydrogen atom from a tertiary alkane $(R)_3C\text{-}H$ is easier than from a secondary alkane $(R)_2CH\text{-}H$ that in turn is less stable and more reactive than a primary alkane $RCH_2\text{-}H$.

A plausible mechanism of grafting in the presence of a radical initiator is the following:

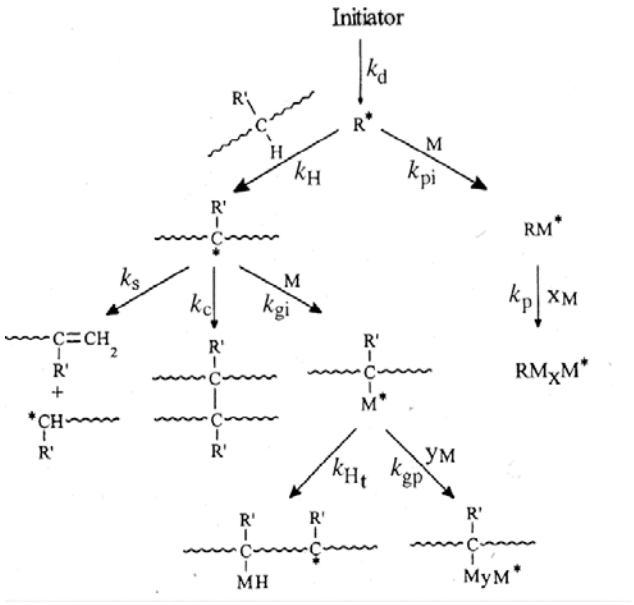

Fig.4.5 Overall scheme of free-radical grafting onto a polymer backbone

Once a primary free radical (R*) is generated by decomposition (k_d) of an initiator, it may follow two completely different reactions pathways in the presence of monomer (M) and polymer: one leading to undesired homopolymerization (k_{pi}) and the other one to grafting (k_h). The former pathway is initiated if the primary radical reacts with a monomer molecule (k_{pi}) forming a monomer radical (RM•). This monomer radical could continue to react with other monomer molecules (k_p), giving to the homopolymer, or more rarely could reacts with the polymer backbone initiating the grafting.

The second pathway, conducing to the grafting, consists in the abstraction of an hydrogen from the polymer backbone by a primary radical (k_h) to form a macroradical, which can react with the monomer molecule, forming a branched macroradical (k_{gi}). In turn, this branched macroradical may continue to react with other monomer molecules forming longer grafted chains (k_{gp}). Anyway, this radical end may also undergo transfer with a hydrogen atom of the same or another polymer backbone forming a new macroradical (k_{ht}). The macroradical, can be subjected also chain scission (k_s) and crosslinking (k_c) whose relative importance depends primarily on the nature of the macroradical.

If the macroradical is highly unstable, the chemical bond (usually a C-C bond) in the neighbourhood of this macroradical may break down to two smaller fragments-chain. This process is termed chain-scission and causes a reduction in the molecular weight. The molecular weight distribution becomes more random and the polydispersivity approaches two. This characteristic is related to the fact that higher molecular weight chains have a greater number of C-C bonds thus is subjected to a greater probability to chain scission. Therefore for broad molecular weight distributions, usually found for polyolefins, the breadth of the molecular weight distribution narrows when chain scission proceeds.

When macroradical is subjected to bimolecular termination by combination long-chain branches are formed (cross-linking and branching). The formation of high molecular weight chains via long chain branching increases melt strength, die swell and improves strain hardening properties. Crosslinking sometimes brings to the original polymer some properties enhancement such as increased service temperature, solvent resistance, flexural modulus, and dimensional stability.

The relative importance of the free-radical grafting with respect to the polymerization depends primarily on the two reaction constant ratios $(k_h+k_{ht})/k_{pi}$ and k_{gi}/k_p. The first ratio is considered as the ratio between the reactivity of the hydrogen atoms of the polymer chain and that of the monomer towards the primary radicals and macroradicals. It can also be viewed as the ratio of the fraction of the primary radicals and macroradical, which abstract hydrogen atoms from the polymer backbone to that of the primary radicals, which react with the monomer. The larger the ratio is, the more macroradicals will be formed from the hydrogen abstraction by the primary radicals as well as by the macroradicals transfer mechanism and consequently, the higher the grafting and the less important the polymerization should be.

The second ratio k_{gi}/k_p, is a measure of the relative capability of the macroradical to initiate grafting with respect to that of the propagating monomer radical to initiate homopolymerization. Obviously, the higher this ratio is, the more monomer molecules will be grafted.

The ratio k_{ht}/k_{gp} is also an important parameter in free-radical grafting because it measures the relative importance between the rate of intramolecular and/or intermolecular macroradical transfer and that of monomer addition to macroradicals. If this ratio is high, the graft length should be short and *vice versa*.

Chemical pre-treatment of the polymer backbone may also generate free-radical sites, which can provide sites for grafting. An example is the direct oxidation of polymer chains by exposing the matrix to ozone that involves the formation of peroxides and hydroperoxides groups on the exposed matrix. These groups may be activated by thermal treatment which generates free radical sites directly linked to the polymer matrix. Ozone can be used as such, anyway it was found that a combination of ozone and UV irradiation

increased the kinetics of the process significantly.[4] Anyway, some polymers undergo to degradation if oxidized by ozone evolving in a decrease of the inherent viscosity and consequently of the molecular weight. This result was reported in a study of ozone oxidation of PVDF, in which it was also observed the presence of –CH=CF- and $–CF_2$-C(O)-CF_2- units, by infrared spectroscopic analysis, revealing a C-H bond scission.[5]

4.2.2 Grafting initiated by ionizing radiation

The irradiation of macromolecules can cause homolytic scission of chemical bonds and thus forms free radicals on the polymer. In this case the medium in which to carry out the irradiation process is important because it influences the type of species formed on the irradiated polymer. Accordingly, in the follow will be explained some examples.

Different types of high-energy radiation are commercially available for graft copolymerization processes. They can be classified into: (1) electromagnetic radiation (photons) such as γ-ray and X-ray, and (2) particulate radiation (charged particles) such as electrons and swift heavy ions. The radioactive isotopes such as Cobalt-60 and Cesium-137, which are fission products of nuclear plants, are the main sources of γ-radiation. Particulate radiations such as electrons are normally obtained from accelerators (electron beam machines), which are commercially available at different designs and energies to modulate depth of penetration in the backbone polymer. Swift heavy ions are another type of particulate radiation, which are produced by ion accelerators (heavy ion beam machines). Energy absorption has been traditionally termed “dose rate” expressed in Gray (Gy), (SI unit) which is equal to 104 erg/g or 1 J/kg).

A grafting process initiated by ionizing radiation can be carried out according to the following two main methods:

(a) simultaneous (direct or mutual) irradiation;

(b) pre-irradiation (post-irradiation), which can be performed either in the presence of air or under vacuum.

Simultaneous irradiation is the simplest irradiation technique for preparation of graft copolymers. In this method a polymer backbone is irradiated in the presence of a monomer available in different forms: vapour, liquid solution or in bulk. Irradiation can be carried out in air, inert atmosphere (e.g. N_2) or preferably under vacuum leading to the formation of active free radicals on both polymer backbone and monomer units. The reaction mechanism in this grafting system can be represented as follows.

Irradiation :

$$P \xrightarrow{\gamma\ rays} P^{\bullet}$$

Initiation :

$$P^{\bullet} + M \rightarrow PM^{\bullet}$$

Propagation :

$$PM^{\bullet} + nM \rightarrow PM^{\bullet}_{n+1}$$

Termination :

$$PM^{\bullet}_{n} + PM^{\bullet}_{m} \rightarrow PM_{n+m}$$

where P is the polymer matrix, M is the monomer unit and P• and M• are their primary radicals, respectively. PM• is the initiated graft chain. PM_n• and PM_m• are the graft growing chains of the copolymer.

Simultaneous graft copolymerization has a serious limitation arising from the high level of homopolymer formation which can be represented as follows.

$$M \xrightarrow{\gamma\ rays} M^{\bullet}$$

$$M^{\bullet} + nM \rightarrow M^{\bullet}_{n+1}$$

$$M^{\bullet}_{n} + M^{\bullet}_{m} \rightarrow M_{n+m}$$

where M_n• and M_m• are the growing chains of the homopolymer.

Pre-irradiation method occurs as a combination of two separated steps: (1) irradiation of the polymer backbone to form active radicals and (2) contact of the irradiated polymer backbone with monomer. If irradiation step is carried out in air or under a flux of oxygen, the generated radicals react with oxygen to form peroxides and hydroperoxides. The stable peroxidic products are then treated with the monomer at higher temperature. In this way the peroxides undergo decomposition to radicals, which then initiate grafting. The overall reaction grafting by pre-irradiation method can be represented by:

Formation of hydroperoxides:

$$PH + O_2 \xrightarrow{\gamma\ rays} POOH$$

Thermal decomposition:

$$POOH \xrightarrow{\Delta T} PO^{\bullet} + OH^{\bullet}$$

Initiation:

$$PO^{\bullet} + M \rightarrow POM^{\bullet}$$

Propagation:

$$POM^{\bullet} + nM \rightarrow POM^{\bullet}_{n+1}$$

Termination:

$$POM^{\bullet}_{n} + POM^{\bullet}_{m} \rightarrow POM_{n+m}$$

where PH is the polymer backbone, POOH is the hydroperoxide group, PO• is the primary radical, POM• is the initial grafted chain and POM_n• is the growing chain. The long storage time of intermediate peroxy trunk polymers before the final grafting step is an obviously a great advantage of this technique.

On the other hand, if irradiation is carried out under vacuum or inert atmosphere, the generated radicals remain trapped on the polymer backbone and initiate grafting in the presence of monomer units according to the following mechanism:

$$PH \xrightarrow{\gamma\ rays} P^{\bullet} + H^{\bullet}$$

$$P^{\bullet} + M \rightarrow PM^{\bullet}$$

The stability of P• and PM• depends mainly on the crystallinity of the polymer backbone, temperature, and storage period of the irradiated films. However, the disadvantage of the technique is that if the polymer is a degrading type, the scission of the base polymer due to its direct irradiation, brings about the formation of block rather than graft copolymers. Also, if the substrate polymer does not have the ability to trap the radicals for a long enough time, subsequent grafting reaction will not follow.

It is not easy to decide which one of the two-irradiation methods is superior. In practice, the pre-irradiation method has been given much attention because of the absence of homopolymer formation and the grafting can be carried out away from radiation sources.

Radiation grafting can also proceed through an ionic mode, with the ions formed through high-energy irradiation. Ionic grafting may be of two different types: cationic or anionic. The polymer is irradiated to form the polymeric ion, and then the macroion reacts with the monomer to form the

grafted co-polymer. The potential advantage of the ionic grafting is the high reaction rate. Thus, small radiation doses are sufficient to obtain the required grafting. A schematic representation of cationic grafting of a vynil monomer is shown in figure 4.6. Analogous mechanisms is involved in the case of anionic grafting.

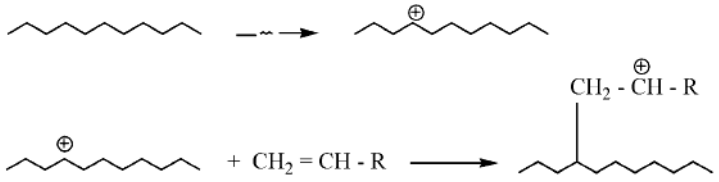

Figure 4.6-Reaction mechanism of a cationic grafting performed in a polymer backbone.[2]

High energy radiation produces ionization and excitation in polymer molecules. These energy-rich species undergo dissociation, abstraction and addition reactions in a sequence of reactions leading to chemical and structural changes. In particular, the molecular changes in polymers may be due to: (i) chain cross-linking, causing an increase in the molecular weight and forming a microscopic network structure; (ii) chain scission, causing a decrease in the molecular weight and substantially changing the polymer material properties; (iii) formation of small molecular products.[6] Concerning the latter, small molecule products result from bond scission followed by abstraction or combination reactions. Another drawback is associated to the possible formation of gaseous products, such as CO_2, which may be trapped in the polymer, and this can lead to subsequent crazing and cracking due to accumulated local stresses.

The extent of each one of these reactions depends on the chemical nature of the polymer and irradiation conditions, i.e., irradiation dose and dose rate. A good example that explains the effect of high energy radiation on polymer is given in figure 4.7, which depicts a plausible mechanism for radiation-induced reactions taking place in poly(vinylidene fluoride) (PVDF) films irradiated by electron beam at ambient conditions and at different doses[7,8].

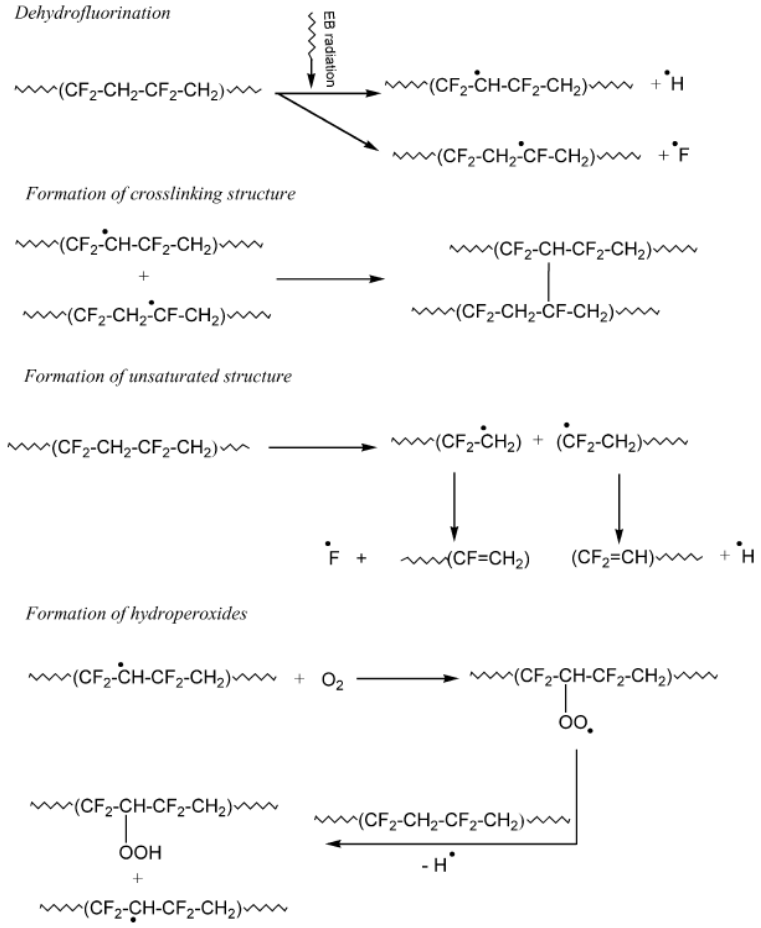

Figure 4.7- Schematic representation of radiation-induced reactions taking place in poly(vinylidene fluoride) upon irradiation by electron beam.[1]

Moreover, most irradiated polymers show a continuing change in properties for a long period after irradiation. These post-irradiation effects may be attributed to (i) trapped radicals which react slowly with the polymer molecules and with oxygen which diffuses into the polymer; (ii) peroxides formed by irradiation in air which slowly decompose with formation of reactive radicals, usually leading to scission; (iii) trapped gases in glassy and crystalline polymers which cause localized stress concentrations. Accordingly, the consequences of these post-irradiation effects in polymer properties are progressive reduction in strength, cracking and embrittlement.
Radiation induced grafting differs from chemical initiation in many aspects. Due to large penetrating power of higher energy radiation, methods using radiation initiation provide the opportunity to carry out grafting at different depths of the base polymer matrix. On the other hand, nuclear radiation energy is usually expensive in comparison with chemical reactions. Length of irradiation time is long and setting up optimum conditions is a huge task. Moreover, it should be well known previously whether the polymer is stable in the radiation range of interest.

4.2.3 Plasma radiation induced grafting

In recent years, the plasma polymerization technique has received increasing interest. Plasma is sometimes referred to as the fourth state of matter. The term was introduced by Langmuir in 1929. It is a partly ionized gas and can be defined as a quasi-neutral particle system in the form of gaseous or fluid-like mixtures of free electrons, ions, and radicals, generally also containing neutral particles (atoms, molecules). Some of these particles may be in an excited state and so they can return to their ground state by photon emission. This process is at least partially responsible for the luminosity of a typical

plasma. In plasma, some electrons are free, rather than bound to molecules or atoms. This means that positive and negative charges can move somewhat independently from each other. Plasma is usually obtained when gases are excited into high energetic states by radio frequency (RF) or electron flux generated from a hot filament discharge. Essentially, radicals formed in the polymer chains by plasma reactions undergo similar reactions to that high-energy irradiation. The energy in plasma is lower than the usual conventional energy (e-beam, γ-irradiation), and as consequence the effects of the plasma on the polymer are milder than those of high-energy irradiation, because of the low level of high activated species, electrons, and ions. Moreover, as the polymer changes are confined only to the depth of a few nanometers at the surface, the bulk properties (degree of polymerization and crystallinity) of the material are not much influenced, unlike to high irradiation energy. Radical sites can be formed with the same techniques shown for high-energy radiations, i.e., preirradiation and simultaneous techniques. The pre-irradiation technique is favoured to minimize the formation of homopolymers. Polymers are first exposed to plasma to create the radicals in the vicinity of the polymer surface, and then contacted to the vapour or to aqueous or organic solution of the monomer.

Different plasmas are available, but for grafting, argon, helium and oxygen plasma are the most used. Typically, Ar or He introduces free radicals, which can react with oxygen to form peroxides or hydroperoxides, Then, the latter functionalities can be used to initiate a graft copolymerization reaction (see Figure 4.8). Note that this method consists in a pre-irradiation grafting technique because the monomer is not subjected to the plasma and thus the grafted polymers will have the same composition as the polymers achieved by conventional polymerizations. In contrast to the pre-irradiation grafting approach, the direct grafting strategy involves the adsorption of a monomer

on the substrate surface, which is then subjected to plasma (Figure 4.9). The plasma will create radicals in the adsorbed monomer layer which will lead to a cross-linked polymer top-layer.

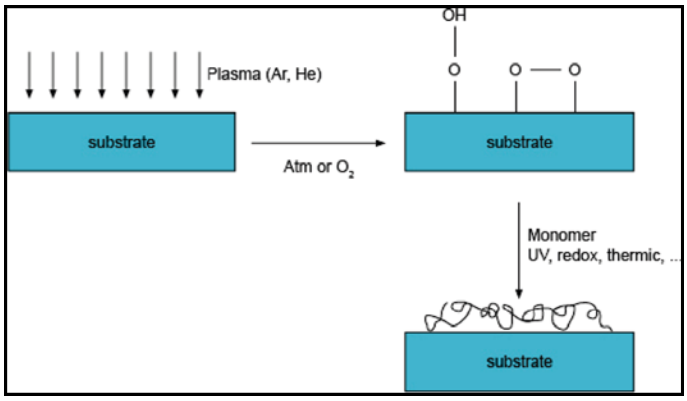

Figure 4.8- Schematic representation of plasma pre-irradiation grafting.

Figure 4.9 Schematic representation of direct grafting and plasma polymerization.

It is worth noting that the plasma induced grafting is very expensive method rather than the chemical and radiation induced grafting, and moreover it is limited to surface modification of the polymer.

4.3 Poly(vinylidenefluoride) as backbone to obtain pH sensitive matrixes

Poly(vinylidenefluoride) (PVDF) has been extensively investigated for its application in the preparation of membranes[9-11] because of its chemical inertness and good processability. Porous PVDF membranes have received much attention from researchers in various fields such as chemical engineering, electronics, textile industry, and food processing. For example, due to their excellent chemical stability, thermal stability and toughness, actually, the PVDF membranes are widely used in microfiltration (MF) and ultrafiltration (UF). Recently, biomaterial science is studying on the possibility to use PVDF-based polymers for biochemical applications, such as selective permeation and protein recognition in order to realize new materials which mime the biological systems. In particular, since living systems are composed of macromolecules, some of which change their shape and, hence, their function in response to environmental stimuli, the effort of recent studies is going to the experimental routes to modify this polymer Therefore, to use PVDF in these applications, it is required it undergoes to reversible changes in its conformation in response to some environmental stimuli, such as temperature, pH[12] and ionic strength. Several approaches have been developed to provide the conventional hydrophobic membranes with hydrophilic properties and pH-sensitivity using techniques (see section 3.2) that induce chemical and physical modification of PVDF membranes. The techniques used have included plasma and ozone treatments, blending with hydrophilic polymers, gamma ray irradiation, and ion beam irradiation.

4.4 Main biomedical applications of PVDF modified membranes

As it will be reported in the chapter 6, the PhD activity was concerned also with the modification of porous pristine PVDF membranes by graft copolymerization of a proper monomer (acrylic acid) to confer hydrophilic properties and pH-sensitivity to the original hydrophobic matrix. Actually, for these systems exist several important biomedical applications, specially concerning the controlled drug release and the selective permeation.

In particular, these membranes are used in oral drug delivery systems to modulate release kinetics by controlling drug diffusion in the release environment or by controlling external solvent penetration in the delivery system. For example, porous membrane can be designed to open its pores and ensure that drug release occurs in region of the gastro-intestinal tract selected according the value of environmental pH.

An interesting application of porous poly(acrylic acid) (PAA) grafted poly(vinylidenefluoride) membranes is shown in the work of Järvinen and coworkers[13] who studied drug release from these matrixes packet as bags at different pH values in vitro. Square-shaped bags (2x2 cm) were formed by placing two PVDF membranes (Millipore; pore size 0.22 μm) on top of each other and hot-sealing three sides to get a membrane bag. The open side served to insert model drug inside the bag after grafting. Bags were irradiated with 25 kGy under nitrogen atmosphere and the unsealed side was protected with a copper plate to avoid hot-sealing after grafting. Immediately after irradiation, bags were immersed at room temperature in a graft solution containing AA that was continuously purged with nitrogen to remove oxygen. Then, bags were soxhlet extracted with water to remove any remaining monomer and dried overnight. Finally, bags were filled manually with model drug (FITC-dextran) and the open side was hot-sealed. The release kinetics were studied from bags at 37.8°C in 900 cm^3 of a 6 mM

phosphate buffer solution at pH 2.0 and 7.0. The ionic strength was adjusted to 0.15 M with NaCl. From figure 4.10 it is possible to see that FITC-dextran release was considerably higher at pH 2.0 than at pH 7.0. Indeed, this is due to changes in the conformation of the grafted PAA chains as a function of pH. As pKa of polyacrylic acid[14] is about 4, at pH 2.0, polymer chains are undissociated resulting in a compact conformation. Accordingly, the pores of the PVDF-PAA membrane are open and the drug can pass through. On the contrary, at pH 7.0, PAA molecules are dissociated and swollen so that pores are partially blocked and drug passage is hindered.

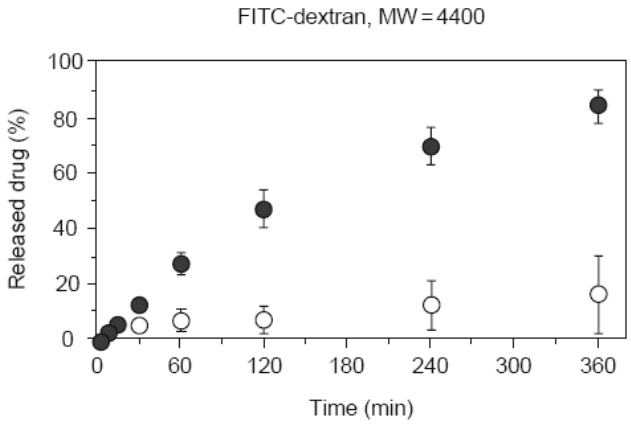

Figure 4.10 - Release of FITC-dextran from membrane bags of 50 wt% PAA grafted PVDF membranes into dissolution medium at pH 2.0 (filled circles) and pH 7.0 (open circles).[12]

S. Åkerman[15] et al. studied the diffusion fluxes of several model drugs across pH sensitive porous PVDF-g-PAA membranes. The results suggested a pH dependent permeation of two neutral model drugs across the membrane, in particular of Caffeine and Mannitol (figure 4.11). Moreover they studied the

influence of the charge of ionic drugs in a range of pH where the permeability was practically constant and it turned out that the cationic drugs permeated the membranes faster in ionized form than in un-ionized form and vice versa in the case of anionic drugs.

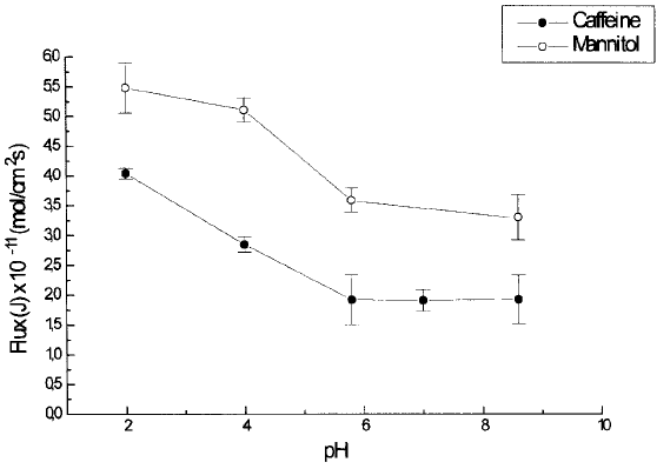

Figure 4.11 - Flux (J) of caffeine and mannitol across the 58wt% PAA grafted PVDF membrane as a function of pH.[15]

Adsorption of acidic and basic drugs onto PVDF-PAA membrane was first studied by Åkerman[16] which found this membrane suitable to separate basic drugs from buffer solution containing proteins. In particular in this study the basic drugs were separated from albumin which was not adsorbed onto the membrane. Then, J. Karppi[17] et all conducted the same study of adsorption from biological fluids, as blood serum, in vitro. It was found that the drugs were adsorbed on the PAA-grafted chains by the mechanism of ion-exchange for which, at physiological pH (7.4), PAA chains are completely dissociated so the membrane surface being negatively charged and it will

exchange their positively charged counter ion (H^+) for preferably a positively charged drug. The adsorbed amounts of several model drugs onto the membrane, that was equal to that disappeared from the initial sample contacted to 50 wt% grafted PVDF–PAA membrane, are shown in table 4.2. The results indicated that basic model drugs were adsorbed onto the PVDF-g–PAA membrane in amount considerably greater than acidic model drugs.

Another very exciting biomedical application is the glucose-responsive permeation of insulin molecules through the gating of PVDF membrane obtained by immobilizing the enzyme glucose oxidase onto poly(acrylic acid) tails[18]. For a glucose-responsive self-regulated insulin release system as this one, stability and response rate are very important and essential, because only a stable system can ensure the safety during therapy and only fast response can ensure the self-regulated insulin release exactly during changes in glucose concentration. To meet both stability and fast response, it is possible to use the glucose responsive gating membranes with porous substrates and linear-grafted functional polymeric gates.

Drug	Behaviour	Adsorbed amount (%)
Alprazolam	(A)	65.9 ± 6.4
Carbamazepine	(A)	7.8 ± 6.7
Clobazam	(A)	32 ± 17.7
Clonazepam	(A)	23.9 ± 3.6
Diazepam	(A)	15.1 ± 2.9
Flunitrazepam	(A)	54.7 ± 17.4
Hydroxycarbazepine	(A)	6.1 ± 3.1
Lamotrigine	(A)	0.4 ± 5
Medazepam	(A)	27.2 ± 6.9
Midazolam	(A)	56.4 ± 14.1
Nitrazepam	(A)	13.4 ± 2.4
Nordiazepam	(A)	11.5 ± 2
Oxazepam	(A)	7.4 ± 1.7
Pentobarbital	(A)	4.9 ± 5.6
Primidone	(A)	9.5 ± 7.4
Temazepam	(A)	42.4 ± 18.5
Zopiclone	(A)	35 ± 17.9
Amitriptyline	(B)	94.1 ± 7.5
Chloropramazine	(B)	83.2 ± 18.6
Chloroprotixen	(B)	82.3 ± 3.5
Citalopram	(B)	98.7 ± 0.2
Clomipramine	(B)	92.6 ± 0.6
Clozapine	(B)	93.4 ± 0.6
Desipramine	(B)	95.8 ± 0.8
Dm-citalopram	(B)	97.5 ± 0.2
Dm-maprotiline	(B)	85.7 ± 5.1
Doxepin	(B)	96.8 ± 0.3
Fluoxetine	(B)	92.2 ± 1.3
Haloperidol	(B)	96.1 ± 0.6
Imipramine	(B)	95.3 ± 0.9
Levomepromazine	(B)	89.6 ± 3.8
Maprotiline	(B)	90.6 ± 3.3
Mianserin	(B)	95.2 ± 1.4
Norclomipramine	(B)	89.8 ± 0.7
Norclozapine	(B)	92.4 ± 0.5
Nordoxepin	(B)	94.9 ± 0.4
Norfluoxetine	(B)	93.4 ± 1.6
Nortrimipramine	(B)	92.1 ± 1.3
Nortriptyline	(B)	93 ± 0.6
Thioridazine	(B)	26.8 ± 15.1
Thiothixen	(B)	65 ± 10.3
Trazodone	(B)	75.6 ± 12.8
Trimipramine	(B)	93.8 ± 1.5

Table 4.2-Amounts of the drugs adsorbed from serum pool onto the 50 wt% grafted PVDF–PAA membrane; A: behaves like acid, B: behaves like base.[17]

In this case a PVDF porous membrane as substrate can provide mechanical strength and dimensional stability and as the PAA grafted chains have freely mobile ends (which are different from the typical crosslinked network structure of the hydrogels that gives rise to relatively immobile chain ends), the response of those membranes to the environmental stimuli could be faster because of the more rapid conformational changes of the functional polymers. The preparation process route and the principle of glucose-responsive control of the permeation through the gating membrane are schematically illustrated in figure 4.12.

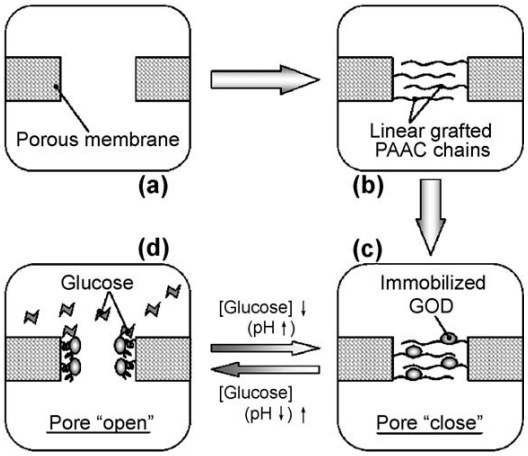

Figure 4.12- Schematic illustration of the preparation process route and the principle of glucose-responsive control of the permeation through the gating membrane: (a) porous membrane substrate; (b) pH-responsive gating membrane with graft linear PAA chains into the pores of the membrane substrate; (c)-(d) glucose-responsive gating membrane prepared by immobilizing glucose oxidase (GOD) onto the PAA-grafted membrane with the pores closed and open respectively.[18]

In particular, in the absence of glucose the pH is close to neutrality (pH 7.4) so the conformation of the grafted PAA chains is greatly expanded due to the repulsion between ionized carboxyl groups. In this way the expanded chains close the membrane gate (figure 4.12-c). When glucose concentration increases, the enzyme glucose oxidase catalyses the oxidation of glucose into gluconic acid, as indicated from the reaction described in equation 3.1, thereby lowering the local pH and protonating the carboxyl groups. Since the PAA chains conformation results compact, the pores are open and the free diffusion of insulin molecules is allowed (figure 4.12-d).

$$Glucose + O_2 + H_2O \xrightarrow{GOD} Gluconic\ acid + H_2O_2 \qquad 3.1$$

4.5 State of the art on the modification of PVDF matrix to obtain pH sensitive porous membranes

Actually, exist several methods to prepare pH sensitive PVDF porous membranes. In particular, concerning the grafting of the monomers acrylic acid (AA) and 4-vinyl pyridine (4-VP), an experimental route[19-22] consists in a pre-activation process of the PVDF chains dissolved in a solution of N-methyl-2-pyrrolidone (NMP) by ozone treatment that generates peroxides and hydroperoxides groups on the polymeric chains. The subsequent step is the thermally induced graft-copolymerization of AA or 4VP on the pre-activated PVDF chains dissolved in a solution of NMP and, finally, the preparation of the membrane for microfiltration (MF) by phase inversion using a bath of water like anti-solvent. In the figure 4.13 are shown the three steps above mentioned.

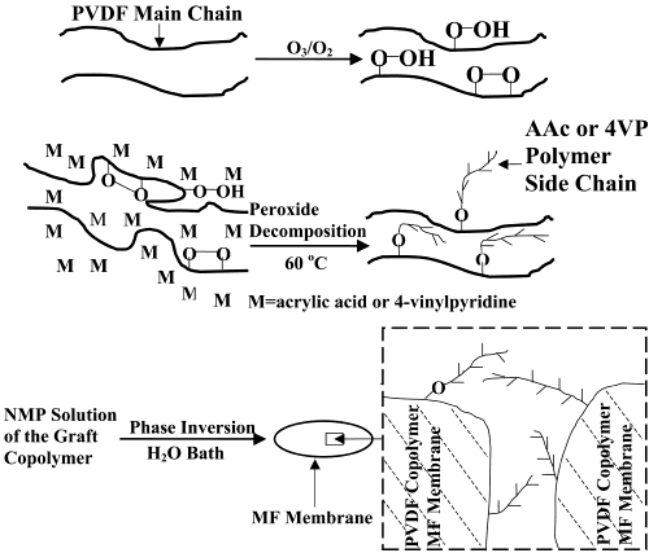

Figure 4.13 – Illustration of the processes of the thermally induced graft copolymerization of AA and 4VP on the ozone preactivated PVDF chains and the preparation of the membranes by phase inversion.[19]

The results of some studies using this method are reported in the following. In particular, in figure 4.14 is reported the comparison between the bulk graft concentration of the 2VP-g-PVDF and 4VP-g-PVDF copolymers (determined by elemental analyses) and the surface graft concentration of the corresponding MF membranes (determined by XPS analyses) obtained by Zhai[21] et al.

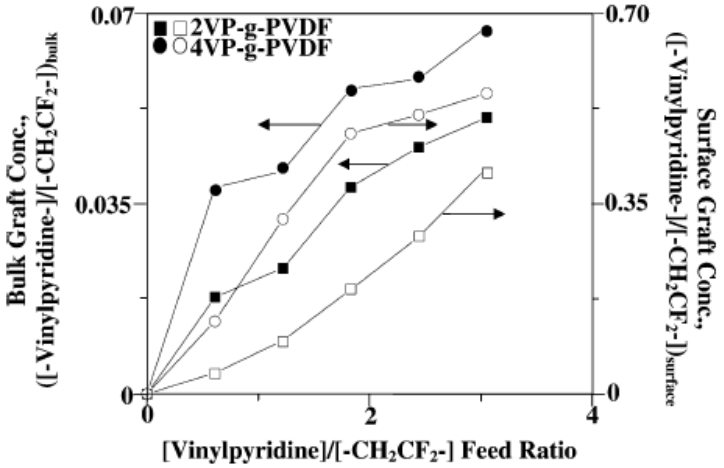

Fig. 4.14 Comparison between the bulk graft concentration and the surface graft concentration of the 2VP-g-PVDF and 4VP-g-PVDF MF membranes cast by phase inversion in water (pH = 6) from the 12 wt.% NMP solutions of the respective graft copolymer.

Thus, the surface graft concentration was always higher than the corresponding bulk value for both types of membranes.

The flux of aqueous solutions of different pH values through the AA-*g*-PVDF, the 4VP-*g*-PVDF, and the pristine PVDF membranes were also investigated.[17] The AAc-*g*-PVDF and the 4VP-*g*-PVDF MF membranes were cast from the 12 wt % NMP solution of the respective copolymer. The results are shown in Figure 4.15. Differing from the flux through the pristine PVDF membrane, the flux of the aqueous solution through all the modified membranes exhibited a pH-dependent behaviour.

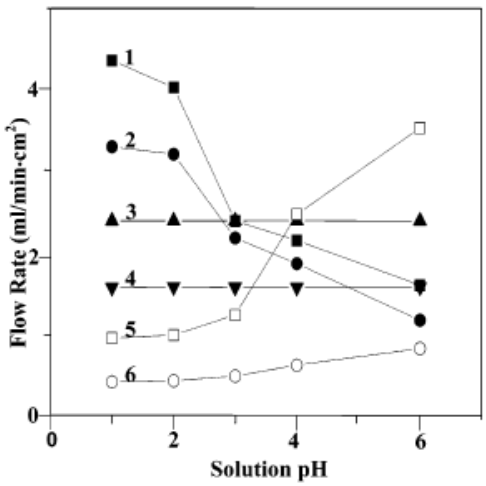

Figure 4.15- pH-dependent water permeability through the pristine PVDF, AAc-*g*-PVDF and 4VP-*g*-PVDF MF membranes. Curves 1 and 2 are obtained from two AA-*g*-PVDF membranes with graft concentrations ([-AA-]/[-CH_2-CF_2-]surface ratios) of 0.97 and 0.13, respectively; Curves 3 and 4 are from fluxes through the commercial PVDF membranes (standard pore diameters: *d*) 0.65 and 0.45 μm, respectively); Curves 5 and 6 are obtained from two 4VP-*g*-PVDF membranes with graft concentrations ([-4VP-]/[-CH_2CF_2-]surface ratios) of 0.55 and 0.13, respectively.

The permeability through the AA-g-PVDF membranes decreases with the increase in the solution pH value from 1 to 6, with the most drastic decrease being observed at solution pH values between 2 and 4. The modification of permeability in response to variations of solution pH may be attributed to the changes in the conformation of the poly(AA) side chains on the surfaces (especially those on the pore surfaces) as explained in section 3.4. While the flux of the aqueous solution through the 4VP-g-PVDF membranes exhibits a reversed pH-dependent behaviour. Indeed, the flow rate increased with the

increase of pH solution from 1 to 6. As a weak base, the pyridine groups of the grafted 4VP side chains are protonated and become complexed in an acid solution. The resulting electrostatic repulsions among the positively charged pyridinium nitrogen atoms overcome the hydrophobic interactions among the alkyl segments of the chains. The uncoiling of the polymer side chains and their interactions with the aqueous solution lead to an extended conformation in the pores. As a result, the effective pore dimensions and thus the permeability of the aqueous solution through the grafted membrane are reduced. Moreover, for both types of membranes, the change of flux in response to pH alterations was enhanced by the increase in the graft concentration.

A drawback of this technique is the use of NMP to dissolve the polymer chains that is a toxic substance for human health so any trace has to be almost totally removed from the final product. Another drawback is due to the ozone treatment that induces uncontrolled radical side reactions on the PVDF chains that cause chain scissions and crosslinks.

The literature reports another route adopted to perform the grafting of acrylic acid on the PVDF backbone, in particular the grafting induced by ionizing radiations[15,23,24] or by plasma, that excite radicals in the polymeric substrate. After this pre-activation step generally the grafting is performed at room temperature dipping the irradiated membrane in an aqueous solution of the monomer. The schematic mechanism of a reaction grafting of AA on a PVDF membrane backbone induced by electron beam[15] is proposed in figure 4.16.

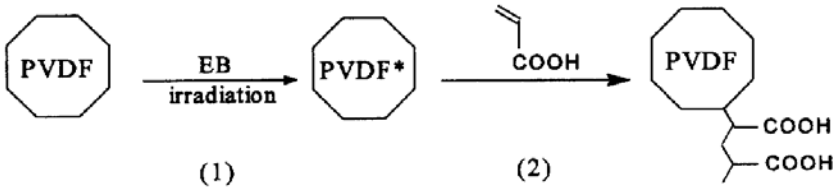

Figure 4.16- Illustration of the grafting mechanism: (1) irradiation of the PVDF membrane to form radicals on the polymer chains; (2) grafting of AA initiated by these macroradicals.

Even if these methods do not use toxic solvents, the plasma species, interacting with the inner matrix, make difficult the control of the uniformity of the distribution of grafted chains over pore surface.

References

[1] M.M. Nasef, E.-S.A. Hegazy, Prog. Polym. Sci. 29 (2004) 499–561

[2] A. Bhattacharya, B.N. Misra, Prog. Polym. Sci. 29 (2004) 767–814

[3] Prasanth KVH, Tharanathan RN., Carbohydr Polym 2003;54(3):43–51.

[4] Walzak, M. J.; Flynn, S.; Foerch, R.; Hill, J. M.; Karbashewski, E.; Lin, A.; Strobel, M., J. Adhes. Sci. Technol. 1995, 9 (9), 1229–1248.

[5] Brondino C., Boutevin B., Parisi J., Schrynemackers J., J. Applaied Polym. Sci., 72, 1999, 611-620

[6] Reichmanis E, Frank C, O'Donnell J, Hill D. Radiation effects on polymeric materials. In: Reichmains E, Frank C, O'Donnell J, editors. Irradiation of polymeric materials. Washington, DC: American Chemical Society; 1993. p. 2.

[7] Nasef M, Saidi H, Dahlan K., Polym Degrad Stab 2002;75:85–92.

[8] Nasef MM, Dahlan KM., Nucl Instrum Meth Phys Res, B 2003;201: 604–14.

[9] M. Khayet, T. Matsuura, Ind. Eng. Chem. Res., Vol. 3, 2001, p. 379.

[10] S. Hietala, S. L. Maunu, F. Sundholm, Macromolecules, Vol. 32, 1999, p. 788.

[11] L. Fan, J. L. Harris, F. A. Roddick, N. A. Booker, Water Res., Vol. 35, 2001, p. 4455.

[12] K. Li, Chem. Eng. Technol., 2002, 25, 2.

[13] Järvinen K, Åkerman S, Svarfvar B, Tarvainen T, Viinikka P, and Paronen P., Pharm. Res. 1998;15(5):802–805.

[14] Yamaki T, Asano M, Maekawa Y, Morita Y, Suwa T, Chen J, Tsubokawa N, Kobayashi K, Kubota H, Yoshida M., Radiat Phys Chem 2003;67:403–7.

[15] S.Åkerman, P.Viinikka, B.Svarfvar, K.Jarvinen, K.Kontturi, J.Nasman, A.Urtti, P.Paronen J. Control. Release 1998, 50, 153.

[16] S.Åkerman, K. Åkerman, J. Karppi, P. Koivu, A. Sundell, P. Paronen, K. Järvinen, Eur. J. Pharm. Sci. 9, 1999, p. 137-143.

[17] J. Karppi, S.Åkerman, K. Åkerman, A. Sundell, K. Nyyssönen, I. Penttilä, Eur. J. Pharm. Biopharm. 67, 2007, 562-568.

[18] L.Y. Chu, Y. Li, J.H. Zhu, H.D. Wang, Y.J. Liang, J. Control. Release 2004, 97, 43.

[19] Guangqun Zhai, Lei Ying, E. T. Kang, K. G. Neoh, Macromolecules 2002, 35, 9653-9656

[20] Lei Ying, Peng Wang, E. T. Kang, K. G. Neoh, Macromolecules 2002, 35, 673-679

[21] Guangqun Zhai, E.T. Kang, K.G. Neoh, J. Membrane Science 217 (2003) 243–259

[22] Guangqun Zhai, Lei Ying, E. T. Kang, K. G. Neoh, J. Mater. Chem., 2002, 12, 3508–3515

[23] J. Hautojärvi, K. Kontturi, J.H. Näsman, B.L. Svarfvar, P. Viinikka, M. Vuoristo, Ind. Eng. Chem. Res. 1996, 35, 450-457.

[24] N. Betz, J. Begue, M. Goncalves, K. Gionnet, G. Déléris, A. Le Moël, Nucl. Instr. And Meth. B 2003, 208, 434-441.

CHAPTER 5

MODIFICATION OF POLYMERS IN SUPERCRITICAL CARBON DIOXIDE

5.1 Advantages of sc-CO_2 as reaction medium in a polymer modification process

The sorption of $scCO_2$ into polymers results in their swelling and changes the mechanical and physical properties of the polymers. The most important effect is the reduction of the glass transition temperature (Tg) of glassy polymers subjected to $scCO_2$, often simply called plasticization. The plasticization of polymers induced by $scCO_2$ has some impacts on many polymer-processing operations. These include viscosity reduction for polymer extrusion and blending, enhancement of the diffusion of additives through polymer matrices for impregnation and extraction, enhancement of monomer diffusion for polymer synthesis. The high viscosity is the major obstacle to the processing of high-molecular-weight polymers and usually this problem is solved by increasing the temperature and/or by the addition of plasticizing agents. However, increasing the temperature requires a higher energy consumption and may lead to thermal degradation. Added plasticizers usually remain in the product, thus affecting its properties and performance. The plasticizing effect of $scCO_2$ on polymers reduces their viscosity, presumably due to the reduction of chain–chain interactions and increasing the interchain distance. It also weakly solvates the molecular

segments of the polymer, thus acting as a "molecular lubricant". Such action also contributes to viscosity reduction in the bulk. It has been demonstrated that the polymer systems for which $scCO_2$ induced viscosity reduction include polymeric liquids (such as polysiloxanes), glassy polymers and their blends.

Previous studies[1-3] demonstrated that it is possible to perform chemical reactions within solid polymer substrates swollen by supercritical carbon dioxide and moreover to carry out chemical modifications in milder conditions than with standard methods of melt modification in extruders or batch mixers. This is extremely important for some polymers, such as poly(tetrafluoroethylene) (PTFE) and polypropylene (PP), for which modification in the melt is always accompanied by degradation. In a modification process of a solid polymer, after the infusion of the reagents (A, B in figure 5.1) into the matrix as a sc-CO_2 solution, the activation step can be run in the presence of CO_2 (in-situ) or subsequent to removal of the solvent by depressurization trapping the reagents in the polymer substrate (ex-situ).

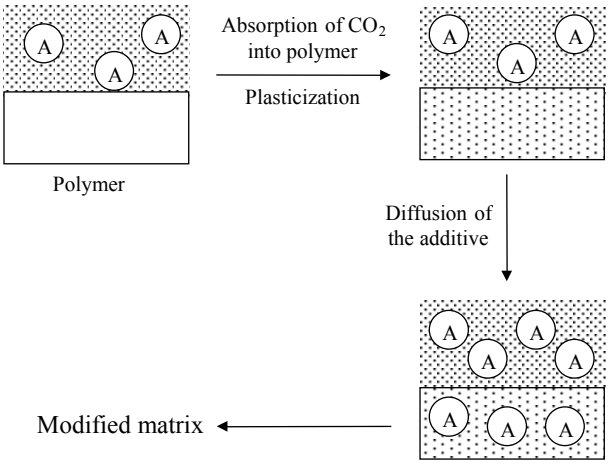

Figure 5.1- Schematic representation of chemical modification of a polymer enhanced by $scCO_2$

Moreover, $scCO_2$ offers several distinct advantages as reaction media in polymer modification process such as the possibility of adjusting the solvent strength over wide ranges by tuning temperature and pressure which control the degree of swelling and the partitioning of reagents between the swollen polymer matrix and the sc-CO_2 solution.

Even if CO_2 is a poor solvent for most polymers it swells them including those that are generally considered solvent-resistant. Several studies demonstrated that the diffusion rates in polymers plasticized by supercritical fluids (SCFs) are considerably increased rather than in no-swollen samples. For example, the work of Berens[4,5] demonstrates that the diffusivity of CO_2 increases by over 2 orders of magnitude when glassy polymers, e.g., poly(methyl methacrylate), are plasticized with CO_2. Other works of Berens[6] and Sand[7] have demonstrated that polymer substrates can be impregnated and modified by swelling the polymer with a solution of a monomer and an initiator in CO_2 followed by rapid venting of the SCF solution. In particular,

Berens used $scCO_2$ to impregnate polycarbonate with poly(ethylene glycol) diacrylate and a photoinitiator. Then, the system was depressurized and subjected to UV photolysis under the ambient condition, resulting in the reaction of acrylates within the matrix of polycarbonate. The final conclusion of the study of Berens on the glassy polymers was that sc-CO_2 plasticizing the substrates accelerates the kinetics of reagent absorption and that the amount of reagent which can be incorporated is limited by the solubility of the latter in the polymer matrix.

5.2 State of the art on radical grafting processes performed in sc-CO_2 on PVDF

Due to the aforementioned advantages, supercritical CO_2 as reaction medium represents a valid alternative to liquid solvents to modify porous membranes by graft copolymerization . In fact, in CO_2/polymer systems the monomers and initiator not only can diffuse into the pores of membranes fast and distribute uniformly, but also their distribution between the bulk of the polymeric substrate and the CO_2 rich fluid phase can be controlled.[8]

Few studies are reported in the literature concerning the graft copolymerization in $scCO_2$ of a backbone polymer using a free radical initiator. Among these, an interesting work is that of Clark et al[9] in which poly(vinylidene fluoride) was grafted with maleic anhydride (MA) monomer via a free-radical mechanism in supercritical carbon dioxide, using benzoyl peroxide (BPO) as free-radical initiator. The Authors suggested a grafting mechanism (figure 5.2) as result of the analysis of the grafted samples carried out by ^1H NMR spectroscopy. According to this mechanism in step 1 the free-radical initiator decomposes into primary radicals. The subsequent step is the hydrogen extraction from the PVDF polymer by a primary radical

(step 2) so producing a macrofluoroalkyl radical which, interacting with the double bond of the monomer, adds a monomer unit (step 3). Termination of the succinyl anhydride radicals occurs by chain transfer to a species containing extractable hydrogen, as shown in step 4. Moreover, the mechanism forecasts the existence of two competing reactions: the recombination (step 5) of the macrofluoroalkyl radical inducing the formation of stable by-products so penalizing the initiator efficiency (an unavoidable problem associated with free-radical polymerization and grafting mechanisms); and the dehydrofluorination that consists in a loss of fluorine from a carbon neighbouring the active center to form a carbon-carbon double bond (Step 6). The latter reaction competes with the addition of monomer units to macroradicals (step 3) so reducing the grafting efficiency.

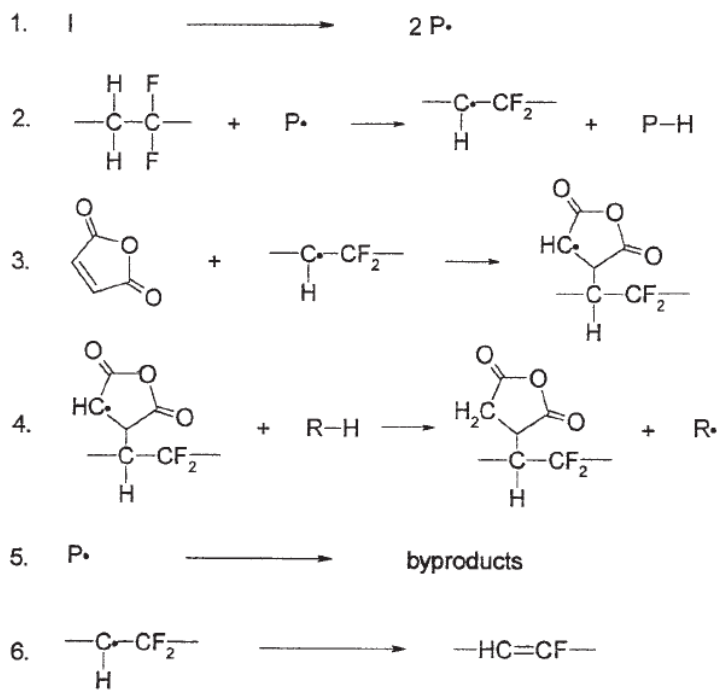

Figure 5.2- PVDF-g-MA grafting mechanism suggested by Lee et al[9]

Moreover, these authors studied the influence of the monomer and initiator loadings, of the reaction temperature and of the treatment time on the level of grafting. In following are reported some experimental results of Clark et al work as confirm of success of this method. Figure 5.3 shows the copolymer grafting level as a function of the initiator loading at two different values of monomer concentration. The results indicated that grafting level increases with maleic anhydride loading for each of the two investigated initiator loadings. The explanation for this trend was that increased monomer concentration promotes the addition of macroradicals to unsaturated monomer thus leading to the formation of grafted macromolecules. While,

concerning the influence of the initiator loading, it was possible to note that grafting level increased with small increases in BPO and then decreased at higher initiator loadings. The initial increasing trend with the peroxide concentration in the region of low BPO loadings was attributed to the prevailing effect of the increased radical concentration and a corresponding increase in hydrogen abstraction from the PVDF homopolymer. The subsequent decrease in graft level at higher BPO loadings was explained with the prevalence of radical reactions (such as steps 5 and 6) which compete with initiation and radical addition (step 2 and 3). A similar behaviour has been observed in the grafting of acrylic acid on polystyrene [10] i.e., where high concentrations of initiators were coupled with larger amount of PAA homopolymers synthesized in the reactor. This result suggested that for these systems the graft level can be optimized with respect to the initiator concentration.

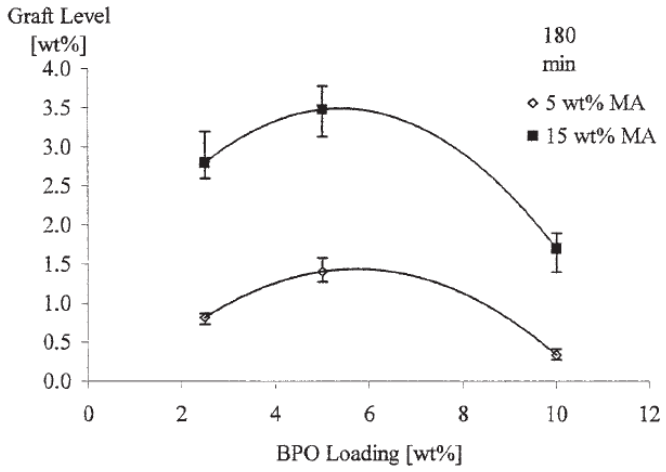

Figure 5.3- Effects of BPO and MA loadings on graft level. The experiments were carried out at 100°C for 180 min.

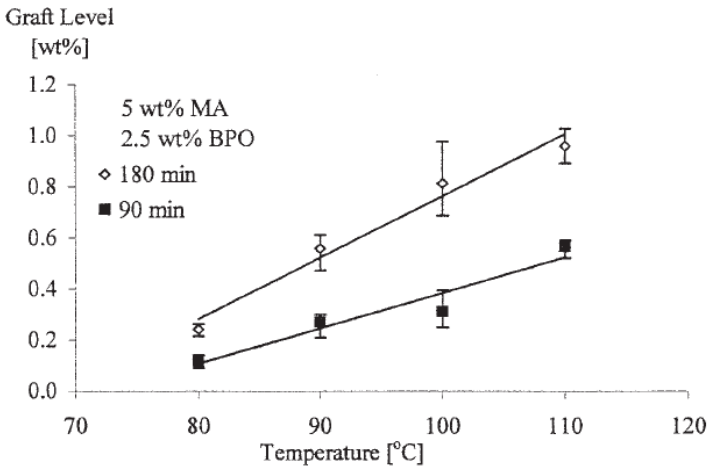

Figure 5.4- Effects of reaction temperature and treatment time on graft level. The experiments were carried out with 5 wt% MA and 2.5 wt% BPO.

Figure 5.4 shows the effect of temperature and time on the graft level exhibited by the copolymers. For both 90 and 180 min reaction times, increasing the experimental temperature increased the graft levels probably because of a major rate of radical generation.

Another important work that supports the possibility of performing grafting reaction on PVDF matrixes in $scCO_2$ is that of G. M. Qiu[11] in which the grafting of a copolymer composed by styrene (St) and maleic anhydride on PVDF porous membranes was successfully performed using supercritical CO_2 as solvent and benzoyl peroxide as initiator. In particular, they have immobilized the poly(maleic anhydride-alt-styrene) segments (SMA) onto the surface of the membrane and inside the pores, to improve the hydrophilicity and biocompatibility of the modified membrane as schematically represented in the following diagram.

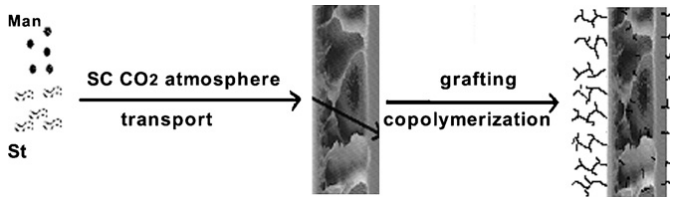

Figure 5.5- Schematic diagram of the graft copolymerization of MA/St on PVDF porous membranes in sc-CO_2.

Specially, they conducted the graft copolymerization of MA and St on the surface of PVDF porous membrane under different conditions in order to investigate the effects of monomer concentrations and soaking pressure on the degree of grafting (Dg). Figure 5.6 shows the effect of monomer concentration on the degree of grafting gravimetrically obtained. The results indicated that Dg increases remarkably with monomer concentration in the range of studied values. Indeed, since the monomer distributes between the $scCO_2$ fluid phase and the PVDF substrate phase during the initial soaking process (before to reach the final reaction temperature), an increase of monomer concentration favours the adsorption of the monomers on the surface of PVDF substrate, which enhances graft copolymerization of St/MA comonomers with PVDF backbone. It is worth evidencing that the monomer concentration studied in this work was relatively low (<0.07 mol/L), and saturation adsorption of the monomers could not be reached.

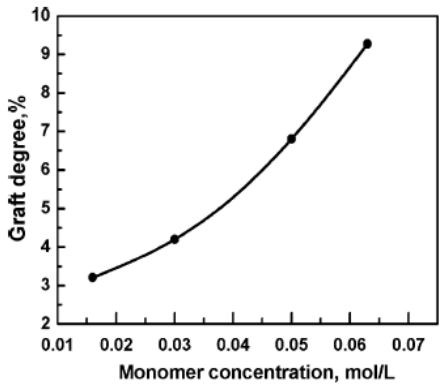

Figure 5.6- Effect of total monomer concentration on the level of grafting of MA/St on PVDF porous membranes in sc-CO_2 ([MA]/[St] mole ratio = 1:1, [BPO]/[monomers] = 1:300, P = 20.5MPa, T = 65 ◦C, reaction time = 20 hours).[11]

Another important result was the behaviour of the level of grafting with the soaking pressure of CO_2 (Figure 5.7). In particular, it was found that the degree of grafting of SMA on the surface of PVDF membrane increased as soaking pressure decreased. That could be attribute to the stronger solvent power of scCO_2 at higher pressures towards the lower molecular weight species. In this way, as consequence, the amounts of monomers and initiator adsorbed on PVDF substrate are reduced, so, penalizing the grafting reaction. This indicates that the Dg of the SMA can also be controlled easily by tuning the soaking pressure.

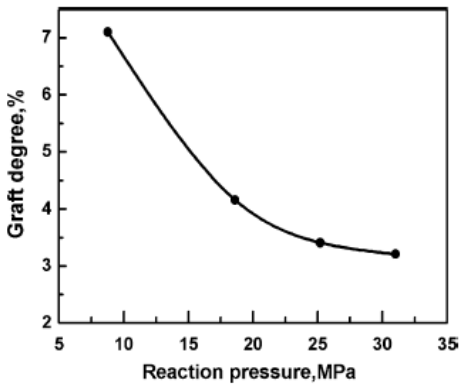

Figure 5.7 - Effect of fluid phase pressure on the level of grafting of MA/St on PVDF porous membranes in sc-CO_2 ([MA]/[St] mole ratio = 1:1, [BPO]/[monomers] = 1/300, total monomer concentration = 0.05 mol/L, T = 65 ◦C, reaction time = 20 hours).[11]

Another interesting work that attests the feasibility of use of carbon dioxide as solvent in a grafting process concerns the grafting of acrylic acid on polypropylene (PP) porous membranes.[12] Indeed, from this study resulted that acrylic acid can be grafted uniformly using scCO_2 as swelling agent of microporous PP membranes. In particular, the work was focused on the study of the influence on the final properties exhibited from the modified membranes of some operative parameters such as monomer concentration, soaking pressure and temperature, reaction time. Concerning the soaking pressure and monomer concentration the trends were both similar to those found in the works previously described in this section. On the other hand, it is interesting to show here the results obtained when the effect of the reaction time and of the temperature on the level of grafting were studied. Figure 5.8 shows the influence of the former parameter: the results indicated

that the Dg increases initially with reaction time and levels off in 24 hours. Authors attributes this behaviour to a total consumption of the initiator and/or to a total polymerization of acrylic acid after 24 hours even if mass balance on low molecular weight species supporting this hypothesis are not reported. Concerning the temperature it has been seen that Dg increases monotonously with the rise of soaking temperature (Figure 5.9), probably because density of CO_2 decreases with increasing temperature at fixed pressure. Therefore, the solvent power of CO_2 is enhanced as the temperature is reduced. As a result, more monomer is dissolved in the fluid phase at the lower investigated temperature, so a lower amount of AA is available for the grafting in the PP phase.

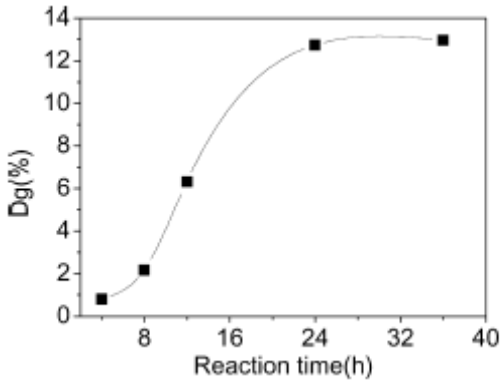

Figure 5.8- Effect of reaction time on degree of grafting with a monomer concentration of 0.19 mol/L (soaking conditions: 35°C, 8 MPa)[12].

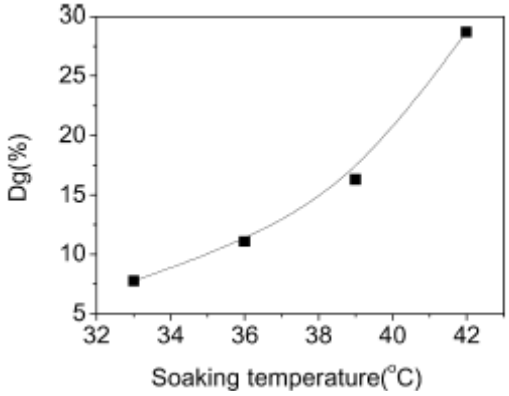

Figure 5.9- Effect of soaking temperature on grafting degree at 9.00 MPa with monomer concentration of 0.32 mol/l (reaction time: 24 h)[12].

References

[1] J.J Watkins, T.J. McCarthy, Macromolecules, 1994, 27, 4845.

[2] Kelyn A. Arora, Alan J. Lesser, and Thomas J. McCarthy, Macromolecules, 1999, 32, 2562

[3] O. Muth, Th. Hirth, H. Vogel, J. Supercrit. Fluids 2000, 17, 65.

[4] Berens, A. R.; Huvard, G. S. In Supercritical Fluid Science and Technology; ACS Symposium Series 406; Johnston, K.P., Penniger, J. M. L., Eds.; American Chemical Society: Washington, DC, 1989.

[5] Berens, A. R.; Huvard, G. S.; Korsmeyer, R. W.; Kunig, F. W., *J.* Appl. Polym. Sci. 1992, 46, 231.

[6] Berens, A. R.; Huvard, G. S.; Korsmeyer, R. W. U.S. Patent 4,820,752, 1986.

[7] Sand, M. L. U.S. Patent 4,598,006,1986.

[8] A.M.Van Herk, H. de Brouwer, B.G. Mander, L.H. Luthjens, M.L. Hom, A. Hummel, Pulsed electron beam polymerization of styrene in latex particles, Macromolecules 29 (1996) 1027–1030.

[9] Kelly Clark, Sunggyu Lee, Polymer Eng. Sci. 2005, 45, 631-639.

[10] S. Subramanian, "Solid Phase Graft Copolymerization of Acrylic Acid Onto Polystyrene," Thesis, University of Akron, Akron, Ohio (1995).

[11] Guang-Ming Qiu, Li-Ping Zhu, Bao-Ku Zhu, You-Yi Xu, Guang-Liang Qiu, J. of Supercritical Fluids 45 (2008) 374–383

[12] Yong Wang, Zhimin Liu*, Buxing Han*, Zexuan Dong, Jiaqiu Wang, Donghai Sun, Ying Huang, Guanwen Chen, Polymer 45 (2004) 855–860

CHAPTER 6

GRAFTING OF ACRYLIC ACID ON PVDF BACKBONE ASSISTED BY SUPERCRITICAL CARBON DIOXIDE

6.1 Introdution

In this work we have studied the preparation of hydrophilic and pH-sensitive PVDF membranes by thermally induced graft polymerization of acrylic acid (AA) on poly(vinilydene fluoride) using supercritical carbon dioxide as solvent and delivering agent to take benefit of $scCO_2$ properties i.e. biocompatibility, easy recovery from the processed polymer by depressurization and good wettability of inner volume of pores. Initially, a pre-oxidation method of the membrane was studied in order to generate peroxide and hydroperoxide groups on the surface, which potentially represent the grafting polymer sites after thermal decomposition of the peroxy bond (O-O). Then another approach was to use a radical initiator as source of free radical to induce radical sites in the solid matrix and perform the grafting reaction. In particular the initiator selected for this study was benzoyl peroxide because it is used in several studies (see chapter 5) for the grafting of vinyl monomers on PVDF in supercritical carbon dioxide. In this way it was possible to exploit the properties of sc-CO_2 as solvent for radical processes. Indeed, it is known that initiator efficiency is improved in sc-CO_2 because solvent-solute cage effects are negligible relative to liquid solvents, and sc-CO_2 doesn't act as a chain transfer agent in radical reactions. The experimental work was opportunely planned in order to understand the

influence of some operative parameters, such as reaction time, monomer and initiator concentration and fluid phase density, on the final properties exhibited of the modified membranes. Moreover, it was investigated the chemical structure of the pristine and modified membranes by ^{1}H NMR and ^{19}F NMR to collect information aimed to hypothesize a possible grafting mechanism. Finally, preliminary results collected from a study on the controlled release of a model drug from a selected grafted membrane at different pH values, will be briefly described.

6.2 Pre-oxidation of the pristine membrane

6.2.1 Materials

Durapore PVDF hydrophobic membranes were used as model substrates. They have an average pore size of 0.22 μm, a diameter of 47 mm, a thickness of about 100 μm and 75% vol/vol porosity. CO_2 was Air Liquide 99.998 pure and O_2 99.5 pure was purchased from Rivoira. All the other chemicals were purchased from Aldrich without further purification.

6.2.2 Experimental procedures and results

The first route used in this work to impart acid functionalities to the PVDF pristine membrane consisted in the ozonization of the substrate to induce the production of peroxide and hydroperoxide units on the pores surface. Initially, it was thought to generate ozone (O_3) according to the work of Otomo[1] et all, in which the authors generated this specie by irradiation of pressurized O_2/CO_2 mixtures under KrF excimer laser irradiation at 248 nm.
To carry out the experiments it was used a constant volume stainless steel high pressure view cell, with a nominal volume of 50 mL and equipped with

two sapphire windows with 180° orientation. The cell containing the pristine membrane was initially purged for about twenty minutes to remove the air and then the oxygen was introduced. Consecutively it was charged CO_2 by mean an ISCO syringe pump. Both gases were charged by weighing the amount introduced up to a prefixed level corresponding to a desired value of density. Then the cell was heated up to 40°C by an heating tape connected to a temperature control system. At set-point temperature two screen lamps, put outside the two windows of the cell, were lighted. The lamps (total power of 14 W) generate a UV radiation centred at 254 nm. The experiments were carried out by irradiation of a supercritical O_2/CO_2 mixture with total molar density of 12 mol/L at 10%mol of oxygen. Anyway, after several efforts, changing the time of exposition up to a maximum of 8 hours, it was not found the presence in the IR spectra of the irradiated membrane of any peak corresponding to the peroxide or hydroperoxide groups. Moreover it was investigated the presence of ozone in the irradiated mixture by a test of ozone[2]. It consisted in the preparation of a liquid mixture containing an aqueous solution of potassium iodide (KI in excess) and chloroform ($CHCl_3$) at 50%vol, which have to be contact with the gaseous mixture under study, maintaining the system under a continuous stirring. Indeed, according to the following reaction:

$$O_3 + 2KI + H_2O \rightarrow O_2 + I_2 + KOH$$

the ozone, eventually produced in the gaseous mixture, have to react with KI to generate iodine. The formation of iodine is evident by the colour change (from colourless to dark violet) of the chloroform phase (stratified in bottom of glass) which extracts iodine from the upper aqueous phase of KI.

After bubbling the gaseous mixtures in the test solution it was not found any colour change in the chloroform phase, so it was deduced that the method used was not appropriated to generate ozone. In particular, that was imputed to a too lower power of the lamps used for the irradiation experiments.
Therefore, the subsequent step of the work was that to use directly an ozone generator for aquarium (Ozone Aqua Medic 300) which is able to produce in continuous 600 mg/h of ozone if it is fed with oxygen. In particular, the pre-oxidation of the membrane was tentatively performed by delivering a flux of oxygen of 0.1 L/min into the ozone generator which converts about 5% of the stream in ozone. The mixture O_2/O_3 was fed to a batch reactor (see description in section) containing the pristine membrane and the times of exposition were changed from few minutes up to 24 hours. After the treatment the membrane was analyzed to IR-ATR spectrophotometer but in the spectrum were no differences rather than the spectrum of pristine membrane. That suggested that very presumably the ozone concentration generated by this instrument it was not sufficient to induce the oxidation of the pristine PVDF matrix. At this point, the further step was to use a radical initiator as source of free radicals to initiate the radical grafting of acrylic acid.

6.3 Grafting induced by benzoyl peroxide

6.3.1 Materials

Aforementioned Durapore PVDF hydrophobic membranes were used as model substrates. Acrylic acid 99% anhydrous (with 200 ppm of monomethyl ether hydroquinone as inhibitor) and ethanol (ACS, 99.8%) were purchased from Aldrich; CO_2 was Air Liquide 99.998 pure. All these chemicals were used without further purification. Benzoyl peroxide (BPO),

purchased from Aldrich (75% remainder water, USP grade), was recrystallized from methanol.

6.3.2 Experimental apparatus and procedures

The experiments were carried out in an AISI 316 fixed volume (27 mL in the completely assembled setup) batch reactor, which details are shown in figure 3.1. The proper amounts of AA and initiator were charged in the reactor together with the PVDF pristine membrane, the vessel was then purged by a controlled flow rate of CO_2 maintained for at least 20 minutes to remove air. After sealing the reactor, CO_2 was added at room temperature by using an ISCO syringe pump according to the scheme represented in figure 3.2. The total amount introduced was measured weighting the vessel with an electronic scale (Sartorius LP 8200S, precision 0.01 g). The vessel was then heated at the reaction temperature (T = 65°C), by an heating tape connected to a temperature controller, and continuously stirred by a magnetic bar, whereas the pressure was recorded by means of the pressure transducer. The time interval to reach the operative temperature was roughly 20 min in each run. At the end of the reaction the reactor was cooled in an ice bath to room temperature and slowly depressurized.

The reactor was then opened and the membrane was recovered, washed at room temperature with ethanol for 1 h to remove unreacted monomer and initiator and at 90°C, in a closed vessel, with the same solvent for 2 h to extract PAA homopolymer formed during the reaction. Then the grafted membrane was dried under vacuum at 40°C overnight. Such procedure was repeated until constant weight of the sample was obtained. At this point it was assumed that the unreacted monomer and PAA homopolymer have been

completely removed. Finally, the degree of grafting (DG) was gravimetrically estimated according to the following equation:

$$DG\ (\%) = 100\ (W_1 - W_0)/W_0 \qquad 6.1$$

where W_0 represents the weight of virgin PVDF membrane and W_1 the weight of modified membrane at the end of aforementioned washing procedure.

6.3.3 Characterization's technique

FTIR spectra of the membranes were obtained from a Perkin-Elmer Spectrum 2000 Explorer FTIR using the attenuated total reflection (ATR) technique, which operates by measuring the changes that occur in a totally internally reflected infrared beam when the beam comes into contact with a sample (Figure 6.1).

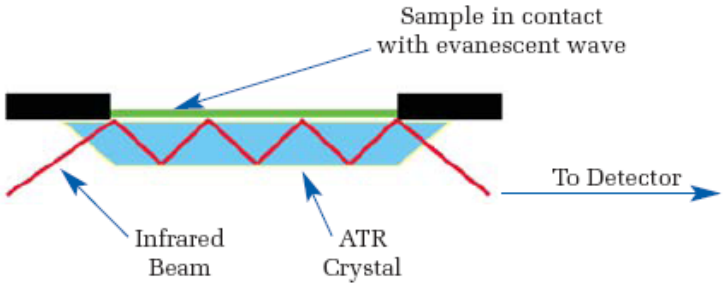

Figure 6.1- A multiple reflection ATR system.

An infrared beam was directed onto ZnSe, an optically dense crystal with a high refractive index. This internal reflectance creates an evanescent wave that extends beyond the surface of the crystal into the sample held in contact

with the crystal. This evanescent wave protrudes only a few microns (0.5 μ - 5 μ) beyond the crystal surface and into the sample. Consequently, there must be good contact between the sample and the crystal surface. In regions of the infrared spectrum where the sample absorbs energy, the evanescent wave will be attenuated or altered. The attenuated energy from each evanescent wave is passed back to the IR beam, which then exits the opposite end of the crystal and is passed to the detector in the IR spectrometer. The system then generates an infrared spectrum. Each spectrum was collect by cumulating 6 scans at a resolution of 1 cm^{-1} using a near-IR fast recovery deuterated triglycine sulphate detector.

The surface morphology of the matrixes was studied by the scanning electron microscopy (SEM), using a Philips scanning electron microscope. The membranes were putted on the sample stubs by means of double-sided adhesive tapes and then were sputter-coated with gold to a thickness of about 200 Å.

Calorimetric analyses of copolymers were performed with a PerkinElmer Jade-DSC calorimeter. A pre-weighed amount of the copolymer (c.a. 3-5 mg) was loaded into the aluminium pan. Then, the sample pan was sealed with an aluminium lid pressed slightly using a metal plunger and placed in the differential scanning calorimeter (DSC), together with an empty pan used as a reference and both were holder under a N_2 flow of 20 ml/min. The sample was heated twice from 18 °C up to 220 °C with a heating rate of 10 °C/min. The cooling rate between the two scans was 10 °C/min too. Since enthalpy or heat capacity changes in the sample cause a difference in its temperature relative to the reference, the instrument records this temperature difference and related that to enthalpy change in the sample. Melting enthalpies, ΔH_m, were determined evaluating the peak areas and melting temperatures, T_m, at the maximum of the peaks. The percent of crystallinity

of the grafted and pristine membranes, χ_c, were then calculated from melting enthalpies values by using equation 5.2 following:

$$\chi_c = \frac{\Delta H_m \times 100}{\Delta H_{100\% cristalline}} \qquad (6.2)$$

where $\Delta H_{100\%cristalline}$ is the heat of fusion of pure crystalline PVDF, which is reported to be 104.6 J/g.[3]

The thermal stability of the copolymers was studied by thermogravimetric analysis (TGA) using a Perkin-Elmer STA 6000 simultaneous thermal analyzer. Samples were inserted in a small crucible made of refractory material, ceramic material, which is chemically unreactive towards most materials. The analysis were performed under a stream of nitrogen, in order to avoid the build-up of decomposition products in the immediate vicinity of the sample, having a flow rate sufficient to sweep volatiles from the furnace, but not so fast as to cool the sample. The samples were heated from 30°C to 700°C at a rate of 10°C/min and the diminution of their weight was recorded by the instrument as temperature function. Generally the reactions by which polymers degrade are: main-chain scission, side group scission and elimination. They usually result in the evolution of volatile products with an accompanying mass change. Also cyclization and cross-linking are possible degradation processes but rarely result in any change of sample mass unless they occur in conjunction with the previous ones.

The water permeability of grafted membranes was investigated by measuring the fluxes through the membranes of aqueous solutions at different values of pH. Before the measure the membrane was immersed in an aqueous HCl solution of a predetermined pH value for about 30 minutes. Then it was inserted in a vacuum filtration unit and a known volume of aqueous HCl

solution of the same pH value was added to the filtration system. The ionic strength of the solution was adjusted to 0.1 mol/l by addition of sodium chloride. The flux was calculated from the volume of solution permeated per unit time and unit area of membrane interested to the flux.

The chemical structure of the samples were investigated by ^{1}H NMR and ^{19}FNMR analysis using dimethylformamide-d_7 as solvent. The analysis were performed by the research group of Prof. Ameduri in Montpellier (France). The NMR spectra were recorded on a Bruker AC 400 instruments, using tetramethylsilane (TMS) and $CFCl_3$ as the references for ^{1}H and ^{19}F nuclei, respectively. Coupling constants are given in hertz (Hz) while the chemical shifts in part per million (ppm). The experimental conditions for recording ^{1}H NMR spectra were the following: flip angle 90°, acquisition time 4.5 s, pulse delay 2 s, number of scans 128. While the ones for ^{19}F NMR were: flip angle 30°, acquisition time 0.7 s, pulse delay 2 s, number of scans 512 and a pulse width of 5 ms.

The caffeine release experiments were studied in vitro at 37±0.2 ◦C by dipping the membrane containing the drug in 50mL of an aqueous buffer solution prepared mixing suitable amounts of sodium chloride, potassium phosphate monobasic, phosphoric acid (for buffer solution at pH 2.5) and sodium phosphate bibasic (for pH 6.8) in water. The solution was stirred by a magnetic stir bar and the drug release was monitored using a PC controlled Avantes fiber optic UV–vis spectrophotometer equipped with a DH2000 light source and a reflection dip probe (optical path 1 cm) that was immersed in the aqueous phase. All connections between components and optical fibers were made with SMA 905 connectors. The signal from each spectrometer was recorded as transmitted intensity and converted in absorbance spectra by the spectrometer manufacturer's software (AVA-Soft version 5, Avantes) running on the PC, using a previously recorded blank

spectrum of the buffer solution at the typical operating conditions. The absorbance of caffeine was located at 272 nm.

6.3.4 Investigation of the phase behaviour of the reaction system

The phase behaviour of the CO_2/AA mixture was investigated under conditions adopted to perform grafting reactions, by visual observation in a constant volume stainless steel high pressure view cell, with a nominal volume of 50 mL and equipped with two sapphire windows with 180° orientation (1.25 in diameter). The vessel had three ports equipped with Swagelock male connectors; one of them was closed by a screw cap and used for loading of the liquid component, a second port was connected to a valve and a pressure transducer, the third male connector was used to insert a Pt100 thermal sensor. The temperature control was ensured by inserting the cell in an electronically controlled heating tape, whereas the pressure was recorded by means of the pressure transducer. After the loading of a proper amount of AA, the cell was purged from air with a small flow rate of carbon dioxide inserted from the valve, maintaining the cap open. After venting, the cell was closed and a weighed amount of CO_2 was loaded up to reach the desired fluid phase density.

The cell was then heated slowly at 65°C and, just after the fluid phase was thermally equilibrated, it was visually observed to determine the number of phases. Because to these measurements it was confirmed that the mixture CO_2/AA was single phase in all the adopted experimental conditions, in agreement with data reported in literature[4].

The graft copolymerization of AA on the PVDF porous membrane was performed under different experimental conditions in order to investigate the effects of monomer and initiator concentrations, reaction time and fluid

phase density on the grafting level and on the final properties exhibited of the modified membranes.

6.3.5 Preliminary experimental investigation

The first step of the experimental work was to analyze some characteristic properties of the pristine membrane, of a membrane subjected to a treatment with only CO_2 and one treated with CO_2 in presence of the radical initiator to understand how the fluid phase and the initiator influence separately the final properties of the matrix. In particular, all of them were characterized by DSC analysis.

	First Heating		Second Heating	
RUN	**T_m (°C)**	**χ_c**	**T_m (°C)**	**χ_c**
1	163.3	45.7	159.4	53.9
2	164.9	43.1	159.0	55.7
3	162.9	44.8	158.6	54.3

Table 6.1 – Thermal cristallinity on first and second heating of (1) PVDF pristine membrane, (2) Membrane pressurized at ρ_{CO2} = 0.5g/mL for 16 h, (3) membrane treated with BPO at molar concentration of 0.15 mM for 16 h and at ρ_{CO2} = 0.5g/mL.

It is well known that PVDF is a partially crystalline polymer arising from its highly symmetrical structure. When it is synthesized by radical polymerization in supercritical CO_2 the degree of cristallinity of the polymer generated in the polymerization process (χ_c on first heating) is usually higher than that of the polymer obtained after the cooling of the melt (χ_c on second

heating) very presumably because of the plasticization effect of the carbon dioxide that improves the mobility of the macromolecular chains and enhances their rate of packing in a more ordinate structure. In this case the behaviour of the pristine membrane is opposite, that is χ_c on first heating was lower than that on second heating. The reason could be attributed to the phase inversion method used by Millipore to produce the membrane. Indeed, during the cooling scan probably the PVDF chains have a sufficient time to reorganize themselves in a more ordinate structure.

Concerning the crystalline content of the two membranes subjected to the above mentioned treatments, the results shown in Table 6.1 (runs 2 and 3) suggested that the fluid phase as well as the initiator do not cause crystallinity changes of the original matrix, on first as well as on second heating. The surface morphology of the pristine membrane was also investigated by SEM analysis and it presents with thin fibrils and a relatively high porosity (Figure 6.2). As comparison in figure it is also shown the surface magnification of the membrane treated with CO_2, which doesn't show appreciable differences.

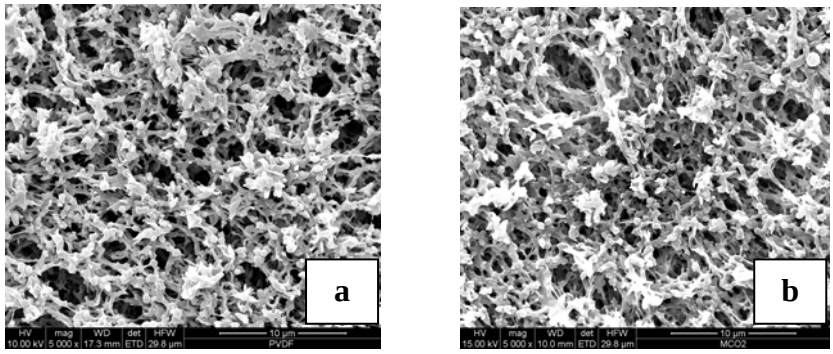

Figure 6.2 – Compare of morphology of a pristine membrane before (a) and then the treatment with CO_2

After these first investigations, a set of grafting experiments were performed and the modified membranes were washed according the aforementioned washing procedure (standard procedure). Before to carry out any membrane characterization, it was important to know if this procedure was efficient for a total removal of the PAA homopolymer, which is inevitably generated during the process. Accordingly, a modified membrane, initially washed with the standard procedure, was subjected to long and severe washing treatments. In particular, it was washed two times with ethanol at 110°C overnight and dried under vacuum at 50°C. Since, the membrane weight at the end of these treatments was the same of that measured after the standard washing procedure, it seems reasonable to conclude that the latter washing procedure is sufficient to remove all the PAA. This result permitted us to assume that the measured DG was really corresponding to the weight increase of the original matrix due to the PAA chains chemically linked to the PVDF matrix.

6.3.6 Theorical considerations on a plausible grafting mechanism

FT-IR/ATR measurements were used to investigate the structure of pristine and modified PVDF membranes. In figure 6.3 are reported the FT-IR/ATR spectra of the virgin membrane, a membrane treated with BPO (run 3, Table 6.1), a modified matrix having a DG = 10.3 % and the spectrum of the homopolymer PAA. The spectrum of pristine matrix exhibits the characteristic peaks of PVDF[5,6] such as that of CF_2 symmetric stretching at 1275 and 875 cm^{-1}, and that of CH_2 wagging deformation at 1409 and 1074 cm-1. After reaction with the initiator the IR spectrum doesn't seem changed. In particular in the spectrum it wasn't detectable the presence of a peak at 1670cm^{-1} characteristic of CH=CF group[7], which was detected in a

previous study (see section 5.2) of radical grafting on PVDF porous membrane of maleic anhydride in sc-CO_2 using BPO as initiator. Moreover that peak is absent in all the spectra of the grafted membranes. Therefore it seems possible to assume that in the conditions adopted in this study the matrixes were not subjected to dehydrofluorination reaction. The spectrum of the grafted membrane (Figure 6.3, c) is characterized by an absorption peak at around 1720 cm^{-1} which is indicative of the stretching of carbonyl groups[5,6] (C=O). This peak was present in all the spectra of the grafted membranes and its absorbance, relative to that of CF_2 peak at 875 cm^{-1}, was proportional to the grafting level of the membranes.

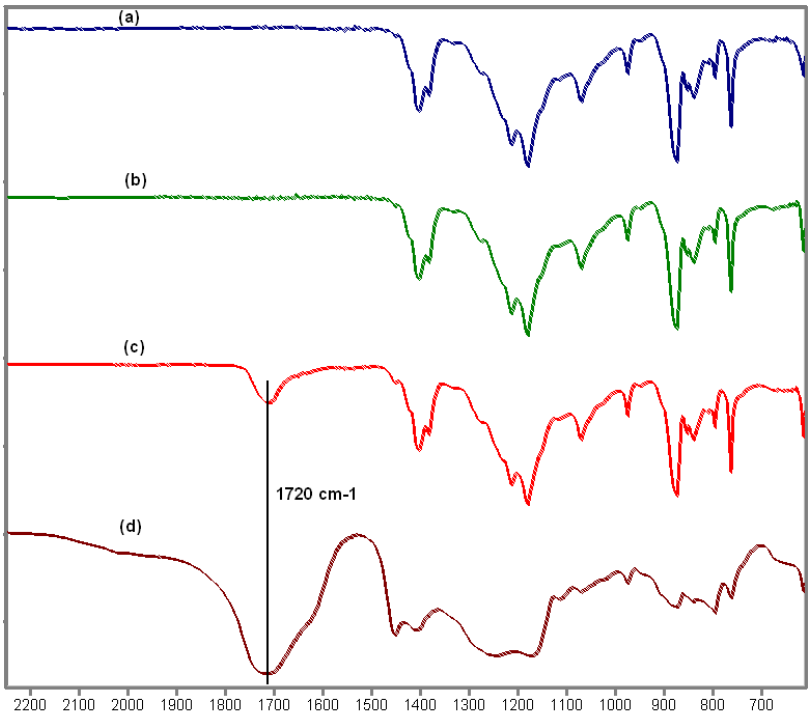

Figure 6.3– FT-IR/ATR Spectra of (a) pristine PVDF, (b) membrane treated with BPO (run 3, Table 6.1), (c) membrane with a DG of 10.3%, (d) PAA homopolymer

From the NMR analysis it was possible to collect information on the chemical microstructure changes of the membrane as consequence of the soaking treatment with CO_2, the reaction with only BPO in sc-CO_2 and the grafting reaction in presence of the monomer. The ^{1}H NMR spectrum of the original matrix is shown in Figure 6.4-a. It presents a multiplet 3.03 ppm, corresponding to C**H$_2$** of the (C**H$_2$**-CF_2) units, which are characteristic of the normal head-to-tail addition of VDF units in the poly(vinylidene fluoride)[7] and a multiplet centered at 2.35 ppm corresponding to that of the unit -CF_2-C**H$_2$**-C**H$_2$**-CF_2-characteristic of the tail-to-tail addition.[7] The DMF peaks are centred at 2.92 and 2.75 ppm, while the peak at 3.5 ppm is attributable to the water probably contained in the solvent.[8] In the case of the membrane soaked with scCO2 in the absence of monomer and initiator (Figure 6.4-b) a small shift of the peaks of about 0.04 ppm to higher values of ppm was noted probably due to a concentration effect. For a similar reason the spectrum of the membrane contacted with BPO alone in scCO_2 results shifted of 0.2 ppm. When ^{1}H NMR spectrum of a sample treated in the presence of AA is considered (Figure 6.5-A, curve 2) it is evident a peak at 1.7 ppm corresponding to the CH_2 of the –CH_2-CH-COOH- unit of the PAA. The other signal at 2.2 ppm characteristic of the CH were not detectable. Moreover, in the region at higher ppm (range from 12 to 14 ppm) appears a small signal for the carboxylic protons COO**H** (Figure 6.5-B)[7].

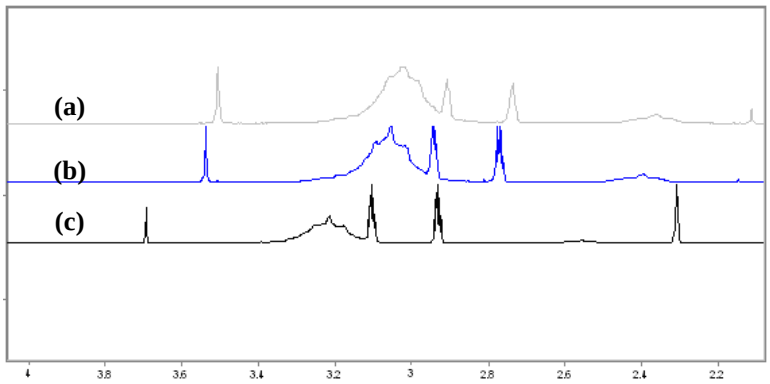

Figure 6.4 – 1H NMR spectra in DMF-d7 of (a) pristine membrane, (b) membrane soaked with CO_2, (c) membrane contacted with BPO in sc-CO_2.

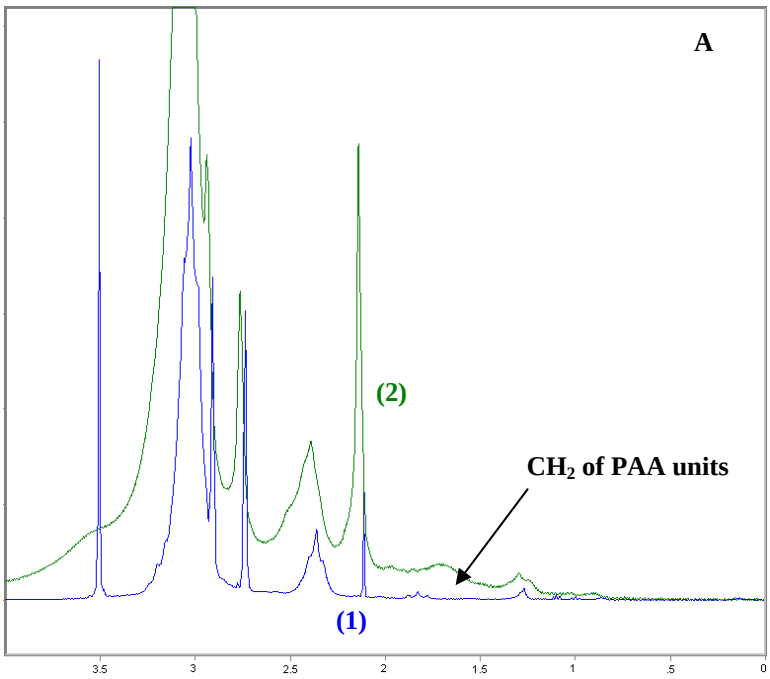

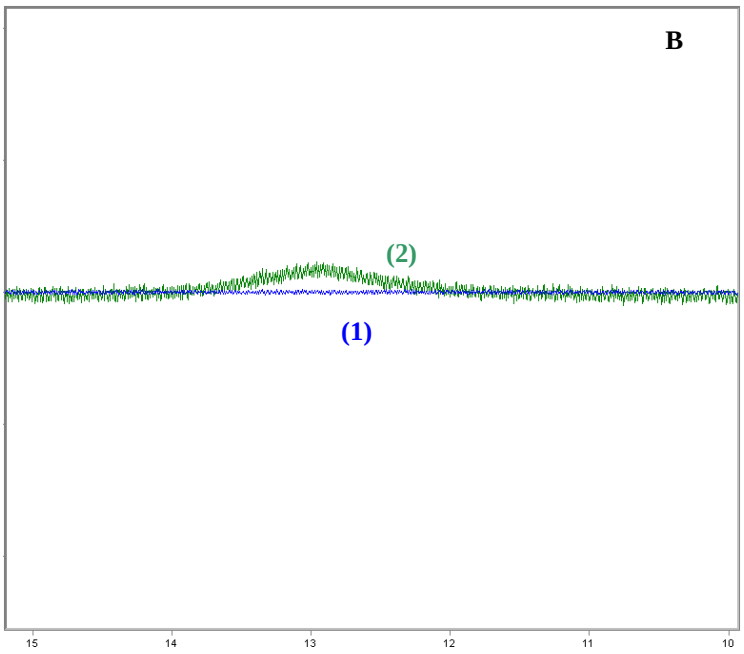

Figure 6.5 –A) ^{1}H NMR spectra in DMF-d7 and B) Magnification of the range in which it is present the signal of the COO**H** of (1) pristine membrane, (2) membrane with a DG = 14.8%, (50°C, [BPO] = 0.5 mM, [AA] = 0.2M, ρ_{CO2} = 0.5 g/mL, 16 h).

The ^{19}F NMR spectra of pristine and modified membrane contain peaks in the range -91, -96 ppm related to CF_2 groups of -$CH_2C\mathbf{F_2}$-$CH_2C\mathbf{F_2}$- sequences assigned to head to tail additions of VDF units and two peaks centred between -114 and -117 ppm corresponding to the -$CH_2C\mathbf{F_2}$-$C\mathbf{F_2}CH_2$- sequence arising from the head-to-head additions of VDF units.[7]

When looking at membranes with gravimetric grafting of 8 and 15 % it seems that peaks are broader, moreover membranes with the highest loading have peaks shifted of about 0.2 ppm (Figure 6.6). Even if the shift could be few meaningful, the broadening of the peak could indicate the modification of the local environment of CF_2 units for the presence of the PAA linked units. Moreover in ^{19}F NMR spectra were not detectable the signals ranging

from -120 to -130 ppm assigned to CH=C**F** groups[7], which represent a potential source of matrix degradation.

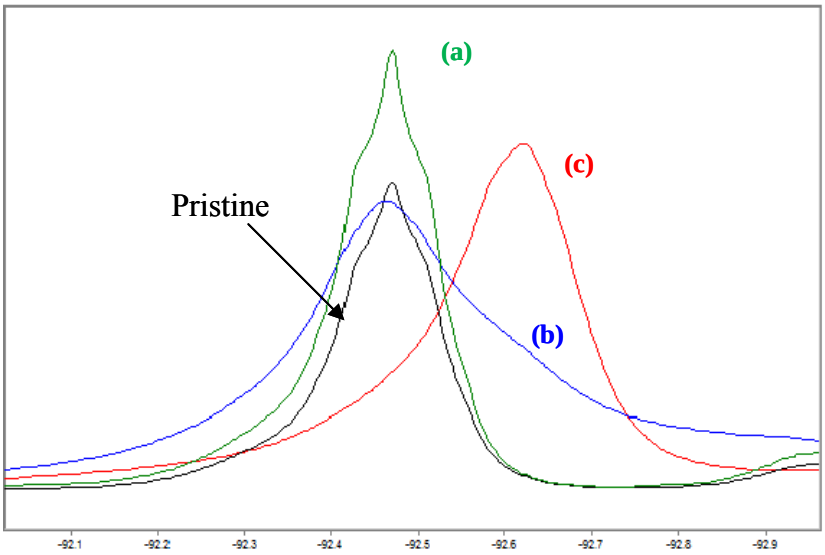

Figure 6.6 – ^{19}F NMR spectra in DMF-d7 of the pristine membrane and of (a) membrane treated with BPO in sc-CO_2, (b) membrane with a DG = 8.5%, (c) membrane with a DG = 14.8%.

According to the results obtained in this study from FT-ATR, ^{1}H and ^{19}F NMR analysis and in the existing literature[4] it was possible to draw an hypothetic grafting mechanism. In particular:

Thermal decomposition of the initiator:

$$\Phi - COO - OOC - \Phi \xrightarrow{\Delta T} 2\ \Phi - COO^{\bullet} \qquad 6.2$$

Initiation:

$$\Phi - COO^{\bullet} + \ -CF_2 - CH_2 - \ \longrightarrow \Phi - COOH + \ -CF_2 - CH^{\bullet} - \qquad 6.3$$

Propagation:

$$-CF_2 - CH^{\bullet} - \ + \ n\ (CH_2 = CH - COOH) \longrightarrow \ -CF_2 - \underset{\displaystyle COOH - CH^{\bullet} - CH_2 - [COOH - CH - CH_2]_{n-1}}{\underset{|}{CH}} - \qquad 6.4$$

Termination:

$$\sim\!\!\sim\!\!\sim - CH_2 - CH^{\bullet} - COOH + RH \longrightarrow -CH_2 - CH_2 - COOH + R^{\bullet} \qquad 6.5$$

Since the system under study, composed by a solid matrix swollen in a supercritical medium, is an heterogeneous system, the initiator and monomer molecules will be partitioned between the two phases: the supercritical and the polymer phase. Concerning the thermal decomposition of the BPO (eq. 6.2), the initiator radicals active to initiate the grafting process will be mainly that produced in the continuous phase (sc-CO_2) because the initiator molecules contained within the solid matrix will be prevalently subjected to the cage effect. Therefore the extraction of the hydrogen radicals from the PVDF matrix (eq. 6.3) will occur almost exclusively by the initiator radicals generated in the continuous phase whose mass transfer rate into the polymer phase is related with interphase area of the membrane. Moreover, the generation of the grafting sites can occurs on the pores surface as well as within the amorphous domains of the matrix, and according the results obtained in this study we suppose that the relative amounts depend very presumably on the experimental conditions used to carry out the reaction.

According the mechanism above shown, successively, the primary radical on the PVDF chain reacts with a molecule of AA to form the radical growing chain (eq. 6.3), which then continues its propagation by addition of other molecules of the monomer (eq. 6.4). We suppose that the latter reactions are

favoured in a supercritical medium because it enhances the kinetics of diffusion of the monomer molecules in the polymer matrix. Finally the termination of the radical macromolecular chain can occur by transferring the radical to another specie, in figure indicated as RH (eq. 6.5). This specie could be a polymer chain or a water molecule present as impurity in acrylic acid.

6.3.7 Study of the influence of the reaction time

Several experiments were performed changing the reaction time, maintaining constant all the other operative conditions. The trend of the degree of grafting DG obtained at different reaction time is plotted in Figure 6.7. To obtain an appreciable level of grafting a reaction time of 8 hours was necessary, it was observed a rapid increase of DG after 16 hours. This behaviour could be attributed to the fact that as reaction time increases the modification moves from the surface to the inner part of the matrix where autoacceleration effects can be possible owing to occlusion phenomena.

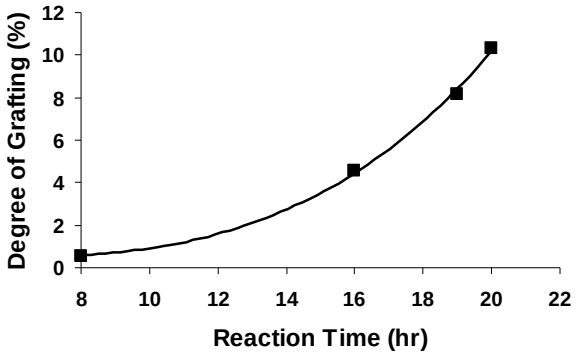

Figure 6.7 - Effect of reaction time on the degree of grafting ([BPO]=0.15mM, [AA]=0.2M, ρ_{CO2}=0.5g/mL, 65°C).

A DSC analysis was carried out to study the modification of crystallinity of the polymeric samples. The results of DSC analysis of the modified membranes at different reaction time indicated that the structural symmetry of pristine PVDF membrane was partially destroyed as a consequence of the graft copolymerization with AA, resulting in a decrease of the crystallinity on first heating with the reaction time (see Table 6.2). Also the crystallinity on second heating decreased with reaction time but in a more prominent way.

			First Heating		Second Heating	
RUN	**Time (h)**	**DG (%)**	**T_m (°C)**	**χ_c**	**T_m (°C)**	**χ_c**
1	8	0.6	163.3	39.9	158.2	53.9
2	16	4.6	163.8	37.7	158.1	48.7
3	19	8.2	163.2	33.3	158.0	40.9
4	20	14.8	162.7	34.7	157.9	38.3

Table 6. 2. Degree of cristallinity (χ_c) on first and on second heating of the grafted membranes: effect of the reaction time. ([BPO]=0.15mM, [AA]=0.2M, ρ_{CO2}=0.5g/mL, T=65°C).

The morphologies of the grafted membranes (runs 1 to 4) were investigated to find a correlation with the reaction time employed to modify the original matrix. The magnifications of the grafted samples (Figure 6.8) show that morphology is significantly different from that of pristine PVDF (Figure 6.2) when time adopted to carry out the experiments was higher than 16 hours.

Indeed, just in those cases the surface seems to have a lower number of pores with decreased sizes and fibrilles tended to become thicker.

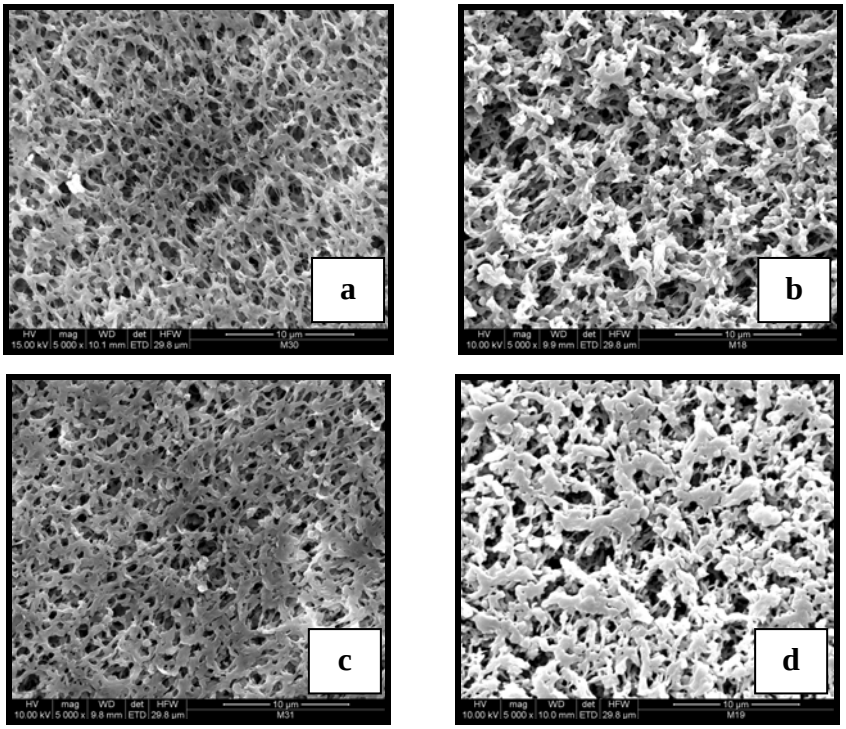

Figure 6.8– SEM micrographs of the grafted membranes processed for 8 h (a), 16 h (b), 19h (c), 20h (d)

6.3.8 Influence of the monomer concentration

Generally, in a grafting system when monomer concentration feed in the reactor increases the final degree of grafting of the polymer progressively increases because the increased monomer concentration promotes the addition of unsaturated molecules of monomer to the macroradicals thus leading to the formation of longer grafted macromolecules. In this case a

not-monotonous trend was obtained in the concentration range examined. The effect of the monomer (AA) concentration on the level of grafting is shown in figure 6.9. In particular, below 0.05 mol/l of AA in the feed the DG increases with the monomer concentration, decreases for higher values and finally increases again for AA concentration higher than 0.2 mol/l. This behaviour could be tentatively attributed to the competition between AA homopolymerization and graft copolymerization with PVDF, which mechanisms and kinetics are explained in section 4.2.1.

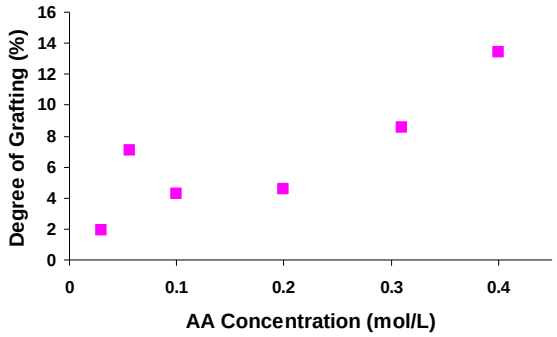

Figura 6.9 -Effect of AA concentration on DG ([BPO]=0.15mM, ρ_{CO2}=0.5g/mL, 65°C, 16 h).

Plotting the crystalline content of the investigated samples versus monomer concentration it is possible to note that both χ_c are almost unchanged for less than a drift of +/- 5 % which could be within the experimental uncertainty of the analytical technique.

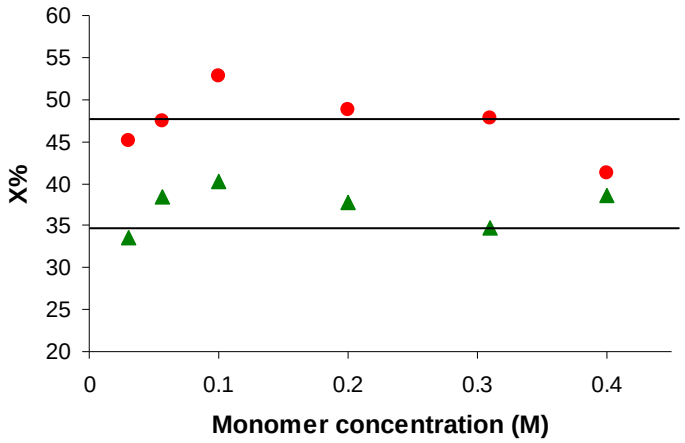

Figura 6.10 - Effect of the AA concentration on the degree of cristallinity (X%) calculated (▲) on first heating and (●) on second heating of the grafted membranes.

The surface morphology of the samples exhibits appreciable differences only processing the membrane with an initial monomer concentration upper than 0.3 mol/L, in fact looking at the corresponding membrane micrographs (Figure 6.11, micrographs e and f) it seems that the pores are more occluded.

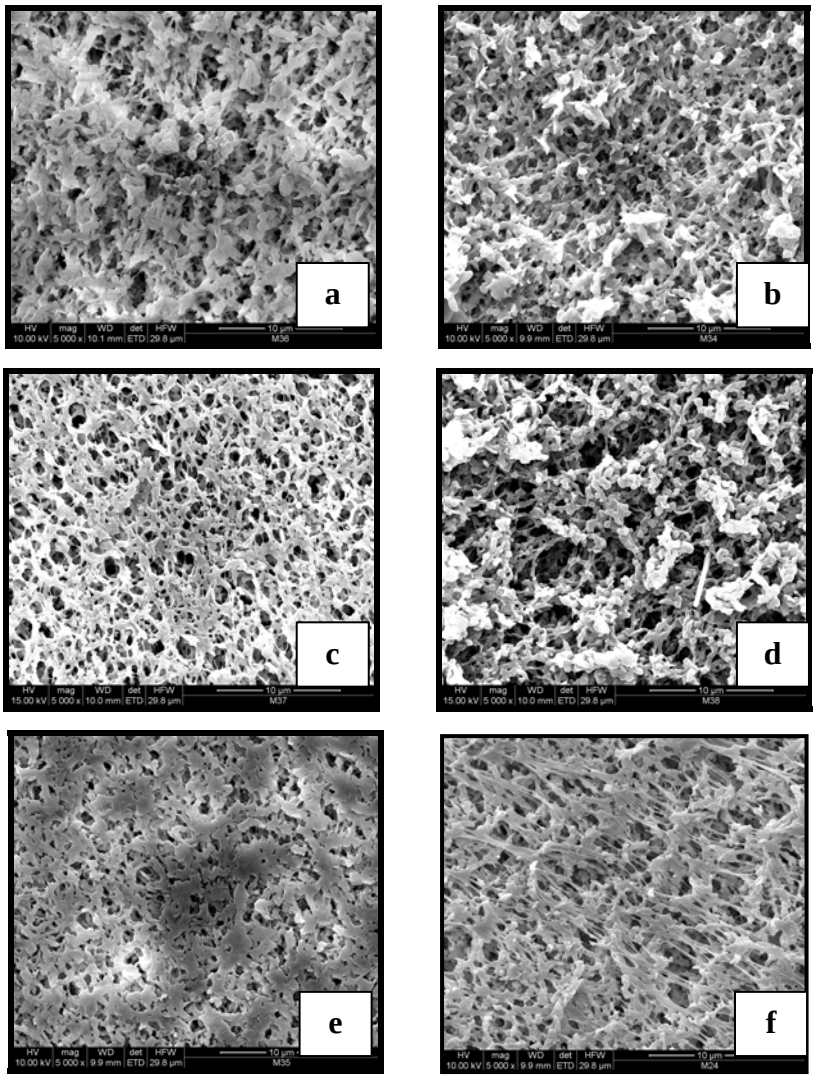

Figure 6.11– SEM micrographs of membranes processed with a [AA] of 0.03M (a), 0.06M (b), 0.1M (c), 0.2 (d), 0.3M (e), 0.4M (f).

6.3.9 Effect of the initiator concentration

Several grafting experiments were performed changing the initial concentration of initiator ([BPO]). The effects of this parameter on the DG

and crystallinity of the processed membranes are shown in Table 6.3. The degree of grafting increased considerably as [BPO] increased, after 8 hours as well as after 16 hours of reaction, while the crystallinity was decreased presumably as consequence of the higher grafting content. The increase of DG could be due to a faster free radical production as peroxide concentration increases that induces a corresponding increase in hydrogen abstraction from the PVDF chains. Indeed, in these conditions more graft copolymerization sites could be generated, where AA molecules can react, at equal reaction time and monomer concentration. Concerning the decrease of χ_c with BPO concentration, it could be attributed to an higher hydrogen abstraction also in the amorphous portions that are located close to the interface of crystalline portions of the original matrix, that can be distorted by the local variation in the polymer composition and microstructure induced by grafting.

				First Heating		Second Heating	
RUN	**Time (h)**	**[BPO] (g/L)**	**DG(%)**	**T_m (°C)**	**χ_c**	**T_m (°C)**	**χ_c**
1	8	0.042	0.56	163.3	39.9	158.2	53.9
2	8	0.118	12.17	164.2	37.4	158.4	40.2
3	16	0.04	4.55	163.9	37.7	158.1	48.7
4	16	0.121	14.84	163.7	31.9	158.1	40.5

Table 6.3- Level of grafting and calorimetric data of selected grafted membranes modified with a [AA]=0.2M, CO2 density =0.5g/mL (Maximum of melting endotherm (Tm) and degree of cristallinity (Xc) on second heating)

The surface modification, in terms of reduction of the pore sizes, due to the higher initiator concentration was more relevant after 16 hours of reaction rather than after 8 hours.

[BPO]=0.04g/L, 8 hours

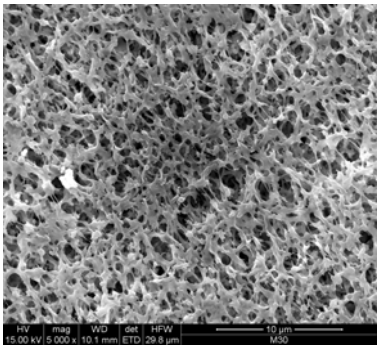

[BPO]=0.12g/L, 8 hours,

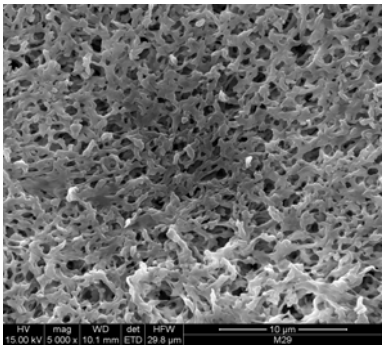

[BPO]=0.04g/L, 16 hours,

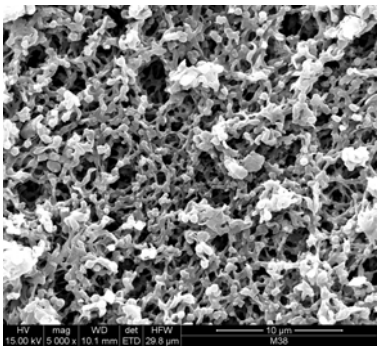

[BPO]=0.12g/L, 16 hours,

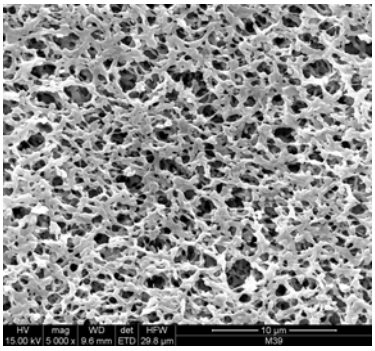

Figure 6.12- SEM micrographs of samples processed at different [BPO]

6.3.10 Study of the influence of fluid phase density

Several experiments were planned changing the fluid phase density in order to study the role of this parameter that can change the partitioning of the radicals and monomer molecules between the two phase. In particular the study of the influence of the fluid phase was aimed to know if it was possible to confine the generation of reaction sites only on the pores surface, which is the portion of the matrix prevalently interested to the water permeation, in order to reduce also the alteration of the crystalline domains. Three sets of experiments were performed (entry 1-6, Table 6.4) changing the density of the fluid phase. The results suggested that the degree of grafting decreased when the density of the fluid phase was increased. This can be explained by the remarkable change of solvency of sc-CO_2 with the change of density. At higher densities, sc-CO_2 has stronger solvent power, and thus more monomer and initiator exists in the supercritical phase, reducing the level of grafting. Moreover, the crystalline content of the membranes processed at high density was sensibly less penalized though high reaction times (run 4, Table 6.4) or high initiator concentration (run 6, Table 6.4) were used. That means that working at high CO_2 density it is possible to protect the bulky structure of the matrix, confining the reaction grafting presumably on the pores surface. Instead, the fluid phase density not has appreciable influences on the surface morphologies of the samples as it is possible to see in figure 6.13.

RUN	Time (h)	[BPO] (g/L)	ρCO_2 (g/ml)	DG (%)	χ_c I Fus.	χ_c II Fus.
1	16	0.04	0.54	4.6	37.7	48.7
2	16	0.04	0.71	2.1	42.3	50.9
3	20	0.04	0.47	10.3	34.7	38.3
4	20	0.04	0.70	5.0	39.5	49.4
5	16	0.12	0.52	14.8	31.9	40.5
6	16	0.13	0.78	3.4	37.0	49.03

Table 6.4 – Effect of CO_2 density on DG and crystalline content ([AA]=0.2 M, 65°C)

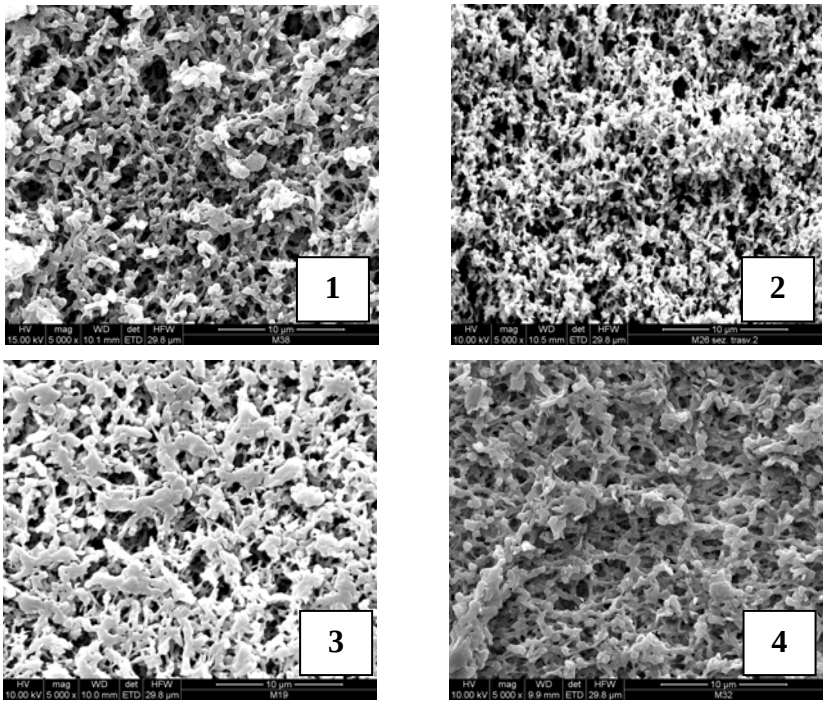

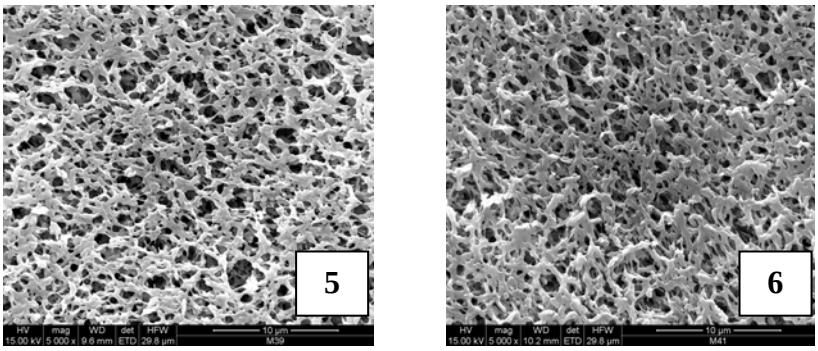

Figure 6.13 – SEM micrographs of grafted membranes (run 1-6) Table : effect of CO2 density

6.3.11 Influence of the DG on the thermal stability and water permeability

From the thermal gravimetric analysis it was possible to compare the thermal stability of the grafted membranes with those of PVDF pristine and polyacrylic acid omopolymer (Figure 6.14). PVDF resulted thermally stable up to about 430°C while PAA starts to decompose at about 200°C. Independently from the operative conditions used to process the membrane, the grafted membranes showed an intermediate behaviour. In particular the extent of the weight loss at about 280°C, corresponding to the PAA grafted chains degradation, increases with the degree of grafting of the sample, while the global thermal stability was comparable to the one of PVDF pristine.

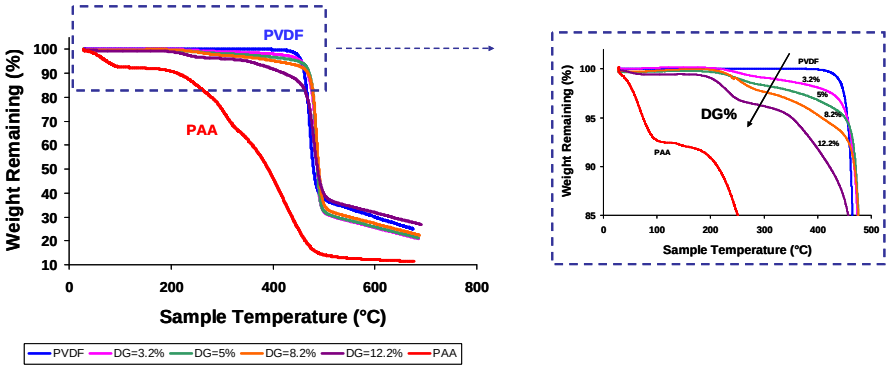

Figura 6.14. Thermal Gravimetric curves of the pristine membrane and grafted membranes compared with that of poly(acrylic acid) (PAA).

The water permeation behaviour of the membranes was examined and they were in all cases pH sensitive (Figure 6.15) contrary to virgin membranes characterized by very low values of flux for each pH value of the solution. The flux changes with the pH of the solution results from the response of the grafted PAA chains on the PVDF substrate to the proton concentration in environment. As a weak polyelectrolyte, PAA molecules adopt coiled or stretched conformation depending on their degree of dissociation or protonation, which is controlled by the pH of the surrounding solution. The conformation of the PAA chains changes from coiled at pH lower than 4 to more stretched at higher pH. The stretched conformation will close the pores partly or even completely provided that the grafted chains are enough and/or longer enough, which results in the decrease in the active pore size, and therefore the permeating flux is correspondingly reduced. The results collected in this work indicated that the grafted membranes have a water permeation that depends on their wettability as a consequence of the grafting of the hydrophilic monomer AA. Indeed, for lower DG (< 2-3 %) the fluxes

result very low because the pores surface was not enough hydrophilic. When DG increases at intermediate values (4-8 %) the water permeability increased notably, while decreased for higher DG (>9%). The latter behaviour is very presumable caused by the blocking effect of the PAA grafted chains anchored onto the pores of the PVDF substrate. Indeed, heavily grafted membranes possess more PAA grafted chains and their average chain length may be longer, and as a result the active pore size is reduced compared with the lightly grafted ones. This suggests that the control of the DG is a crucial aspect to obtain pH sensitive membranes with desired permeability.

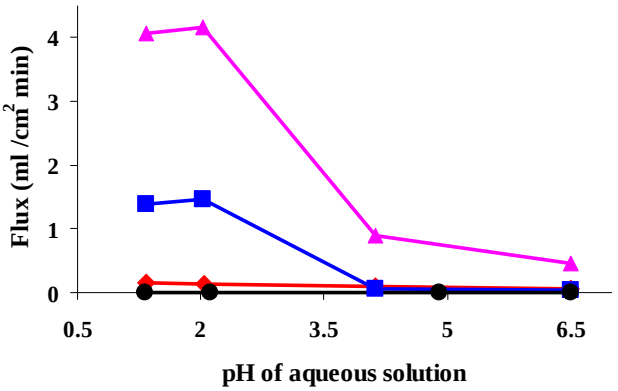

Figure 6.15 – Water permeability of grafted membranes with a DG of (●) 0.6%, (♦) 2.7%, (■) 8.2%, (▲) 4.6%.

6.4 Preliminary study on the controlled release of a model drug

To carry out some preliminary experiments of drug release from a grafted membrane, caffeine was selected as model drug because it belongs to class 1

in the biopharmaceutical classification system which means it has high permeability and solubility. In the figure 6.16 are shown the release profiles at 37°C of caffeine encapsulated in a grafted membrane in buffer solution at pH 2,5 (curve a) and 6,8 (curve b). The membrane selected for the experiments was that having an intermediate level of grafting (4.6%), that had higher water permeation (plot ▲ in Figure 6.15). The concentration profiles obtained for the grafted membrane were lower than the free dissolution of the pure caffeine but faster than the dissolution from the pristine membrane, moreover the dissolution profile in acid buffer was faster than that obtained in basic condition. Therefore it was confirmed that the release of the model drug from the grafted membrane was pH sensitive.

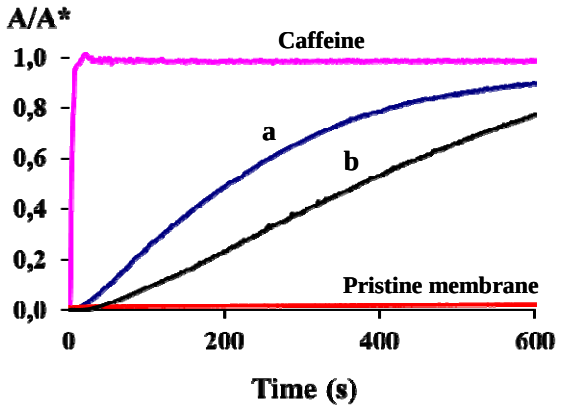

Figure 6.16 - Release profiles at 37°C of caffeine encapsulated in a grafted PVDF membrane (DG of 4.6%) in buffer solutions at pH a) 2.5, b) 6.8, compared with that from pristine membrane. A* is the absorbance of pure caffeine measured at infinite release time.

6.5 Conclusions

Grafting of AA on PVDF membranes was successfully performed in $scCO_2$ using the radical initiator benzoyl peroxide as source of radicals to initiate the grafting reaction. Results collected from ^{1}H NMR analysis indicated the presence of some functionalities typical of PAA chains in the spectra of the membranes with higher loading of grafting, moreover the ^{19}F NMR spectra of these membranes are characterized by the presence of peaks of CF_2 units broader than that of pristine matrix, due probably to the modification of the local environment of CF_2 groups for the presence of the PAA linked units. Both FT-ATR and NMR analyses of the samples does not give evidence of the presence of –CH=CF- groups arising from dehydrofluorination of the matrix. Therefore, accordingly the results obtained from FT-ATR and NMR analysis and the existent literature, it was possible to suggest a grafting mechanism of AA on PVDF membranes based also on the information collected from the study of the reaction locus in the heterogeneous copolymerization process of VDF and HFP in sc-CO_2, since even this grafting process occurs under heterogeneous conditions.

The results collected from the study of the influence of the operative parameters suggested that the grafting degree can be tuned by controlling the monomer and initiator concentrations, the reaction time and the carbon dioxide density. Flux measurements across the pristine and the grafted membranes at different pH-values demonstrated that a pH-sensitive behaviour was obtained after the grafting process and that the level of grafting influences notably the water permeability. Characterization by DSC of grafted membranes at the highest investigated densities suggested that at these conditions the reaction occurred mainly on the pore surface, with lower alteration of the bulk properties of the membrane. This could be tentatively explained considering that in these operative conditions AA and BPO

partitioning is biased towards the continuous phase. The thermal stability of the grafted matrixes was the same of that of pristine membrane, less than a previous step of degradation corresponding to the PAA chains.

Finally, preliminary results from drug release experiments suggested that it is possible to use PVDF membranes modified by graft copolymerization of AA in $scCO_2$ as vehicles of drugs with high solubility and permeability.

References:

[1] J. Otomo, Y. Oshima, A. Takami, S. Koda, J. Phys. Chem A, 2000, 104, 3332-3340.

[2] H. Guérin, Traité de Manipulation et d'analyse des gaz, Masson et Cie Editeurs

[3] Gaur, U.; Wunderlich, B. B.; Wunderlich, B. J Phys Chem Ref Data

1983, 12, 29–63.

[4] Kelly Clark, Sunggyu Lee, Polymer Eng. Sci. 2005, 45, 631-639.

[5] L. Bardet, G. Cassanas-Fabre, M. Alain, J. Mol. Struct., 24, 153, 1975

[6] D. Lin-Vien, N. B. Colthup, W. G. Fately, J. G. Grasselli, The Handbook of Infrared and Raman Characteristic Frequencies of Organic Molecules, Academic Press, San Diego, 1991.

[7] R. Saint-Loup, A. Manseri, B. Ameduri, B. Lebret, P. Vignane, Macromolecules 2002, 35, 1524-1536

[8] S. Inceoglu, S.C. Olugebefola, M.H. ACAR, A. MAYES, Designed Monomers and Polymers, Vol. 7, No. 1–2, pp. 181– 189, 2004.

Publications and Communications

L.I. Costa, G. Storti, M. Morbidelli, L. Ferro, O. Scialdone, G. Filardo, A. Galia, «*Copolymerization of VDF and HFP in Supercritical Carbon Dioxide: Experimental Evidence of the Role of the Polymer Phase In Determing Bimodal Molecular Weight Distributions»* Macromolecules, 43, 23, 9714-9723.

L.I. Costa, G. Storti, M. Morbidelli, L. Ferro, O. Scialdone, G. Filardo, A. Galia, «*Copolymerization of VDF and HFP in Supercritical Carbon Dioxide: A Robust Approach for Modeling Precipitation and Dispersion Kinetics*» Submitted to Macromolecular Reaction and Engineering.

L. Ferro, O. Scialdone, A. Galia, "*Preparation of pH Sensitive Poly(vinilydenefluoride) Porous Membranes by Grafting of Acrylic Acid Assisted by Supercritical Carbon Dioxide*", in preparation.

L.I. Costa, G. Storti, M. Morbidelli, L. Ferro, A. Galia, G. Filardo,, «*Robust Modeling of Precipitation and Dispersion Copolymerization of fluorinated monomers in Supercritical Carbon Dioxide*» 2010 AIChE meeting, Salt Lake City UT, USA, 07-12/11/2010.

L.I. Costa, G. Storti, M. Morbidelli, L. Ferro, A. Galia, G. Filardo,, «*Modeling of Precipitation and Dispersion Copolymerization of fluorinated monomers in Supercritical Carbon Dioxide*» 10th International workshop on Polymer Reaction Engineering, Hamburg, 10-13/10/2010

A. Galia, L. Ferro, G. Filardo, O. Scialdone, "*Modification of Poly(vinilydenefluoride) Porous Membranes by Grafting of Acrylic Acid Assisted by Supercritical Carbon Dioxide*", Sorrento, Italy, 8-11/09/10.

A. Galia, L. Ferro, V. Firetto G. Filardo, O. Scialdone, «*Preparation of pH sensitive poly(vinilydenefluoride) porous membranes by grafting of acrylic acid assisted by supercritical carbon dioxide*", Graz, Austria, 09-12/05/2010